Thermoluminescence of synthetic quartz annealed beyond its second phase inversion temperature

Zuko Mthwesi

Supervisor: Professor Makaiko L. Chithambo

A thesis submitted for the degree of Masters of Science

Faculty of Science

March 16, 2017

Dedication: *I dedicate this work to my family and late brother. Also not forgetting the whole department of Physics members.*

Acknowledgement

I would like to say thank you to my supervisor Professor Makaiko L.Chithambo. I appreciate all the work, you gave me through out the project.

Thank you to National Research Foundation (NRF) for funding my studies. Also Rhodes university, my postgraduate friends and staff.

I THANK YOU

Contents

List of Figures

List of Tables

Abstract

Thermoluminescence of synthetic quartz annealed at 1000 ^{0}C for 10 minutes has been studied. The aim was to study mechanisms of thermoluminescence in annealed synthetic quartz and to discuss the results in terms of the physics of point defects. The sample was irradiated with a beta dose of 10 Gy of beta radiation and then heated at a linear heating rate of 1 ^{0}C.s^{-1} up to 500 ^{0}C. The thermoluminescence (TL) glow curve consists of three glow peaks. Peak I at 74 ^{0}C (main peak) with high intensity as compared to the other two peaks. Peak II at 144 ^{0}C is more intense than peak III at 180 ^{0}C. This study was on the main peak (MP) at 74 ^{0}C and peak III at 180 ^{0}C. Kinetic analysis was carried out to determine the trap depth E, frequency factor s and the order of kinetics b of both peaks using the initial rise, peak shape, variable heating rate, glow curve deconvolution and isothermal TL methods. The values of kinetic parameters obtained were around 0.7 to 1.0 eV for trap depth and in the interval of 10^8 to 10^{15} s^{-1} for frequency factor for both peaks.

The effect of heating rate from 0.5 to 5 ^{0}C.s^{-1} on the TL peak intensity and peak temperature was observed. Also the effect of thermal quenching was observed at high heating rates. Since the TL glow curve has overlapping TL peaks, the T_m-T_{stop} method from 54 ^{0}C up to 64 ^{0}C and E -T_{stop} methods were introduced where a first order single peak was observed.

Phototransfered thermoluminescence (PTTL) was investigated and characterized by three peaks. First PTTL peak I at 72 ^{0}C, peak II at 134 ^{0}C and peak III at 176 ^{0}C.

Analysis was carried out on peaks I and III for the effect of dose dependence from 20-200 Gy. Thermal fading was observed on PTTL peaks I and III, after storage time of 30 minutes.

Chapter 1

Introduction

1.1 Types of defects

Imperfections that exist at atomic sites in a crystal structure are known as point defects. Defects sometimes are introduced in materials to improve their properties. Irradiation with energetic particles can create defects in the crystal. Usually the defects introduce localized energy levels between the conduction and valence bands within the energy band gap.

Missing atoms at lattice point are called vacancies. Extra atoms in between lattice points are called interstitials. Foreign atoms replacing host atoms are called impurities. Extrinsic defects are formed by foreign atoms and intrinsic defects form by displacement of host atoms by Eduardo [1]. Insulators and semiconductors materials exhibit these defects because of the size of their energy gap.

1.2 Luminescence in solids

Luminescence is the emission of light from a previously irradiated material. After irradiation, stimulation may occur either thermally or optically. The luminescence materials may be insulators or semiconductors. Such materials absorb energy during radiation and later release the absorbed energy as light of a longer wavelength. During irradiation, electrons in the valence band absorb energy and become excited. These electrons move to the conduction band. Once in the conduction band, the electrons are metastable and can make a transition to some energy levels within the band gap which are known as luminescence centre. If the process is radiative, luminescence is emitted by McKeever and Chen [2].

The emission of light can be classified into two processes, phosphorescence and fluorescence by McKeever and Chen [2]. This depends on the characteristic lifetime (τ) between absorption of the excitation energy and emission of the luminescence.

1.2.1 Comparison between fluorescence and phosphorescence

The time between excitation and emission of luminescence describes fluorescence and phosphorescence. Irradiation excites electrons from the valence band to the conduction band. The excited electrons are metastable. This causes them to transit to the valence band releasing light in the process. If the time of the whole process $\tau \leqslant 10^{-8}$ s, the process is known as fluorescence.

Figure 1.1 shows the fluorescence process. Transition 1 shows the excitation of electrons from the valence to the conduction band. Transition 2 shows electrons transiting from the conduction to the valence band. Luminescence is emitted during transition 2.

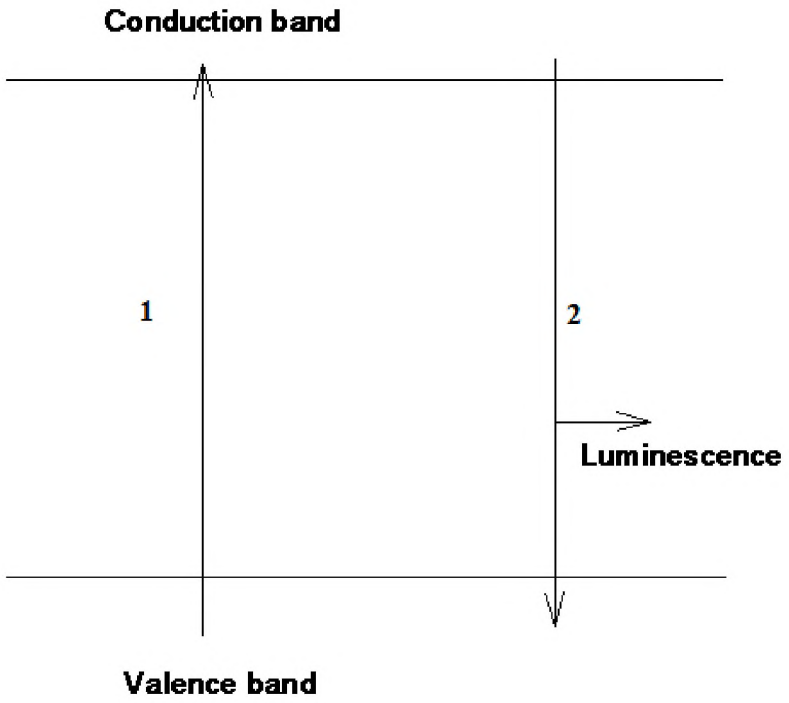

Figure 1.1: Transitions 1 and 2 showing absorption and emission involved in the process of fluorescence.

When $\tau \geq 10^{-8}$ s, due to delay of electrons releasing luminescence, the process is called phosphorescence by McKeever and Chen [2]. The cause of this is because the electrons delay releasing luminescence. Figure 1.2 shows the phosphorescence process. Transition 1 shows the excitation of electrons from the valence to the conduction band. In transition 2, electrons are

trapped at a point defect acting as an electron trap. Transition 3 shows electrons escaping the electron trap to the valence band. Transition 4 shows the emission of luminescence. The lifetime, τ, of the electron remaining in the trap at temperature T, is given by

$$\tau = s^{-1} \exp\left(\frac{E}{kT}\right), \tag{1.1}$$

where s is the frequency factor measured in Hz, E is the trap depth of the electron trap below the conduction band, k is Boltzmann's constant and T is temperature in K by McKeever [3]. Equation (1.1) is used in the case of phosphorescence.

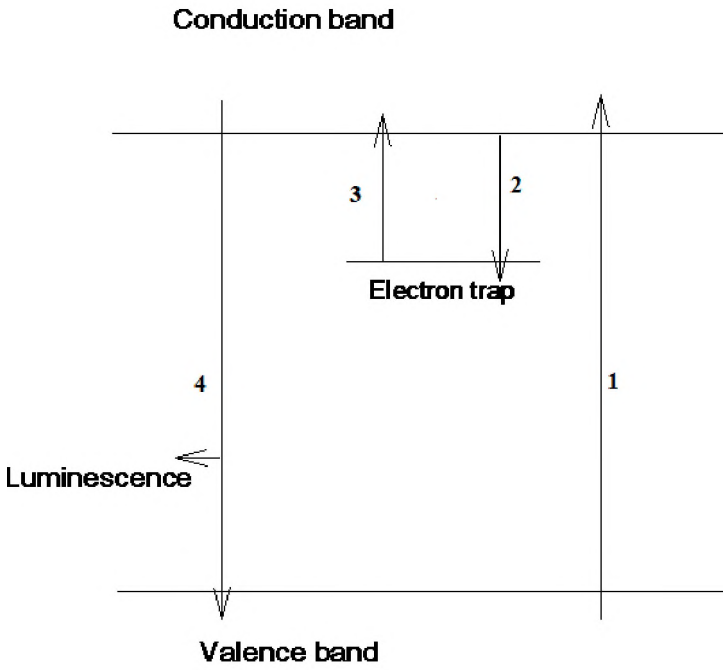

Figure 1.2: Four transitions showing the process of phosphorescence. Transition 1 shows excitation of electrons to the conduction band, transition 2 shows an electron get trap in an electron trap. Transition 3 shows escaping of electrons from the trap. Transition 4 shows emission of luminescence.

A reasonable idea to distinguish the two processes is to consider and analyse the effect of temperature on the decay of the luminescence intensity. Phosphorescence is strongly affected by temperature whereas fluorescence is independent of temperature by McKeever [3].

1.3 Luminescence processes

Various luminescence processes are given different names which reflect the type of radiation used to excite the emission. There are many luminescence processes that characterise the phosphor materials that release the absorbed energy in the form light.

Crystalloluminescence is produced during crystallisation. Piezoluminescence (PL) is produced by the action of pressure on certain solids. When the material is exposed to external sources such as γ , β particles and α rays the luminescence released is known as radioluminescence (RL)by McKeever [3]. Luminescence can be generated by mechanical energy to produce triboluminescence (TBL). Biochemical energy leads to bioluminescence (BL) and sound waves produce sonoluminescence (SL) from by McKeever [3]. Stimulation by heat or optical methods is classified as thermally or optically stimulated luminescence (TL or OSL) by McKeever [3]. If the excitation is done by an electron beam, the luminescence is called cathodoluminescence (CL).

1.4 Natural and synthetic quartz

Quartz is a naturally occurring mineral formed through various geological processes under high temperatures and pressure of most minerals that are in the earth's crust. It is a natural form of silicon dioxide known as crystal quartz. The vast majority contain quartz (SO_2), feldspar, olivine and other minerals. The largest group of minerals are silicates. Synthetic quartz is a single crystal grown using the hydrothermal synthesis method for use in industries. This method uses heat treatment and pressure to synthesize the scraps of natural quartz and The crystal system is trigonal. When the quartz is annealed, it passes under a process of heating and cooling the crystal. In order to remove internal stresses and make the crystal to be hardness and ductility. During the process some atoms migrate in the crystal lattice and number of dislocation decreases.

The basic type of defects in quartz are extrinsic and intrinsic defects such as missing oxygen or silicon atoms. Natural and synthetic quartz has luminescence properties. This has caused its extensive use in dating and retrospective dosimetry. In working with quartz, one should consider the phase transition as temperature increases. The usual phase transition takes place at 573 ^{0}C and 870 ^{0}C by McKeever [3]. The physical properties of natural and synthetic quartz may not be the same.

The sample of study was annealed beyond its second phase inversion temperature. The second phase of quartz, is when the temperature is above 850^{0}C. When annealing the sample above 850^{0}C result on transforming the usual phase transition of the sample. The main aim is to study mecha-

nisms of thermoluminescence in annealed synthetic quartz and to discuss the results in terms of the physics of point defects.

1.5 Synopsis of the thesis

Chapter 1 is the introduction of types of defects that are present in the crystal. The fundamentals of luminescence properties and processes are also explained.

Chapter 2 focuses on thermoluminescence (TL) theory literature and applications including TL theoretical models. In this chapter, the order of kinetics is also explained. The characteristics of TL glow curves were discussed in details. Six different methods were used to extract kinetic parameters on the TL glow curve. These are the initial rise, peak shape, variable heating rate, glow curve deconvolution and isothermal analysis.

Chapter 3 explains more about instrumentation that was used to perform the measurements in the study. The sample preparation is explained.

Chapter 4 is about the experimental results obtained during experiments using the methods mentioned in chapter two. Only peaks I and III were analysed.

Chapter 5 is the summary and conclusion of all the experimental results that were obtained in chapter four.

Chapter 2

Thermoluminescence theory

2.1 Introduction

Thermoluminescence (TL) has been used in different ways to study phosphor materials. Thermoluminescence is the emission of light from a previously irradiated insulator or semiconductor when it is heated at a controlled rate. The light is emitted as a function of temperature and resulting plot is called a glow curve by Furetta [4]. The glow curve is made up of one or more peaks some of which may be overlapping. The focus in this chapter is to present the theory of TL.

2.2 Basic theory

In order for thermoluminescence to be possible the material must be a semiconductor or insulator. During irradiation, electrons in the valence band absorb energy. The excited electrons then move to the conduction band. Some of the electrons in the conduction band get trapped at electron traps. Heating the material causes the trapped electrons to move from the trap back to the conduction band. Some of the electrons transit down to recombine with holes at the luminescence center. If the transition is radiative, luminescence is emitted. These processes are illustrated in figure 2.1.

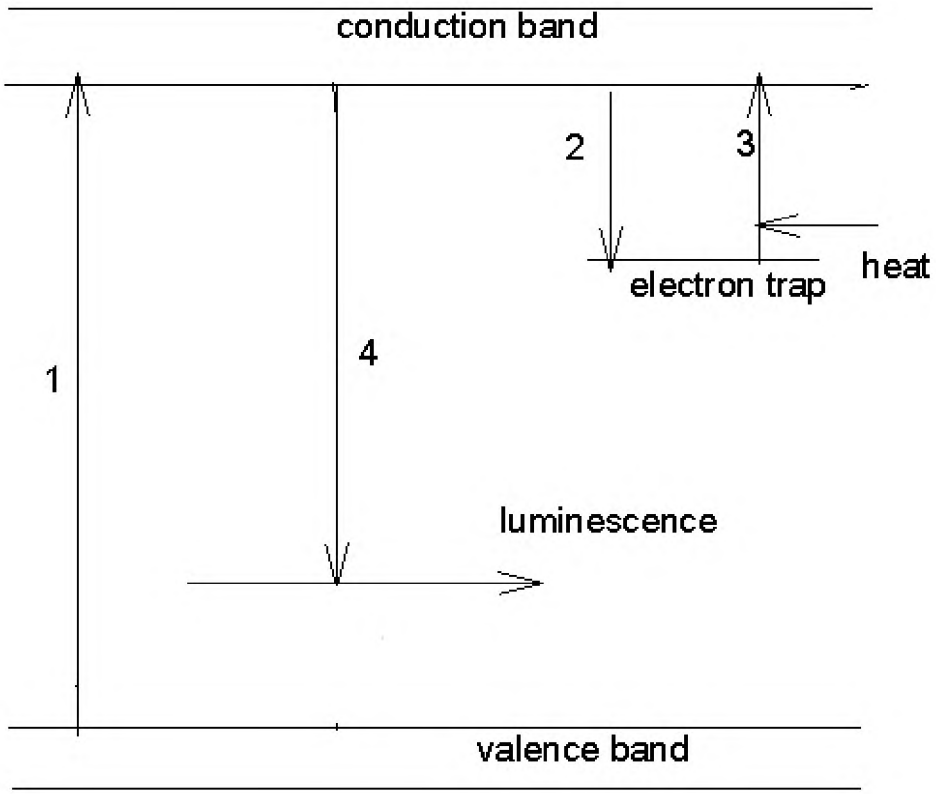

Figure 2.1: Energy band scheme to explain TL. Transition 1 shows the irradiation stage, exciting electrons to the conduction band. Transition 2 shows trapping of electrons from the conduction band into the electron trap. Transition 3 shows electrons transiting to the conduction band after thermal stimulation by heat. Transition 4 is the movement of electrons from the conduction band to the recombination center.

2.3 Models of Thermoluminescence

Point defects act as electron traps and hole traps in crystal structure. Electrons are trapped in these electron traps until they are thermally stimulated as was shown in figure 2.1. The TL intensity I_{TL} that is emitted is proportional to the rate of recombination of electrons and holes at the

luminescence center,

$$I_{TL} = -\frac{dn}{dt} \tag{2.1}$$

where n is the concentration of trapped electrons.

2.3.1 Simple model of thermoluminescence

In 1945, Randall and Wilkins used a mathematical representation originated from studies of phosphorescence by Randall and Wilkins [5]. Their mathematical treatment was based on the energy band model and yielded the well known first order expression. In first order kinetics the probability of electrons escaping the electron traps is more than that of retrapping. In the simple model it is assumed that between the valence and conduction bands, there exist two types of defects as shown in figure 2.1. One type acts as an electron trap and the other as a luminescence center (LC). The electron trap is close to the conduction band. The energy gap between electron trap and the bottom of the conduction band is called the trap depth. The trap depth E is the energy required to liberate electrons from the electron trap to the conduction band. On the other hand,the luminescence center (LC) is close to the valence band (VB). The probability of an electron escaping the trap per unit time is given by an Arrhenius equation by Furetta [4],

$$p = s \exp\left(\frac{-E}{kT}\right) \tag{2.2}$$

where p is the probability of an electron escaping the trap, s is the frequency factor (in Hz), E is the trap depth (in eV), k is Boltzmann's constant and T is the temperature.

In the case of TL, a sample is heated at a linear heating rate, $\beta = \mathrm{dT/dt}$. The intensity of TL is proportional to the rate of concentration of electrons escaping the trapping centres and is given as

$$I = -\frac{dn}{dt} = p\,n \tag{2.3}$$

Since $p = s \exp\left(\frac{-E}{kT}\right)$, equation (2.3) becomes

$$I = -\frac{dn}{dt} = -n\,s \exp\left(\frac{-E}{kT}\right) \tag{2.4}$$

By integrating equation (2.4) and replacing dt by $\frac{dT}{\beta}$, we get

$$\int_{n_0}^{n} \frac{1}{n} dn = \left(\frac{s}{\beta}\right) \int_{T_0}^{T} \exp\left(\frac{-E}{kT}\right) dT \tag{2.5}$$

from which

$$ln(n) - ln(n_0) = ln\left(\frac{n}{n_0}\right) = \left(\frac{s}{\beta}\right)\int_{T_0}^{T} \exp\left(\frac{-E}{kT}\right) dT \tag{2.6}$$

$$n = n_0 \exp\left[\left(\frac{s}{\beta}\right)\int_{T_0}^{T} \exp\left(\frac{-E}{kT}\right) dT\right]. \tag{2.7}$$

Since TL is proportional to the rate of electrons escaping trapping centres, then the intensity is given as

$$I_{TL} = n_0 s \exp\left[\left(\frac{s}{\beta}\right)\int_{T_0}^{T} \exp\left(\frac{-E}{kT}\right) dT\right]. \tag{2.8}$$

At the peak maximum $T = T_m$. The decrease of the second exponential is much faster than the increase of the first exponential and $I(T)$ decreases until the traps are emptied. At T equal to T_m

$$\frac{dI}{dT} = 0. \tag{2.9}$$

Written in terms of a logarithm derivative, equation (2.9) becomes.

$$\frac{d(lnI)}{dT} = \frac{I}{dT}\left(\frac{dI}{dT}\right) \tag{2.10}$$

From equation (2.10) we get

$$\left[\frac{d(lnI)}{dT}\right] = \frac{E}{kT_m^2} - \frac{s}{\beta}\exp\left(\frac{-E}{kT_m}\right) = 0 \tag{2.11}$$

$$\frac{\beta E}{kT_m^2} = s\exp\left(\frac{-E}{kT_m}\right) \tag{2.12}$$

hence

$$s = \left(\frac{\beta.E}{k.{T_m}^2}\right)\exp\left(\frac{E}{k.T_m}\right) \tag{2.13}$$

2.3.2 General order model

An intermediate case where first and second order kinetics are invalid is called general order kinetics by May and Partridge [6].

The assumption is that the number of charge carries found in the single energy level is proportional to n^b. The probability or rate of escape of charges from the electron trap is given as:

$$I_{TL} = \frac{dn}{dt} = -s'n^b \exp\left(\frac{-E}{kT}\right) \tag{2.14}$$

where the order of kinetics b is such that $1 < b < 2$ and s' is the pre-exponential factor ($\mathrm{cm}^{3(b-1)}$). Rearranging equation (2.14) we have,

$$\frac{dn}{n^b} = -s' \exp\left(\frac{-E}{kT}\right) dt. \tag{2.15}$$

Integrating equation (2.15) we find

$$n = n_0 \left[1 + s''(b-1)t \exp\left(\frac{-E}{kT}\right)\right]^{\frac{1}{1-b}} \tag{2.16}$$

where $s'' = s n_0^{b-1}$ ($\mathrm{cm}^{3(b-1)}$).
For a linear heating rate $dT/dt = \beta$, equation (2.16) becomes

$$I_{TL} = s'' n_0 \exp\left(\frac{-E}{kT}\right) \left[1 + \frac{s''(b-1)}{\beta} \exp\left(\frac{-E}{kT}\right)\right]^{-\frac{b}{b-1}} \tag{2.17}$$

The corresponding pre-exponential factor is given as

$$s'' = \left[\frac{kT_m^2 b \exp\left(\frac{-E}{kT_m}\right)}{\beta E} - \frac{(b-1)\int_{T_0}^{T} \exp\left(\frac{-E}{kT'}\right) dT'}{\beta}\right]^{-1} \tag{2.18}$$

2.4 Orders of kinetics

Glow curves can be analysed on the basis of first, second or general order kinetics.

2.4.1 First order kinetics

When retrapping of electrons is negligible the behaviour is called first order kinetics. In this case the recombination probability as compared with retrapping probability becomes

$$m\sigma_{mn} >> (N-n)\sigma_n. \tag{2.19}$$

where $(N-n)\sigma_n$ is the retrapping probability, σ_n is the retrapping cross section for free carriers. Also $m\sigma_{mn}$ is the recombination probability and σ_{mn} is the recombination cross section for free carriers by McKeever and Chen [2]. Under the conditions of first order kinetics, equation (2.14) becomes

$$I_{TL} = \frac{dn}{dt} = ns \exp\left(\frac{-E}{kT}\right). \tag{2.20}$$

By integrating equation (2.20) using a constant heating rate $\beta = dT/dt$ we get,

$$n = n_0 \exp\left[\left(-\frac{s}{\beta}\right)\int_{T_0}^{T} \exp\left(\frac{-E}{kT}\right) dT\right]. \tag{2.21}$$

Substituting equation (2.21) into equation (2.20) leads to

$$I_{TL} = sn_0 \exp\left(\frac{-E}{kT}\right) \exp\left[\left(\frac{-s}{\beta}\right)\int_{T_0}^{T} \exp\left(\frac{-E}{k\theta}\right) d\theta\right] \tag{2.22}$$

where n_0 is the initial value of n and θ is a dummy variable representing temperature.

The shape of the TL glow peak is narrow under first order kinetics and wider on the low temperature side than on its high temperature side. Its shape is asymmetric and geometric factor is given as $\mu = \frac{\tau}{\omega} = 0.42$ which determine first order of kinetics by Chen [7]. In first order processes the position of the peak temperature is independent of initial trapped charge concentration.

2.4.2 Second order kinetics

Garlick and Gibson [8] proposed that if retrapping is dominant then

$$\sigma_{mn} << (N - n)\sigma_n. \tag{2.23}$$

For a fixed heating rate the peak temperature and shape are strongly dependent on the initial trapped charge concentration n_0. The TL peak shift to the lower temperatures as the heating rate increases. Its shape is asymmetric and geometric factor is 0.52 which determine first order of kinetics. The equation for second order kinetics is given as,

$$I_{TL} = \frac{dn}{dt} = n^2 s \frac{\sigma_n}{N\sigma_{mn}} \exp\left(\frac{-E}{kT}\right). \tag{2.24}$$

With the assumption that $\sigma_{mn} = \sigma_n$ made by Garlick and Gibson [8] for second order kinetics, integrating equation (2.24) produces

$$I_{TL} = s\frac{n^2}{N} \exp\left(\frac{-E}{kT}\right)\left[1 + \left(\frac{n_0 s}{\beta N}\right)\int_{T_0}^{T} \exp\left(\frac{-E}{k\theta}\right) d\theta\right]^{-2}. \tag{2.25}$$

2.4.3 General order kinetics

General order kinetics results when the situation is between first and second order kinetics. Equation (2.26) was written by May and Partridge [6] reviewed from Chen and McKeever [2] for the case where first and second order kinetics does not apply. The formula for general order kinetics is given as

$$I(T) = \frac{dn}{dt} = n^b s' \exp\left(\frac{-E}{kT}\right) \tag{2.26}$$

where s' has the unit $m^{3(b-1)}\ s^{-1}$ and b is the general order parameter. Integrating equation (2.26), for $b \neq 1$ leads to,

$$I(T) = s'' n_0 \exp\left(\frac{-E}{kT}\right)\left[1 + \left(\frac{s''(b-1)}{\beta}\right)\int_{T_0}^{T} \exp\left(\frac{-E}{k\theta}\right) d\theta\right]^{\frac{-b}{b-1}} \tag{2.27}$$

where now $s'' = s'(n_0)^{b-1}$.

Equation (2.27) is not a general expression when introducing all three orders of kinetics. The more general order kinetics was given as,

$$I_{TL} = -\frac{dn}{dt} = \left(\frac{n^b}{N^{b-1}}\right) s \exp\left(\frac{-E}{kT}\right) \tag{2.28}$$

Equation (2.28) can be easily reduced to first or second order kinetics, if $b = 1$ or 2.

2.5 Methods of analysis

Kinetic analysis of thermoluminescence uses various methods to evaluate kinetic parameters such as trap depth E, order of kinetics b and frequency factor s of a TL glow peak by Mckeever [3].

2.5.1 Initial rise method

The initial rise method (IRM) was first suggested by Garlick and Gibson [8]. The method is applied in the initial rising part of the TL glow curve. The rising part must not exceed 15 % of the maximum intensity. At these low temperatures the assumption is that the concentration of trapped electrons remain constant by Mckeever [3]. Since the dependence of the amount of trapped electrons on temperature is ignored in this temperatures region, the thermoluminescence emission is described mathematically as

$$I(T) = C \exp\left(\frac{-E}{kT}\right) \tag{2.29}$$

where $I(T)$ is thermoluminescence intensity, C is a constant, E is the trap depth (eV), k is Boltzmann's constant and T is temperature in kelvin (K).

Equation (2.29) can be re-written as

$$\ln(I(T)) = \frac{-E}{kT} + lnC \tag{2.30}$$

A plot of $ln(I)$ against $1/kT$ gives a straight line with slope equal to E. The disadvantage of this method is that it uses the rising part of the TL glow peak which may sometimes give errors because of overlapping peaks.

2.5.2 T_m-T_{stop} technique

Some methods were suggested in the literature for composite or overlapping glow peaks by Mckeever [3], because the initial rise method may fail to give correct values of trap depths. One example is the thermal cleaning technique. The sample is heated above the peak temperature of the first TL glow peak and then cooled to room temperature. The process is repeated for all the TL glow peaks if there is more than one. This produces a clean initial rise curve that is easy to analyse.

Another partial technique was introduced by Mckeever [3] is known as T_m -T_{stop} technique. The sample is irradiated then heated at a linear rate up to a certain temperature T_{stop} that corresponds with a low temperature of the TL glow peak. After cooling, the process is repeated but T_{stop} temperature by is increased 2 °C to 5 °C. A Plot of T_m against T_{stop} stands for a single peak if a flat line is produced. For overlapping peaks staircase curve is produced. The technique allows for the estimation of the number and position of the individual peaks that were hidden and overlapping in original TL glow peaks. Plotting E as a function of T_{stop} will also give the similar results as the T_m -T_{stop} technique.

2.5.3 Peak-shape method

Figure 2.2 shows the geometrical properties of a TL glow peak by Chen [9]. The following are shape parameters definition,

$$\tau = T_m - T_1 \tag{2.31}$$

$$\delta = T_2 - T_m \tag{2.32}$$

$$\omega = T_2 - T_1 \tag{2.33}$$

where T_m is the peak temperature, T_1 and T_2 are temperatures at half intensity $I_m/2$, τ is the half-width at low temperature side of the peak, δ

is the half-width at high temperature side of the peak, ω is the total half width and μ is the geometric factor or symmetrical factor $\mu = \frac{\tau}{\omega}$.

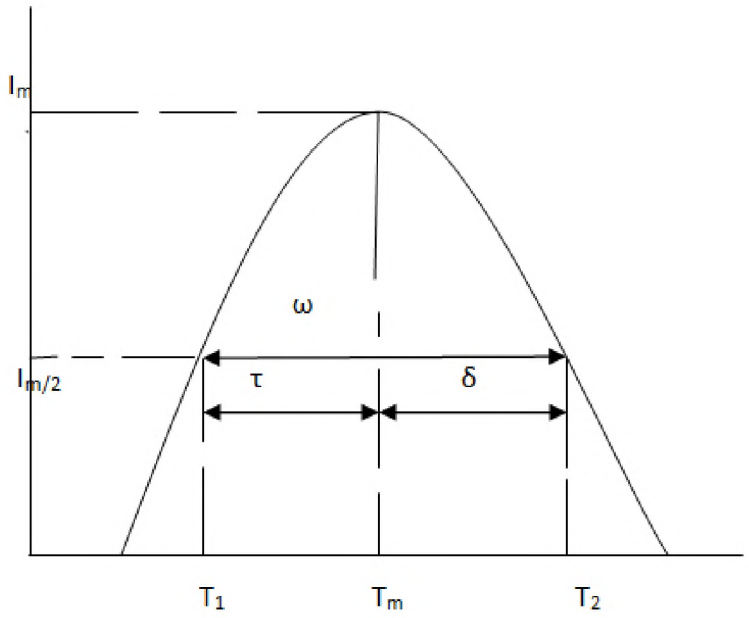

Figure 2.2: Peak shape method procedure using geometric parameters (from Chen [9]).

First order and second order kinetics have their values of the geometric factor as 0.42 and 0.52 respectively. For evaluation of trap depth E, one uses

$$E_\alpha = C_\alpha \left(\frac{kT_m^2}{\alpha} \right) - b_\alpha (2kT_m) \tag{2.34}$$

where α can be δ, ω and τ.

C and b are constants, k is Boltzmann's constant and T_m peak temperature. C_α and b_α are given as follows,

$$C_\tau = 1.510 + 3.0(\mu - 0.42) \quad b_\alpha = 1.58 + 4.2(\mu - 0.42) \tag{2.35}$$

$$C_\delta = 0.976 + 7.3(\mu - 0.42) \quad b_\delta = 0 \tag{2.36}$$

$$C_\omega = 2.52 + 10.2(\mu - 0.42) \quad b_\omega = 1. \tag{2.37}$$

The disadvantage of peak shape method, is the choice of T_1 and T_2 on TL glow peak during experimental results this may give inaccurate results on the trap depth, E, since the two parameters depend on half intensity,$I_{m/2}$.

2.5.4 Variable heating rate method

As the heating rate increases from one measurement to another, the centroid of the current peak associated with a trap shifts to higher temperatures. Variable heating rate method (VHR) is also used to evaluate kinetic parameters such as the trap depth E and the frequency factor s. Evaluation of the value of E can be based on two different heating rates which correspond to two peak temperature by Hoogenstraaten [10].

$$E = \left[\frac{kT_{m1}T_{m2}}{T_{m1} - T_{m2}}\right] ln \left[\frac{\beta_1}{\beta_2}\left(\frac{T_{m2}}{T_{m1}}\right)^2\right] \tag{2.38}$$

where T_{m1} and T_{m2} are the peak temperatures corresponding to heating rates β_1 and β_2. E can also be estimated from the two intensities as,

$$E = \left[\frac{kT_{m1}T_{m2}}{T_{m1} - T_{m2}}\right] \ln\left(\frac{I_{m1}}{I_{m2}}\right) \tag{2.39}$$

where I_{m1} intensity corresponding to T_{m1} , I_{m2} is the intensity corresponding to T_{m2}. The choice of two peak temperatures and maximum intensities is arbitrary.

A slightly different method from the first order kinetics equation (2.39), uses several heating rates. Applying logarithms both side, we get

$$ln\left(\frac{T_m^2}{\beta}\right) = \frac{E}{kT_m} + ln\left(\frac{E}{sk}\right) \tag{2.40}$$

where s is the frequency in s^{-1}.

From the equation (2.40), a plot of $ln(T_m^2/\beta)$ versus $1/kT$ gives a straight line of slope of E and intercept $ln(E/sk)$. The frequency factor can be evaluated from the intercept.

The major challenge in variable heating rate method, is that they need good thermal contact between the sample and the holder as the heating rate increases.

2.5.5 Whole curve method

The whole curve method (WCM) uses the area under a TL glow peak by Pagonis [16].

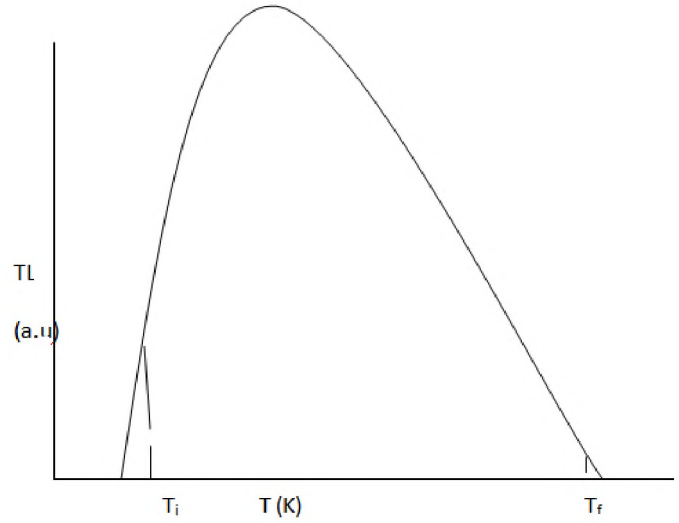

Figure 2.3: Whole curve method procedure, showing the the integrated area from T_1 to T_2.

With reference to figure 2.3, the area under the peak is calculated according to the following equation by Pagonis [16],

$$n = \int_{T_i}^{T_f} I dt \tag{2.41}$$

where n is the area under the peak between T_i and T_f ,where T_i and T_f are temperatures at the beginning and end of the peak respectively and I is the intensity.

Substituting $\beta = dT/dt$ in equation (2.41) leads to

$$n = \frac{1}{\beta} \int_{T_i}^{T_f} I dT \tag{2.42}$$

where β is the heating rate $({}^0C \cdot s^{-1})$.

After integration equation (2.42) becomes,

$$ln\left[\frac{I}{n(T)}\right] = ln\frac{s}{\beta} - \frac{E}{kT}. \tag{2.43}$$

A plot of $ln(I/n(T))$ versus $1/kT$ has a slope of $-E$ and an intercept equal to $ln(s/\beta)$. In the case of general order kinetics, equation (2.43) can be written as

$$ln\left[\frac{I}{n(T)^b}\right] = ln\frac{s}{\beta} - \frac{E}{kT}. \tag{2.44}$$

If the order of kinetics b is unknown several values of b can be used and the best straight line chosen. By plotting $ln(I/n(T)^b$ versus $1/kT$ the best straight line gives the value of E. The first disadvantage of WCM, is the choice of T_i and T_f when calculating the area under the curve. Secondly the values of b when we chose the best straight line.

2.5.6 Glow curve deconvolution method

Experimental data is analysed by the glow curve deconvolution method (GCDM) using the equation,

$$I(T) = I_m b^{\frac{b}{b-1}} \exp\left[\frac{E}{kT}.\frac{T-T_m}{T_m}\right]\left[(b-1)(1-\triangle)\frac{T^2}{T_m^2}\exp\left[\frac{E}{kT}.\frac{T-T_m}{T_m}\right] + Z_m\right]^{-\frac{b}{b-1}} \tag{2.45}$$

where I is the glow peak intensity, I_m is the maximum glow peak intensity, E is the trap depth, $\triangle = \frac{2kT}{E}$ and $Z_m = 1 + (b-1)/\triangle_m$ by Kitis [11]. The parameter b is called order of kinetics. Kinetic parameters such as the trap depth and kinetic order are obtained using curve-fitting using equation (2.45). The advantage of using this method is that they involves two quantities which are measured experimentally, T_m and I_m. The trap depth E can be treated as a varying parameter.

The goodness of fit is tested by the figure or merit (FOM) given as:

$$FOM = \frac{\Sigma|Y_{exp} - Y_{fit}|}{\Sigma Y_{fit}}, \tag{2.46}$$

where Y_{exp} is experimental data and Y_{fit} is the fitted results. The disadvantage, is that when fitting the TL glow curve the rising part of TL glow curve may be compose of overlapping peak.

2.5.7 Isothermal method

This method uses a plot of intensity as the function of time at a constant temperatures by Mckeever and Chen [12]. Experimental measurements consist of heating the sample after irradiation to a specific chosen temperatures below the maximum temperature on the rising part of the main peak and then keeping the sample at this temperature for some time. The simplest form of the intensity as a function of time is given as

$$I(t) = I_0 \exp(-pt) \tag{2.47}$$

$$\tag{2.48}$$

or

$$I(t) = I_0 \exp\left(-s \exp\left(\frac{-E}{kT}\right) t\right) \tag{2.49}$$

where I_0 is the intensity at $t = 0$, p is the probability of thermal stimulation. For the case of a series of isothermal measurements at different temperatures (T_i).

$$ln(p) = \frac{E}{kT_i} + ln(s) \tag{2.50}$$

Plotting $ln(p)$ against $1/kT$ and the graph will give a straight line with slope E (trap depth) and intercept equal to ln(s) from which s can be found.

In the case of using only two different temperatures to evaluate E and s, one finds

$$E = k\frac{ln\left(\frac{T_1}{T_2}\right)}{(1/T_1 - 1/T_2)} \tag{2.51}$$

The application of isothermal decay analysis for general order kinetics has been suggested by May and Partridge [6] and Inabe et al Nanto [13] as

$$I = I_0 \left[1 + s' n_0^{b-1}(b-1)t \exp\left(\frac{-E}{KT}\right)\right]^{-b/b-1} \tag{2.52}$$

where $I_0 = s' n_0^b \exp\left(\frac{-E}{kT}\right)$.

The challenge in this method, is the number choice of specific chosen constant temperatures below the T_M on the rising part as it may compose of overlapping peaks and also the time to keep the sample on those temperatures.

2.6 Phototransferred thermoluminescence

Phototransferred thermoluminescence (PTTL) can be explained by the energy level scheme shown in figure 2.4. Figure 2.4 shows PTTL model with three trapping centres, deep trap (DT), shallow trap (ST) and luminescence center (LC). The DT is governed by N_2, n_2 and A_2 parameters. The shallow trap (ST) is governed by N_1, n_1 and A_1. The luminescence centre (LC) is governed by m, M and A_m. PTTL is a tool that shows transfer of charges from deep traps to shallow traps. The charges are then released to luminescence center (LC) where the luminescence emission take place by Santo [14]. This is just thermoluminescence emission caused by movement of charges from shallow traps to the luminescence center.

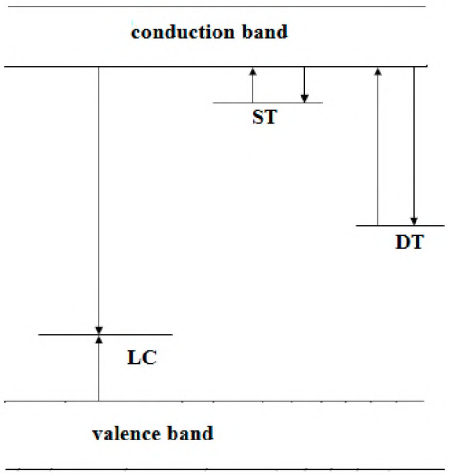

Figure 2.4: A model of PTTL showing a, deep trap (DT), shallow (ST) and luminescence center LC.

PTTL is carried out by few steps, firstly the electrons and holes are released from the valence band by irradiating the sample. Some of these electrons get trapped at electron traps by Botter [15]. Secondly the glow peaks are erased by heating the sample to a pre-decided temperature then cooled to room temperature. Thirdly, light of a suitable wavelength is used to excite charges from deep traps to into shallow traps by Santo [14]. The deep trap in this case acts as a donor and shallow traps as acceptor. After illumination for a particular time, the sample is heated to produce thermo-luminescence.

2.6.1 PTTL models

The simplest PTTL model involves one deep trap, one shallow trap and one luminescence center as shown in figure 2.4. The rate equations during the illumination time are given as

$$\frac{dn_2}{dt} = n_c(N_2 - n_2)A_2 - n_2 f_2 \tag{2.53}$$

$$\frac{dn_1}{dt} = n_c(N_1 - n_1)A_1 \tag{2.54}$$

and

$$\frac{dm}{dt} = -n_c m A_m = \frac{m}{\tau}. \tag{2.55}$$

where $\tau = 1/(n_c A_m)$ is a lifetime, f is frequency factor from deep trap during illumination time by Mckeever and Chen [12].

Equations (2.53), (2.54) and (2.55) show the process of filling the traps during irradiation. During this process electrons are trapped in shallow traps and also in deep traps. At the same time the holes are generated in the valence band N_h, n_v.

The second step is to heat the sample to the temperature that is suitable to remove all electrons in the shallow traps. The following equations apply during the heating stage,

$$\frac{dn_1}{dt} = -sn_1 \exp\left(\frac{-E}{kT}\right) + A_1(N_1 - n_1)n_c \tag{2.56}$$

$$\frac{dn_2}{dt} = A_2(N_2 - n_2)n_c \tag{2.57}$$

$$\frac{dn_v}{dt} = 0 \tag{2.58}$$

$$\frac{dm}{dt} = A_m m n_c \tag{2.59}$$

$$\frac{dn_1}{dt} + \frac{dn_2}{dt} + \frac{dn_c}{dt} = \frac{dm}{dt} \tag{2.60}$$

After preheating it is assumed that there are no electrons in the shallow trap. The term $n_v = 0$ because the are no additional hole in the valence band. During phototransfer process $s\, n_1 \exp(-E/kT) = 0$. Since the illumination is performed at the room temperature during this time no electrons from the shallow trap play role.

The idea now is to excite electrons in the deep trap known as donor traps. This stage is performed at room temperature to keep the electrons in shallow trap stable.

It can be shown that as $t \to \infty$ the maximum PTTL intensity becomes,

$$S_{PTTL}(\infty) = \frac{C n_1^2 \infty}{N_2} \tag{2.61}$$

where $S_{PTTL}(\infty)$ is the PTTL intensity. The concentration of electrons in the shallow trap may increase during illumination time and the number of holes decreases. At some point the number of electrons in shallow trap is equal to the number of holes in the luminescence center. PTTL intensity

at $t \to \infty$ will decrease following the number of holes in the luminescence center, thus

$$n_1 + n_2 + n_c = m \tag{2.62}$$

The above equation describes the competition and conditions of charge neutrality to explain the PTTL as a behaviour of time by McKeever and Chen [12]. That is why the relationship between shallow trap and luminescence center with illumination time must be considered Botter [15]. Thus

$$S_{PTTL} = min(n_1, m) \tag{2.63}$$

PTTL follows the behaviour of electrons in the shallow traps since there are enough holes to accommodate electrons during illumination time, then PTTL will increase as n_1 increases. The model explains PTTL intensity as an increasing function of the illumination time in the case of two traps and one luminescence center.

Chapter 3

Experimental details

All the measurements were performed using a Risø TL/OSL DA-20 luminescence Reader as shown in figure 3.1. The reader is made up of two essential components: a Reader and a controller. Figure3.1: the reader consists of three components: a light detection system, an irradiation source and a luminescence stimulation system. The Reader enables both measurements of thermoluminescence and optically stimulated luminescence.

3.1 Components of the RISØ TL/OSL DA-20 READER

The Risø TL/OSL Reader enables automated measurement of thermoluminescence (TL) and optically stimulated luminescence (OSL). The Risø TL/OSL Reader consists of two separate components the controller and the reader as shown in figure 3.1.

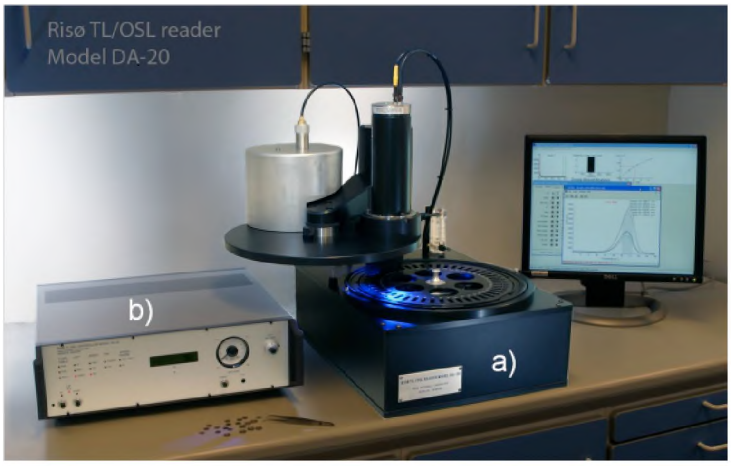

Figure 3.1: The Risø TL/OSL instrument showing the Reader (a) and the controller (b).

Samples are loaded onto a sample carousel that can accommodate up to 48 samples. The sample carousel is placed within the sample chamber which can be programmed to have nitrogen atmosphere maintained by nitrogen flow. The sample is lifted through slots on the sample carousel into the measurement position by a lift which also functions as a heating element. In the measurement position, the sample can be stimulated thermally or optically. Thermal stimulation is obtained by linearly increasing the temperature of the heating element and optical stimulation is done by different light sources focussed onto the sample position. The emitted luminescence is measured by the light detection system.

3.2 The reader

3.2.1 Light detection system

The light detection system consists of a photomultiplier (PMT) tube and suitable detection filters. The detection filters define the spectral detection window. Examples of detection filters are the Hoya U-340 (7.5 mm thick), Schott BG 39 (2 mm thick) and Corning 7-59 (4 mm thick). The photomultiplier detects the luminescence signal. The PMT in the Risø TL/OSL reader is an EMI 9235 PMT. This has maximum detection efficiency between 200-400 nm.

3.2.2 Irradiation Source

Samples can be irradiated using beta ^{90}Sr/ ^{90}Y beta source which produces beta particles with a maximum energy of 2.27 MeV. The dose rate is approximately 0.1 Gy/s.

3.2.3 Luminescence stimulation system

The Risø TL/OSL reader consists of two luminescence stimulation systems, that is a heating system and a light stimulation system. The TL measurements are made using the heating system and OSL measurements are made using the light stimulation system.

(a) Heating system

The heating element and lift mechanism are located underneath the photomultiplier tube. The heating system has two functions. It heats the sample and lifts the sample into the measurement position. Heating is done by a controlled current through the heating element. The heating system is able to heat samples up to 700 ^{0}C at constant heating rates (β) from 0.01 to 20

^{0}C.s^{-1}. The heating strip can be cooled by nitrogen flow which also protects the heating element from oxidation at high temperatures.

(b) Optical stimulation system

All OSL measurements are performed under control of an optical stimulation system. The optical stimulation system is equipped with blue light emitting diodes. The blue LEDs are NICHIA type NSPB-500AS with a peak wavelength of 470 nm (FWHM=20 nm). The blue LEDs are arranged in 4 clusters each containing seven individual LEDs. The total power from 28 LEDs is 100 mW/cm^2.

3.3 Sample preparation

Measurements were made on an annealed synthetic quartz sample obtained from Sawyer Research Products (Ohio, USA). The sample was annealed at 1000 ^{0}C for 10 minutes to improve its sensitivity and remove residual charge from electron trap. The sample in powder form. The sample was in granular form of grain size 90-500 μm was placed on stainless steel discs of diameter 10 mm and thickness 0.3 mm. The sample was then irradiated different doses using a ^{90}Sr/ ^{90}Y beta source at a dose rate of 0.1028 Gy/s. All of the measurements were carried out in nitrogen atmosphere. This ensured that there was good thermal contact between the sample and the heating element. The results shown are in averages of several measurements as explained throughout the thesis.

Chapter 4

Results and discussions

The sample of synthetic quartz was irradiated with beta radiation of 10 Gy then was heated up to 500 ^{0}C. The kinetic analysis show main peak at 74 ^{0}C for a heating rate of 1 ^{0}C.s^{-1} and dose 10 Gy. Several methods were used to evaluate kinetic parameters. These are the initial rise, peak shape, variable heating rate, whole glow curve, glow curve deconvolution and isothermal methods. The analysis was done on the main peak (74 ^{0}C). The kinetic parameters found are the trap depth E, frequency factor s and order of kinetics b. Only the main peak was studied because the intensity for two other peaks was too low to used compared with the main peak. Thermal quenching and fading was observed during experimental studies.

4.1 Characteristics of thermoluminescence glow curves

A sample annealed at 1000 ^{0}C for 10 minutes was used. The sample was heated at 1 ^{0}C.s^{-1} after irradiation to 10 Gy.

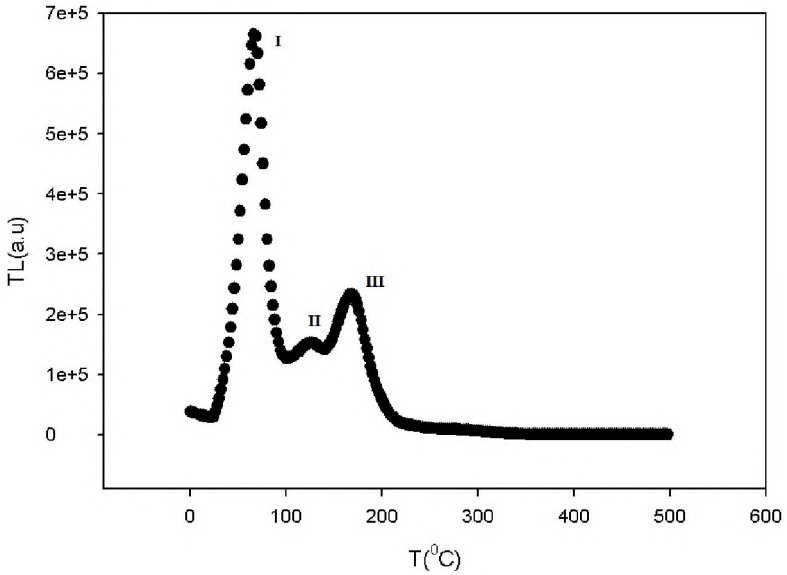

Figure 4.1: TL intensity against temperature for annealed synthetic quartz.

The glow curve is shown in figure 4.1 Three glow peaks were observed in the TL glow curve which represent electron trap in the sample. The main peak I occurs at 74 ^{0}C . There is another peak II at 144 ^{0}C with lower intensity and a weak peak III at 168 ^{0}C as shown in figure 4.1.

Figure 4.2 shows the same graph on a logarithmic scale. This scaling assists to show some TL glow peaks which are not easy to see on the linear scale. A fourth peak (labelled IV) can be seen.

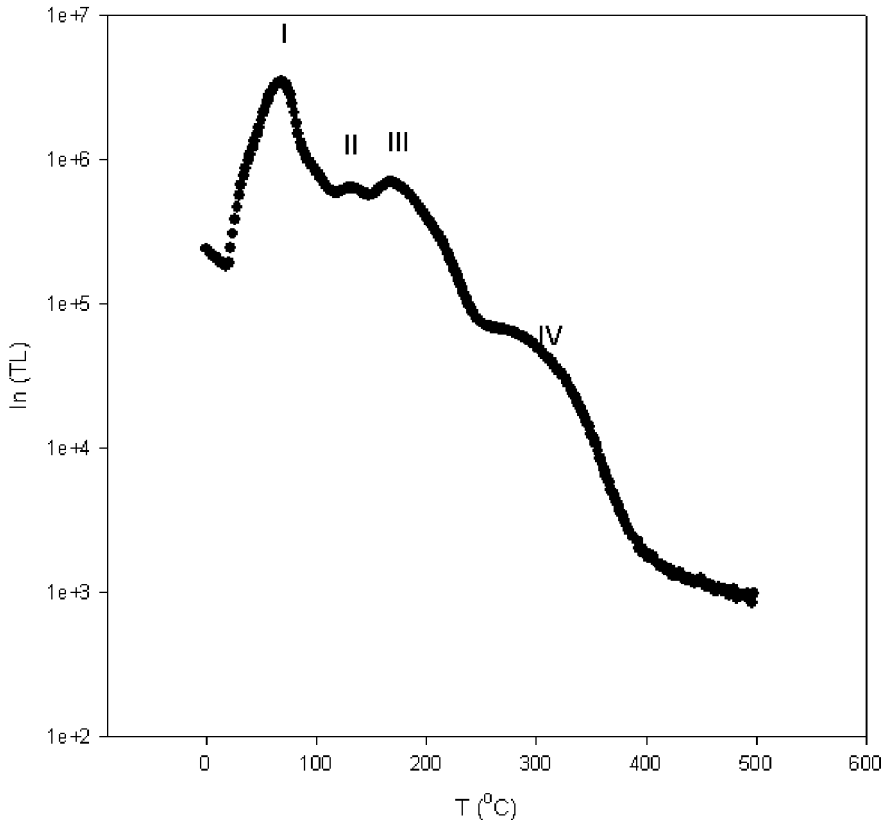

Figure 4.2: ln(TL) against temperature for synthetic quartz.

The log(TL) against temperature is shown in figure 4.2. Four peaks were found in linear scale. The main peak I at 74 ^{0}C, peak II at 144 ^{0}C, peak III at 168 ^{0}C and peak IV at 286 ^{0}C.

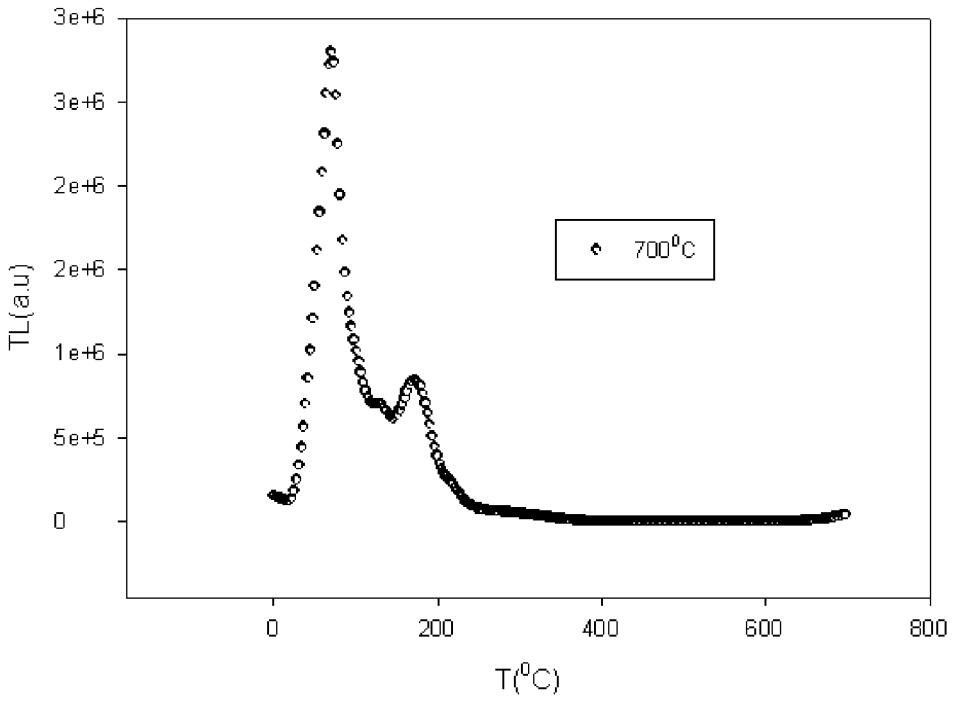

Figure 4.3: TL glow curve heated up to 700 ^{0}C.

Figure 4.3 shows the glow curve of a sample irradiated with 100 Gy and then heated up to 700 ^{0}C at 1 ^{0}C.s^{-1}. The glow curve shows peak I at 70 ^{0}C, peak II at 138 ^{0}C and peak III at 176 ^{0}C. The aim was to observe if there are any electron traps at high temperatures beyond 500 ^{0}C. As illustrated in figure 4.3, there were no peaks found beyond 500 ^{0}C.

4.2 Kinetic analysis

The analysis of finding the parameters (E, μ and s) was focusing on five kinetic analysis methods, Initial rise, peak shape, variable heating rate, whole glow peak and isothermal methods. Two techniques, T_m-T_{stop} and thermal quenching were also employed.

4.3 Initial rise method on the main 74 ^{0}C

The TL glow curve was observed to have three glow peaks after the irradiation to 10 Gy and heating rate of 1 ^{0}C.s^{-1} as shown in figure 4.1. Evaluation of kinetic parameters using initial rise method was done by plotting $ln(TL)$

against $1/kT$ as shown in figure 4.4. The data points in the graph correspond to $10-15\%$ of maximum intensity. These points were taken on rising side of main peak at 74 ^{0}C. The slope of the graph gave the value of the trap depth E to be 0.86 $\pm$ 0.00 eV. The frequency factor was evaluated for first order kinetics and was s=3.45 $\times$ 10^{11} s^{-1}.

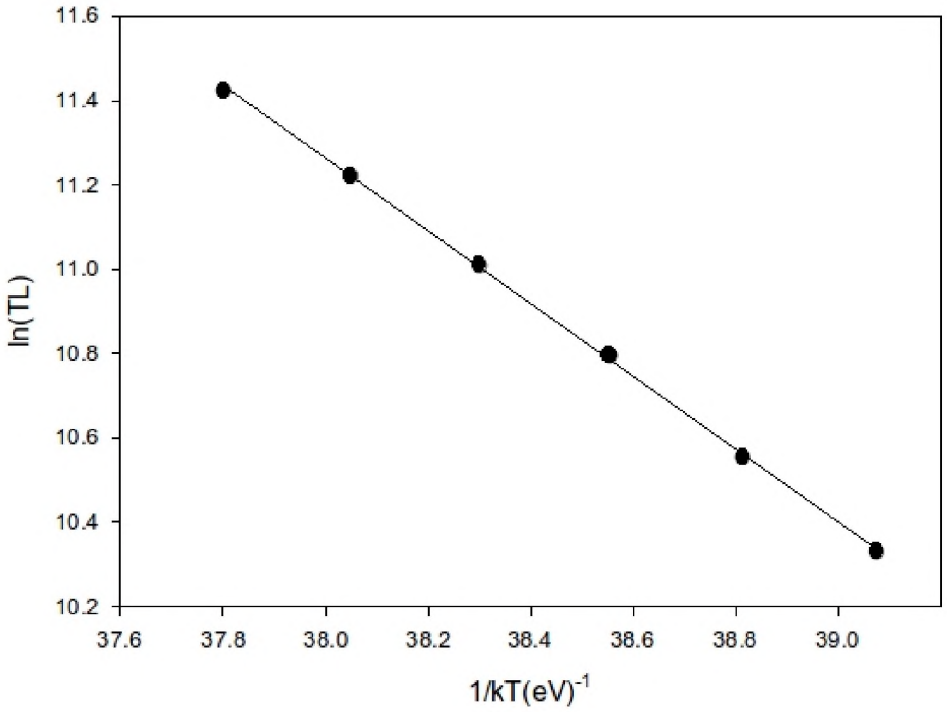

Figure 4.4: Application of the initial rise method for peak (I).

Changing the heating rate from 0.5 to 4 ^{0}C.s^{-1} did not affect the value of E as shown in figure 4.5.

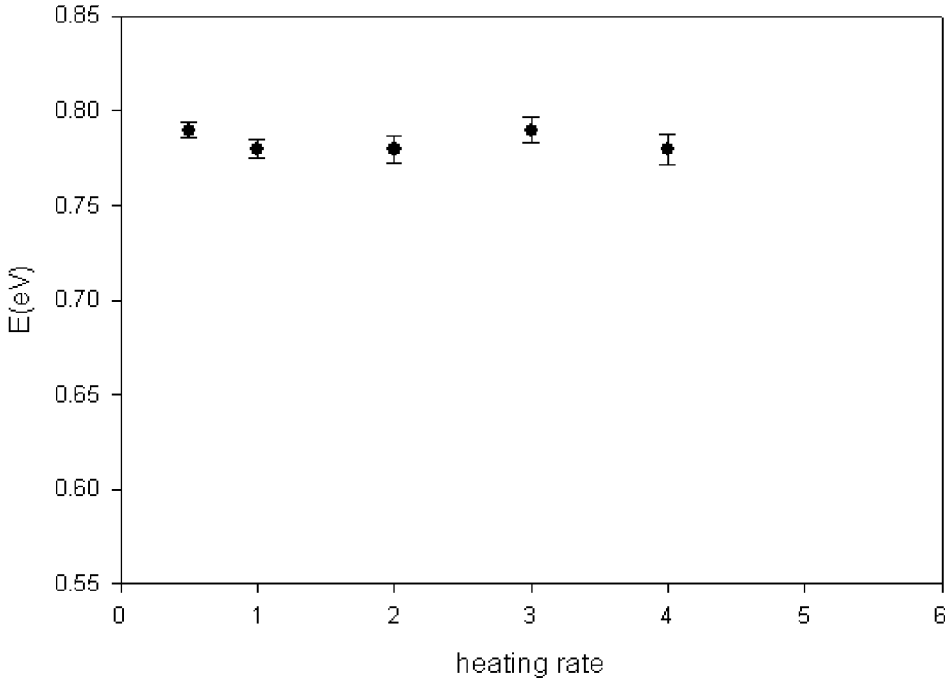

Figure 4.5: The trap depth E against heating rates (from 0.5 to 4 ^{0} C.s^{-1}). The value of E was calculated using the initial rise method.

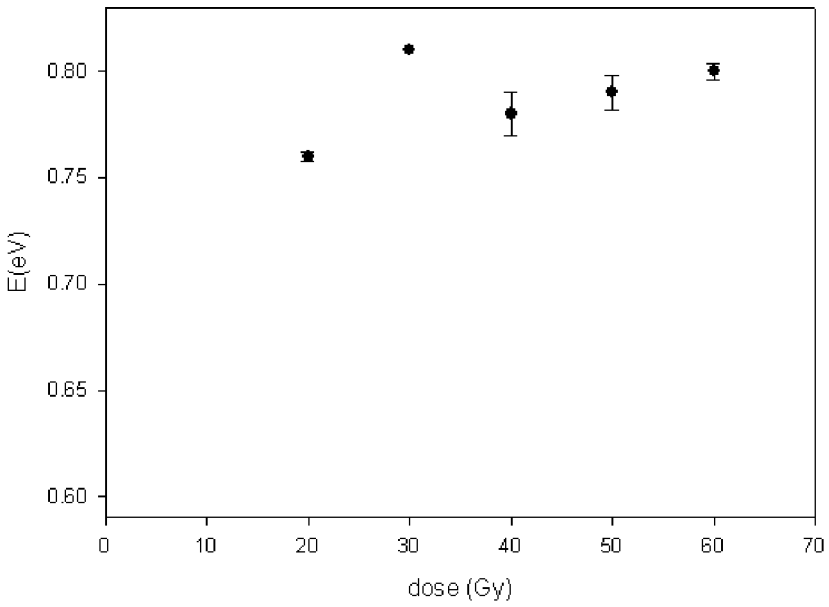

Figure 4.6: Trap depth E against doses from 20 to 60 Gy.

The analysis for E against dose was performed for doses from 20 to 60 Gy. The relationship was illustrated in figure 4.6.

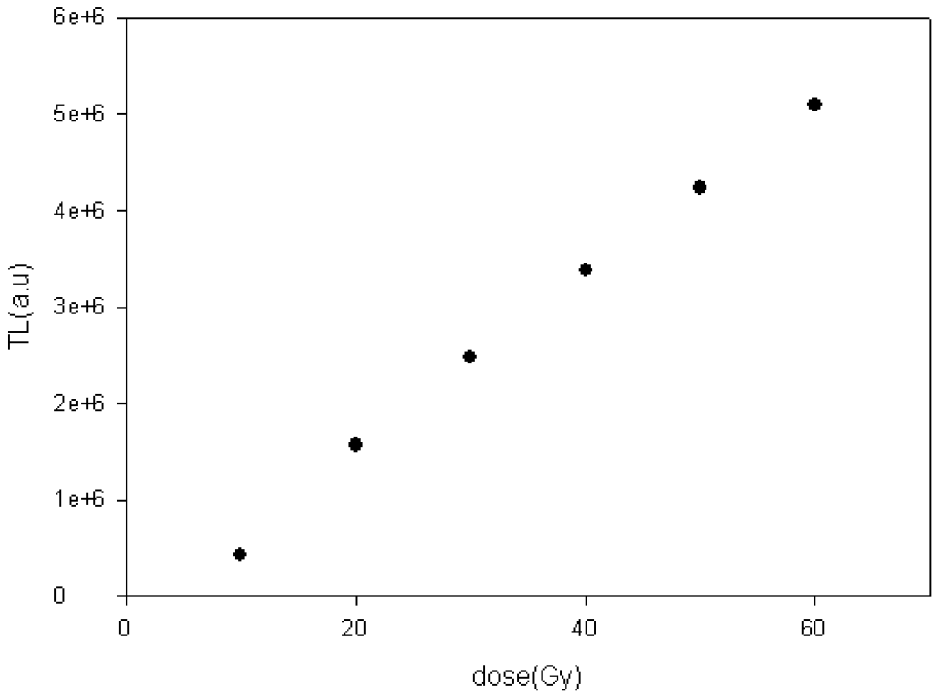

Figure 4.7: The TL maximum intensity against dose. The TL was measured at 1 ^{0}C.s^{-1}

Table 4.1: The values of heating rates, peak temperatures, trap depths and average trap depth evaluated using the initial rise method.

heating rates (^{0}C.s^{-1})	T$_m$ (^{0}C)	E (eV)
0.5	64	0.79 ± 0.03
1	72	0.78 ± 0.03
2	80	0.78 ± 0.03
3	84	0.79 ± 0.03
4	86	0.76 ± 0.03

There is not much difference between the values of the trap depth as the dose increases. The trap depth is independent of the dose from 10 to 60 Gy. The average value of trap depth using initial rise method was 0.75 ± 0.02 eV.

Figure 4.7 shows the relationship between TL against dose for low doses from 10 to 60 Gy. The intensity increases as dose increases and the increase showed a linear trend.

4.3.1 Application of the T_m-T_{stop} technique on the main peak at 74 ^{0}C

TL glow peaks sometimes contain overlapping peaks. In order to find the number of overlapping peaks and their positions, the T_m-T_{stop} technique was employed. Here the sample was irradiated with a dose of 10 Gy, then heated at a linear heating rate of 1 ^{0}C.s^{-1} up to 500 ^{0}C. The peak temperature was observed at 74 ^{0}C for main peak. Applying the method, temperatures from 54 to 64 ^{0}C were chosen with a step of $\triangle T$= 2 ^{0}C. In the first step, the sample was heated up to 54 ^{0}C then cooled to room temperature. The peak temperature was noted at 80 ^{0}C. The sample was heated up to 500 ^{0}C then cooled down to room temperature, then heated again. The peak temperature was noted again. The procedure was repeated up to 64 ^{0}C on same sample. The graph of peak temperature (T_m) against T_{stop} is shown in figure 4.8b.

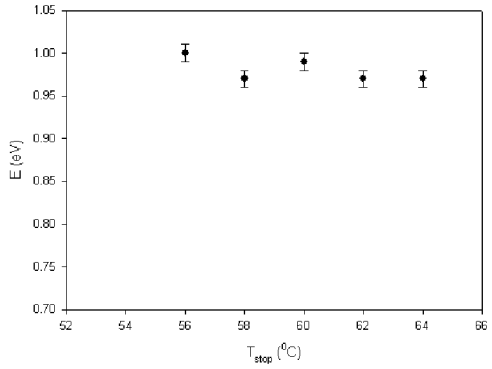

(a) Trap depth (E) plotted against T_{stop}.

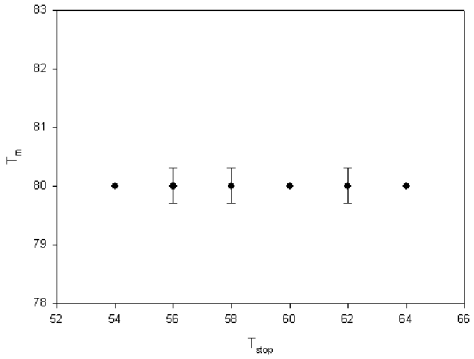

(b) T_m (in ^{0}C) against T_{stop}(in ^{0}C).

Figure 4.8: Two figures (a and b) showing E and T_M plotted against T_{stop}

The peak temperature was was not affected by increasing the preheating temperature from 54 to 64 ^{0}C, T_{stop}. The behaviour explains that there is only a single peak subject to first order kinetics. The peak is found at 80 ^{0}C.

Similarly for the E-T_{stop} technique, the evaluation of trap depth E was computed using the initial rise method. The average value of the trap depth was found to be 0.94$\pm$0.001 eV. The plot of E against T_{stp} is shown in figure 4.8a. The trap depth was observed to be independent of T_{stop} which show an evidence of peak corresponding with first order kinetics. Each values of trap depth correspond with each peak temperatures as shown in both figure 4.8b and 4.8a. The techniques both agree and show the first order kinetics.

4.4 Application of the peak shape method on the main peak at 74 ^{0}C

Figure 4.9 shows a glow curve corresponding to 10 Gy of irradiation and heating at 1 ^{0}C.s^{-1}. The figure 4.9 was scaled down up to 110 ^{0}C to obtain a single clean peak. The main peak was at 74 ^{0}C.

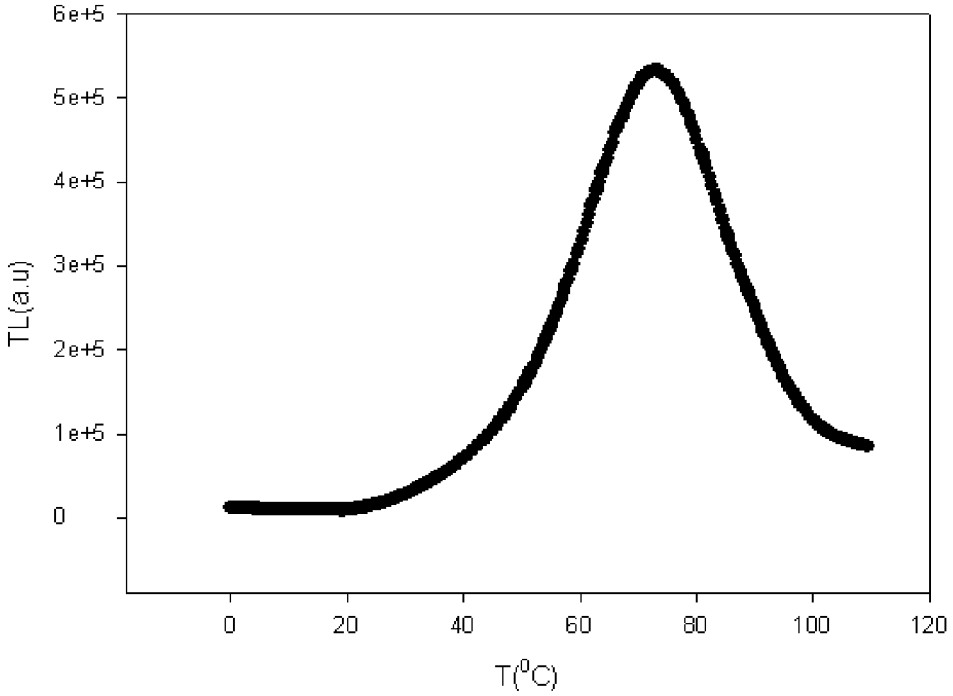

Figure 4.9: TL glow curve (of main peak) scaled up to 110 ^{0}C.

Kinetic parameters were evaluated using the peak shape method. T_1, T_2 and T_m were found to be 57 ^{0}C, 88 ^{0}C and 74 ^{0}C. The geometric parameters τ, δ, ω, and μ were calculated using equations (2.31), (2.32), (2.33) and (2.34) by Chen [9] . Also the geometric details are shown in figure 2.2.

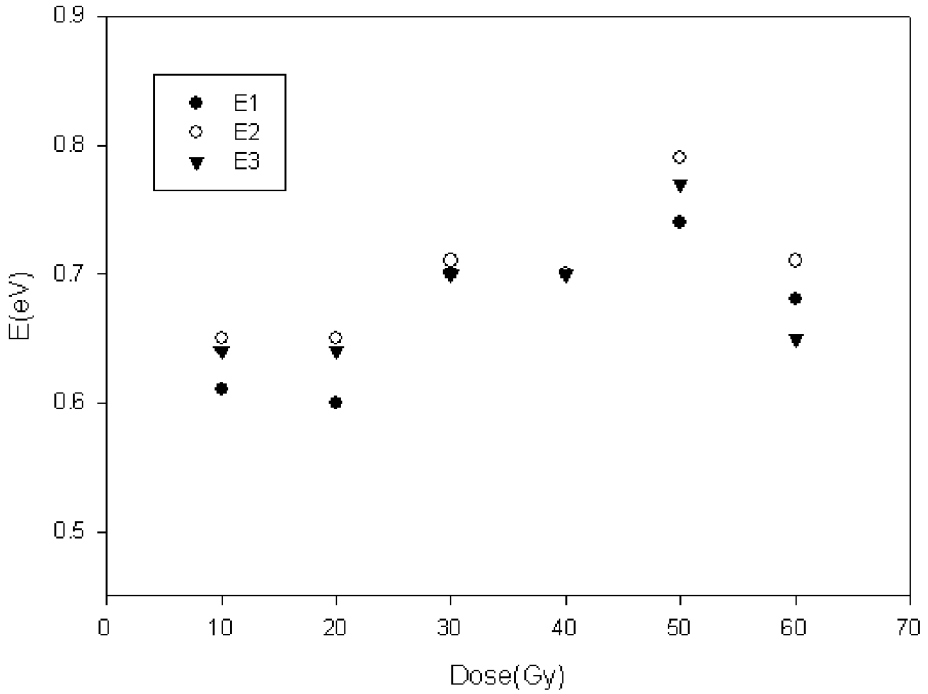

Figure 4.10: $E_\tau(E1)$, $E_\delta(E2)$ and $E_\omega(E3)$ against dose.

E_τ, E_δ and $E\omega$ found from the peak shape method are as shown in figure 4.10. By using equation (2.34), the values of trap depth were found to be 0.86 ± 0.02, 0.94 ± 0.02 and 0.87 ± 0.01 eV. The frequency factor was of the order of 2.34×10^{11}, 1.55×10^{12} and 6.78×10^{11} s^{-1}. The symmetry factor was found to be 0.45 ± 0.03 which is consistent with first order kinetics. The average value of trap depth was 0.89 ± 0.02 eV.

Table 4.2: Values of heating rate, symmetric factor and trap depths E_τ, E_δ and E_ω and average trap depths.

heating rates(^{0}C.s^{-1})	μ	E_τ (eV)	$E\delta$ (eV)	E_ω (eV)
0.5	0.39 ± 0.05	0.64± 0.01	0.61± 0.02	0.63± 0.02
1	0.43± 0.02	0.8± 0.02	0.81± 0.02	0.82± 0.02
2	0.40± 0.02	0.79± 0.03	0.74± 0.02	0.77± 0.02
3	0.46± 0.03	0.98± 0.02	0.91± 0.05	0.98± 0.03
4	0.41± 0.04	0.76± 0.01	0.76± 0.02	0.77± 0.02
5	0.44± 0.04	1.01± 0.02	0.82± 0.03	0.82± 0.04
Average	0.45±0.02	0.83± 0.02	0.80± 0.01	0.80± 0.03

The calculations were also done for different doses from 10 to 60 Gy. Figure 4.10 shows the effect of dose on trap depths. The average value of the trap depth and symmetric factor were found to be 0.70 ± 0.01 eV and 0.45 ± 0.02. As dose increases there is not much difference between the values of trap depths.

Table 4.3: The values of dose symmetric factor and trap depths E_τ, E_δ and E_ω and average trap depths computed using the peak shape method.

Dose (Gy)	μ	$E_\tau(eV)$	$E_\delta(eV)$	$E_\omega(eV)$
10	0.40± 0.03	0.61± 0.03	0.65± 0.03	0.64± 0.04
20	0.48± 0.03	0.60± 0.02	0.65± 0.02	0.64± 0.03
30	0.43± 0.03	0.70± 0.03	0.71± 0.02	0.70± 0.02
40	0.41± 0.02	0.70± 0.04	0.70± 0.05	0.70± 0.03
50	0.46± 0.02	0.74± 0.02	0.79± 0.02	0.77± 0.03
60	0.50± 0.03	0.68± 0.01	0.71± 0.02	0.65± 0.02
Average	0.45± 0.02	0.70± 0.04	0.70± 0.03	0.68± 0.02

4.5 Application of the variable heating rate method on the main peak at 74 ^{0}C

Many measurements were taken at different heating rates from 0.5 to 5 ^{0}C.s^{-1} corresponding to a constant dose of 10 Gy. With increase of heat rates, the peak temperatures are shifted to higher temperatures according to the literature by Furreta [16]. Figure 4.1 shows the glow curve of a sample irradiated with dose of 10 Gy and heated at 1 ^{0}C.s^{-1} up to 500 ^{0}C. The variable heating rate (VHR) method uses different heating rates. To evaluate kinetic parameters using VHR method two peak temperatures and two heating rates were used. The trap depth was evaluated using equation (2.38). The value was found to be 0.84 ± 0.05 eV. Since several experiments were taken the parameters, T_m and β were recorded and the choice of these two parameters T_m and β was arbitrary. That is from the data we randomly choose two in each parameters (T_m and β). So from this procedure the results sometimes may not be more accurate but giving a reasonable results as compare with other methods.

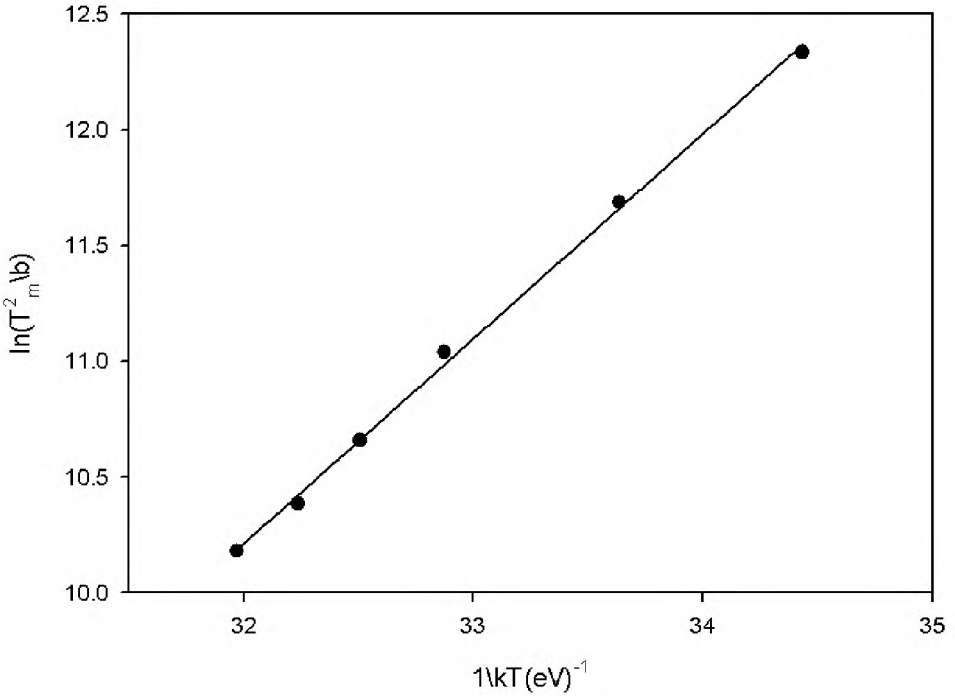

Figure 4.11: The graph of $ln\left(\frac{T_m^2}{\beta}\right)$ against $1/kT$ to evaluate trap depth E .

Another VHR method by Hoogenstraaten [10] was used to evaluate trap depth and frequency factor using equation (2.40). The value of E found from the slope of $ln\left(\frac{T_m^2}{\beta}\right)$ against $1/kT$ was 0.89 ± 0.01 eV. The frequency factor determined from the intercept was $3.5{\times}10^{11}$ s^{-1}.

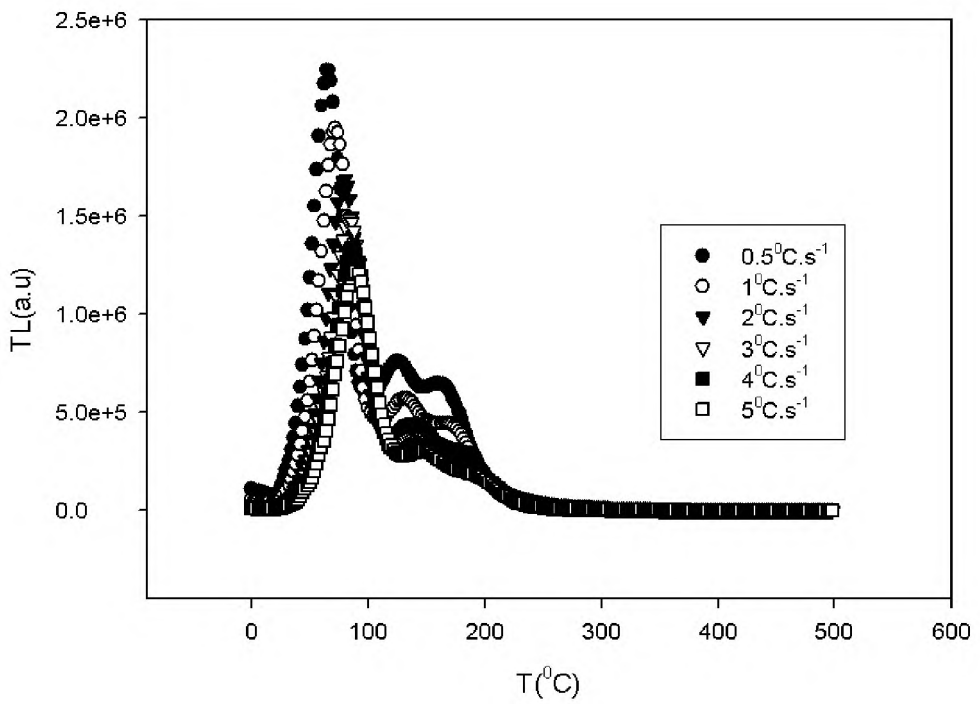

Figure 4.12: The effect of heating rate on glow peaks .

Figure 4.12 shows TL glow curves measured at different heating rates. The peak intensity decreases as the heat rate increases. This is also shown in figure 4.13a. The cause of this behaviour is thermal quenching effect whose efficient increases as the temperature increases. The glow curve glow peak shifts to higher temperatures values as result of the increases of the heating rate.

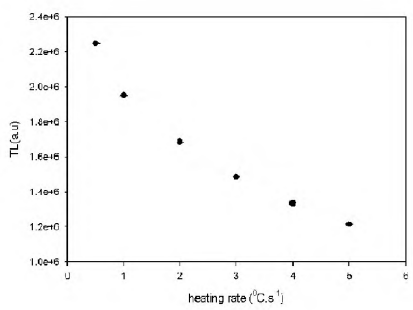

(a) TL peak intensity against heating rate.

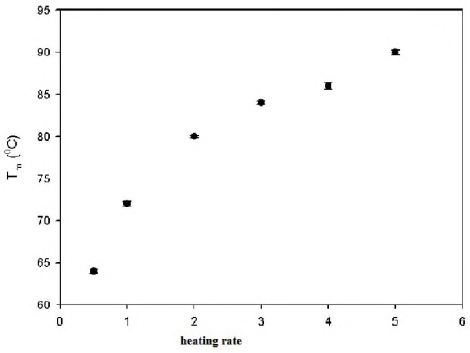

(b) T_M against heating rate.

Figure 4.13: Two figures (a and b) showing TL peak intensity and T_M plotted against heating rate.

As the heating rate increase, the peak intensity decreases as shown in figure 4.13a. In figure 4.13b shows as peak temperature increases, the heating rate increases.

4.5.1 Thermal quenching on TL glow curve

During kinetic analysis of TL glow curve it was observed that there are external factors affecting the TL glow curve analysis. Thermal quenching was found to have the effect on the higher heating rates as was shown figure 4.13a. By using various heating rates from 0.5 to 5 ^{0}C.s^{-1} the TL glow peak was observed to shift to higher temperatures. Thermal quenching affect experimental data in TL measurements. When taking a series of TL measurements with different heating rates the thermal quenching effect is observed. The fact that as heating rate increases TL intensity decrease. This kind of behaviour is mostly observed at higher temperatures where the luminescence is quenched. More intensely so that the whole area under the TL peak decreases.

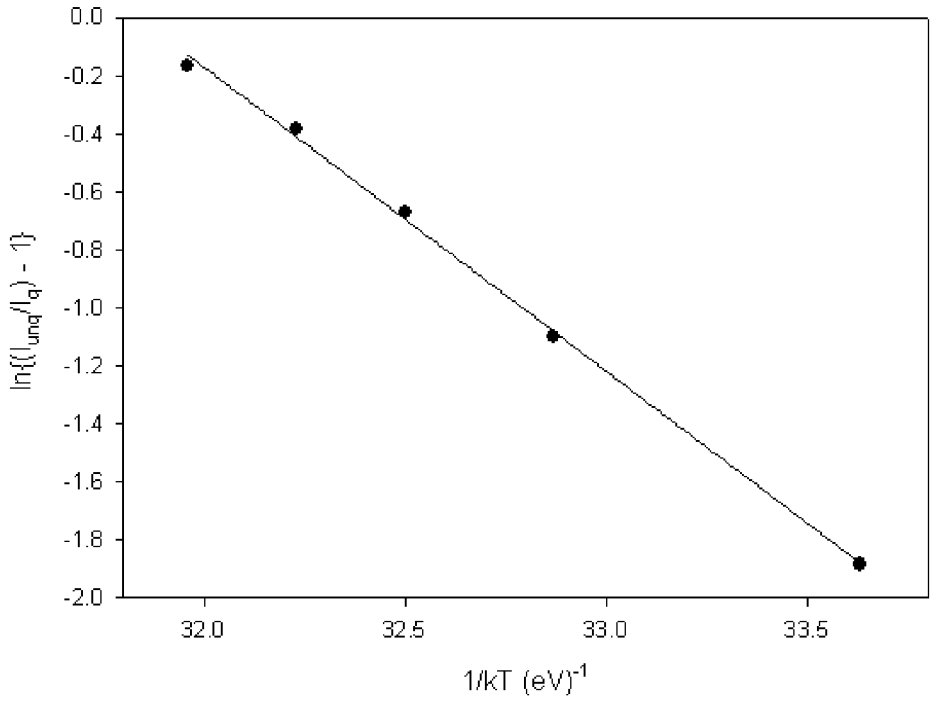

Figure 4.14: The plot of $\ln((I_{UNQ}/I_Q) - 1)$ against $1/kT_m$ for evaluation of thermal quenching parameters W and C.

Thermal quenching effect is when luminescence efficiency decrease with increase in temperature, since is a factor dependent on temperature. Thermal quenching is a problem on evaluation of trap depth by McKeever [3]. Quenching may be caused of competition between radiation and non radiation transitions during heating of the sample. Therefore it must be corrected.

The equation for thermal quenching is given as,

$$I_Q(T) = I_{UNQ}(T)\eta(T) \tag{4.1}$$

where

$$\eta(T) = \frac{1}{1 + C\exp(-W/kT)}. \tag{4.2}$$

$I_Q(T)$ is the quenched TL intensity, I_{UNQ} is the unquenched TL intensity usually noted at the lowest heating rate where the thermal quenching is small, $\eta(T)$ quenching factor function, W the activation energy of thermal quenching and C is a constant.

Rearranging the two equations (4.1) and (4.2) we get,

$$ln((I_{UNQ}/I_Q) - 1) = \frac{1}{kT_m}W + lnC \tag{4.3}$$

The plot of $\ln(I_{UNQ}/I_Q) - 1$ against $1/kT_m$ is shown in figure 4.14. This is a straight line with the value of thermal activation energy $W = 1.05 \pm 0.03$ eV. The parameter C was found to be 3.27×10^{14}.

At high heating rates the probability of thermal quenching on peak intensity is too high. At low heating rates, it is believed that the effect of thermal quenching on luminescence is small. So in this case the lowest heating rate was 0.5 ^{0}C.s^{-1}. At 0.5 ^{0}C.s^{-1} the TL peak intensity was chosen to be thermal unquenched.

4.6 Analysis of using glow curve peak method on the main peak at 74 ^{0}C

The whole glow peak method focusses on the area under the glow peak by integrating from the initial temperature (T_i) on the rising side to the final temperature (T_f) on the decreasing side of the peak. The sample was irradiated up to 10 Gy and heated at 1 ^{0}C.s^{-1} up to 500 ^{0}C. The chosen temperatures from the main peak were 52 ^{0}C and 106 ^{0}C. The TL peak shown in figure 4.15 is the main peak at 74 ^{0}C, although it appears to be in 80^{0}C.

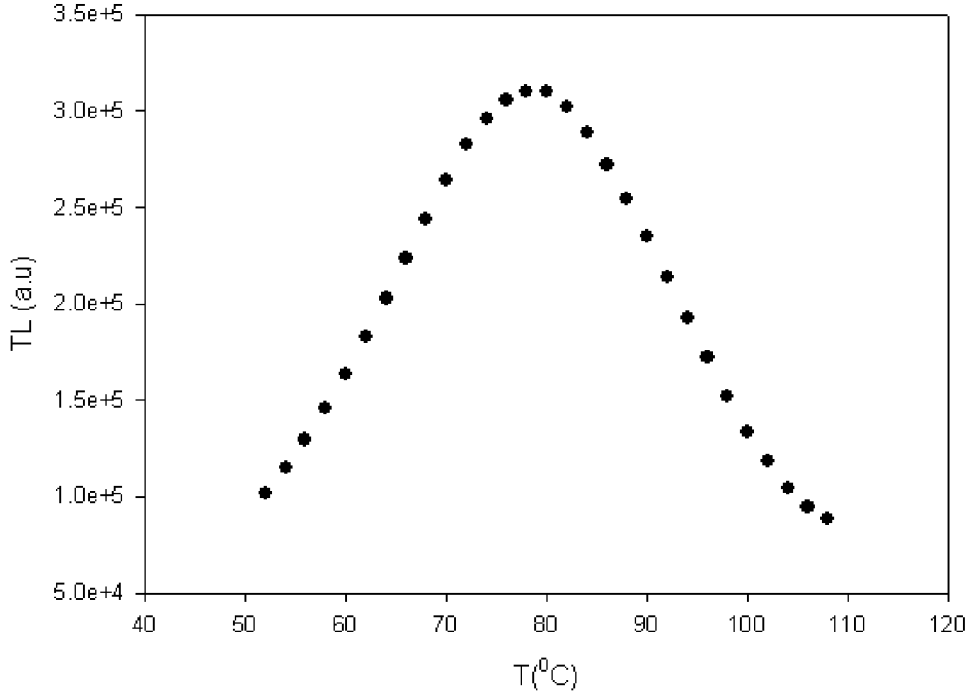

Figure 4.15: Single peak TL ($a.u$) versus temperature (^{0}C).

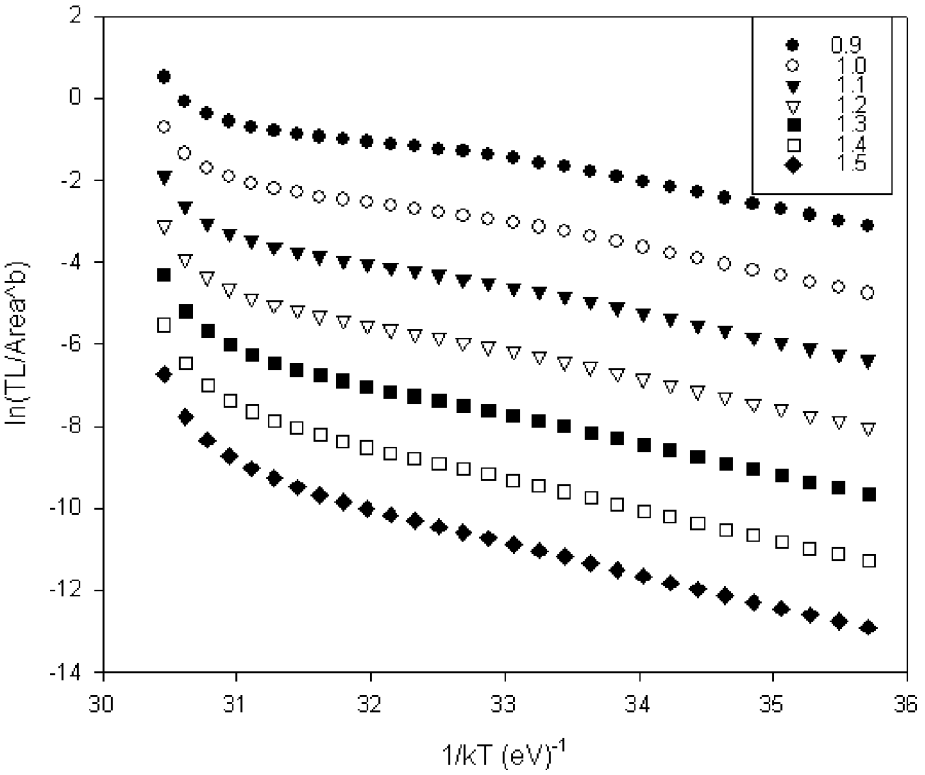

Figure 4.16: $ln(TL/area^b)$ versus $1/kT$ for different values of b.

Kinetic parameters were also evaluated using the whole glow curve method. Figure 4.15 shows a single TL glow peak with the portion of main peak from 52 ^{0}C to 106 ^{0}C. Figure 4.16 shows the plots of $\ln(area^b)$ against $1/kT$, for different values of b. All the graphs were fitted as a straight line.

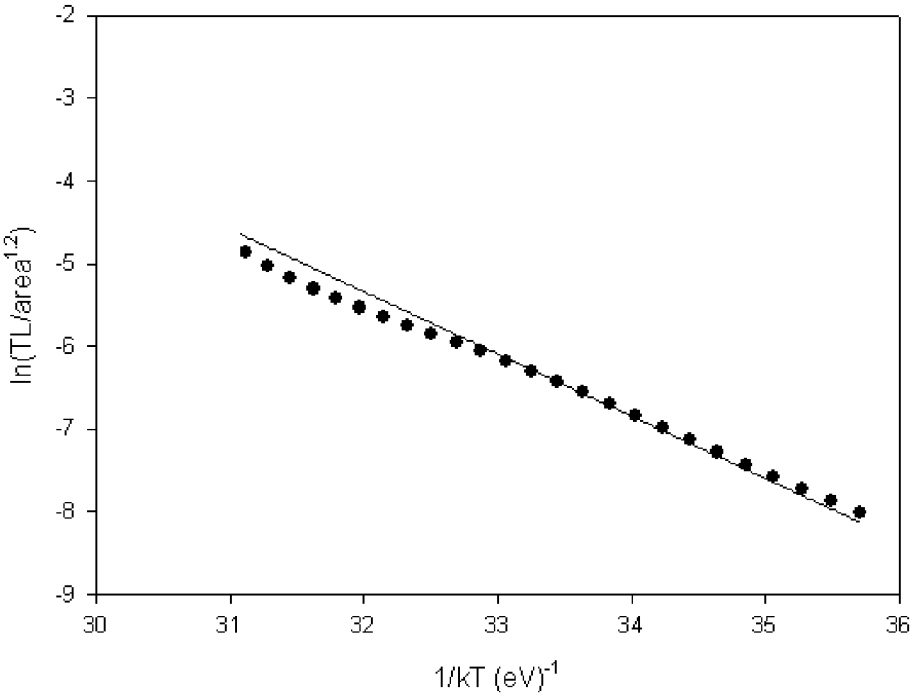

Figure 4.17: $ln(TL/area^{1.2})$ versus $1/kT$, for $b = 1.2$. The slope of the graph yields the value of $E = 0.80 \pm 0.06$.

The best fit was for $b = 1.2$ as shown in figure 4.17, all other values of b were not giving reasonable values. To evaluate kinetic parameters equation (2.44) was used and the value of trap depth was found to be 0.80 ± 0.06 eV. The frequency factor was 1.38×10^9 s^{-1}. Since $b = 1.2$, which is closer to 1, then the order of kinetics is concluded to be first order kinetics.

4.7 Curve fitting of the main peak (74 ^{0}C)

The experimental results were analysed on the basis of first order kinetics. The equation relies on two parameters, I_m (maximum TL intensity) and T_m (peak temperature in K corresponds with I_m). The kinetic parameter that was chosen to be adjustable was trap depth, E, by Kitis [11].

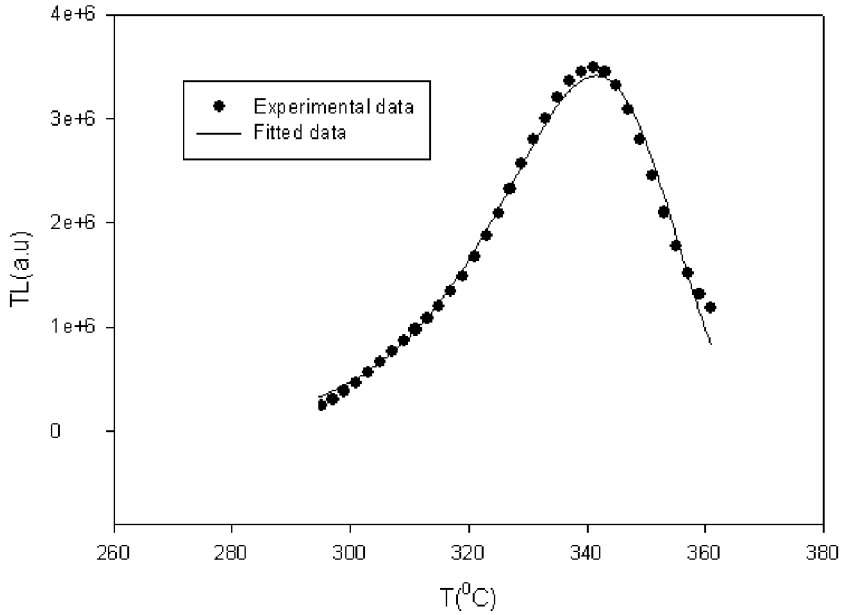

Figure 4.18: Curve fitting analysis to evaluate the trap depth E for peak I (at 74 ^{0}C). The circle represent experimental data and the line for fitting data the best fit.

The experimental data were fitted to equation (2.45) as shown in figure 4.18.The heating rate during data collection was 1 ^{0}C.s^{-1}. The TL glow peak was fitted using different values of trap depth. The accuracy of the fit was find to be R^2=0.74, which indicate that the possible reason may be the presence of overlapping peaks on the rising part of the TL glow curve. The values of E were chosen between 0.7 to 1.0 eV for first order kinetics.

The FOM for the value of the trap depth E = 1.0 was equal to 7.4 % and 3 % for the trap depth of E = 0.9 eV. The one with low FOM gives best fit. By comparing the two percentages, the value of E was found to be 0.9 $\pm$ 0.02 eV. For evaluation of the frequency factor for first order kinetics, was 1.8 $\times$ 10^{12} s^{-1}.

4.8 Analysis of phosphorescence associated with the main peak at 74 ^{0}C

Phosphorescence is the decay of thermally stimulated luminescence as a function of time at a specific constant temperature. Six different temperatures from 54 ^{0}C to 64 ^{0}C were chosen on the rising side of the TL glow

peak. At each of the temperatures, phosphorescence was recorded and the plots are shown in figure 4.19.

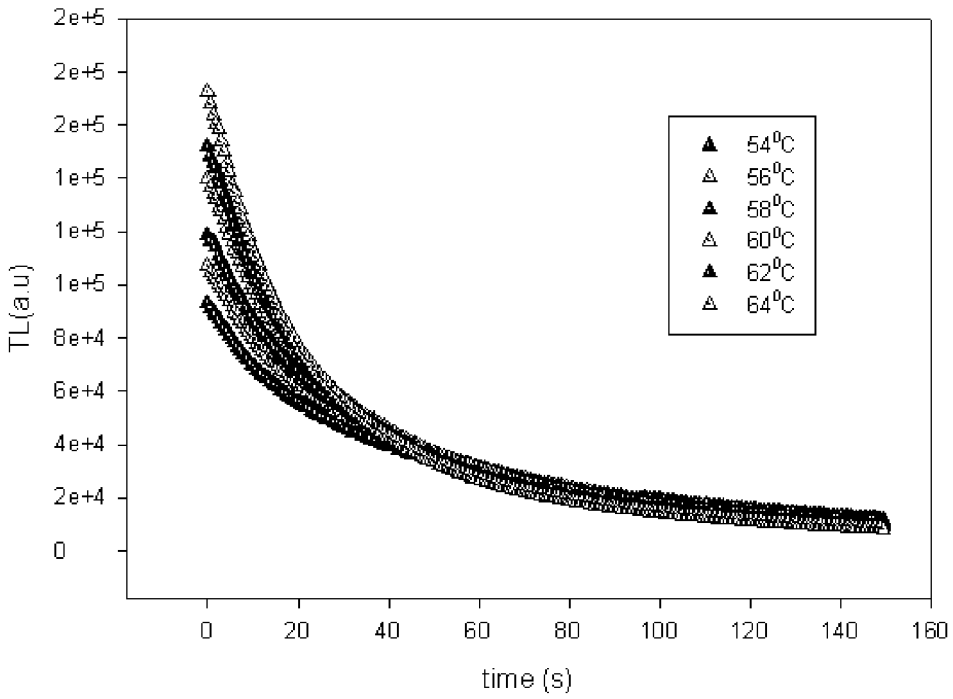

Figure 4.19: The TL intensity against time for six isothermal curves at six different constant temperatures from 54 ^{0}C to 64 ^{0}C.

Each isothermal curve from 54 ^{0}C to 64 ^{0}C was analysed using the exponential decay curve for first order kinetics as given in equation (2.50). $ln(TL)$ was plotted against time. In each graph a straight line was observed and the slope was found. The slope for the six measurements were plotted against $1/kT$ as shown in figure 4.20. In the plot, a straight line with slope of E= 0.73 $\pm$ 0.03 eV was obtained. The frequency factor s was found to be 9.6$\times$ 10^{15} s^{-1}.

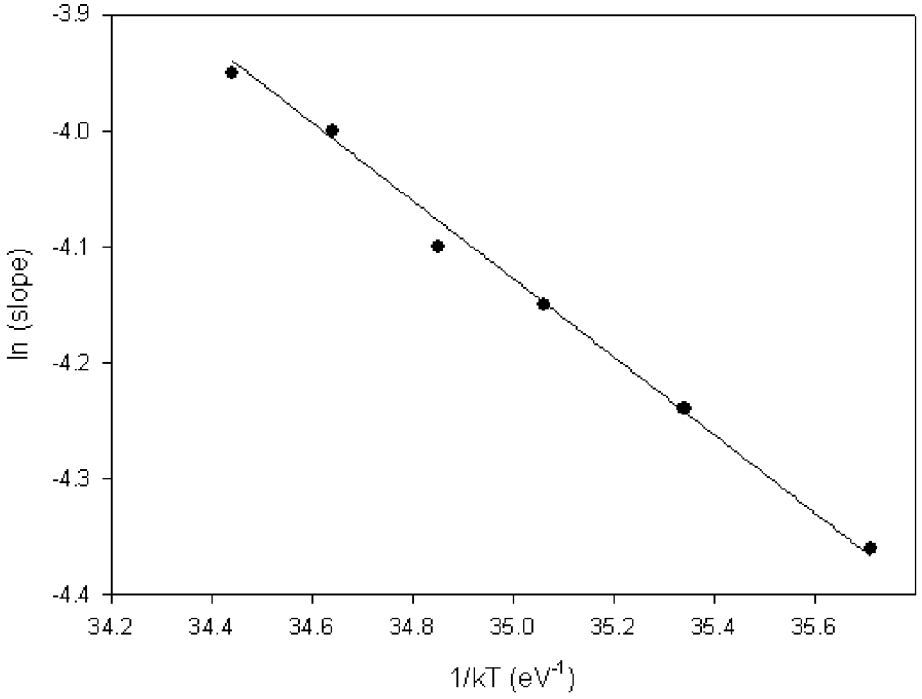

Figure 4.20: The plot of ln(slope) against 1/kT used to evaluate the kinetic parameter E.

4.8.1 Dose dependence of the isothermal decay curve at 54 ^{0}C

The sample was irradiated with beta radiation doses from 20 to 150 Gy at room temperature. The values of maximum TL intensity for each dose was noted. The TL peak intensity was plotted against beta radiation dose as shown in figure 4.21. The TL peak intensity was fitted by $Y(D)$ where $Y(D)$ denotes experimental TL peak intensities at the given beta radiation doses. The experimental data was fitted by the following equation,

$$Y(D) = Ae^{BD}. \tag{4.4}$$

where D is the given dose in (Gy) and $Y(D)$ is the function of dose. The superlinearity index $g(D)$ gives the change in the slope of the beta radiation dose response. The supralinearity index $f(D)$ is the amount of deviation from linearity by Pagonis [16]. The equations for the indices are:

$$g(D) = \left[\frac{DY''(D)}{Y'(D)}\right] + 1, \tag{4.5}$$

and

$$f(D) = \frac{\frac{Y(D)}{D}}{\left(\frac{Y(D_1)}{D_1}\right)}. \tag{4.6}$$

where $Y'(D)$ and $Y''(D)$ are first and second order derivative of $y(D)$, D is given beta radiation dose in Gy and D_1 is the normalized beta radiation dose corresponding with $Y(D_1)$.

Equations (4.5) and (4.6) are used to evaluate the functions $g(D)$ and $f(D)$ to determine for which doses TL response is linear, superlinear, supralinear or sublinear by Pagonis [16].

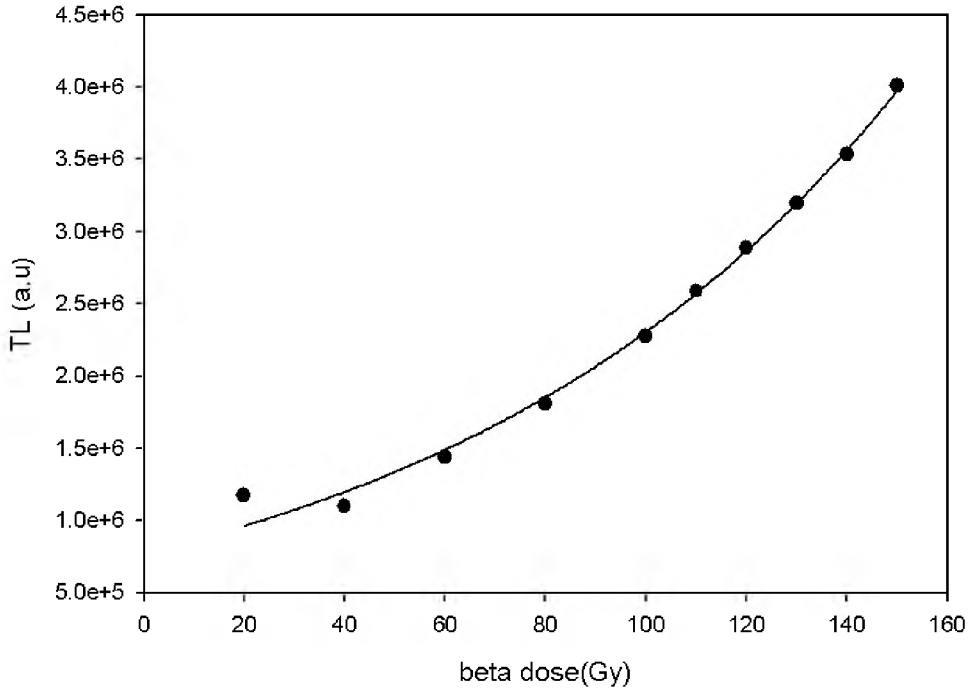

Figure 4.21: TL intensity against beta radiation dose from 20 to 150 Gy.

Figure 4.22 shows the index $g(D)$ against dose. The value of $g(D) > 1$. This behaviour means that dose response was superlinear.

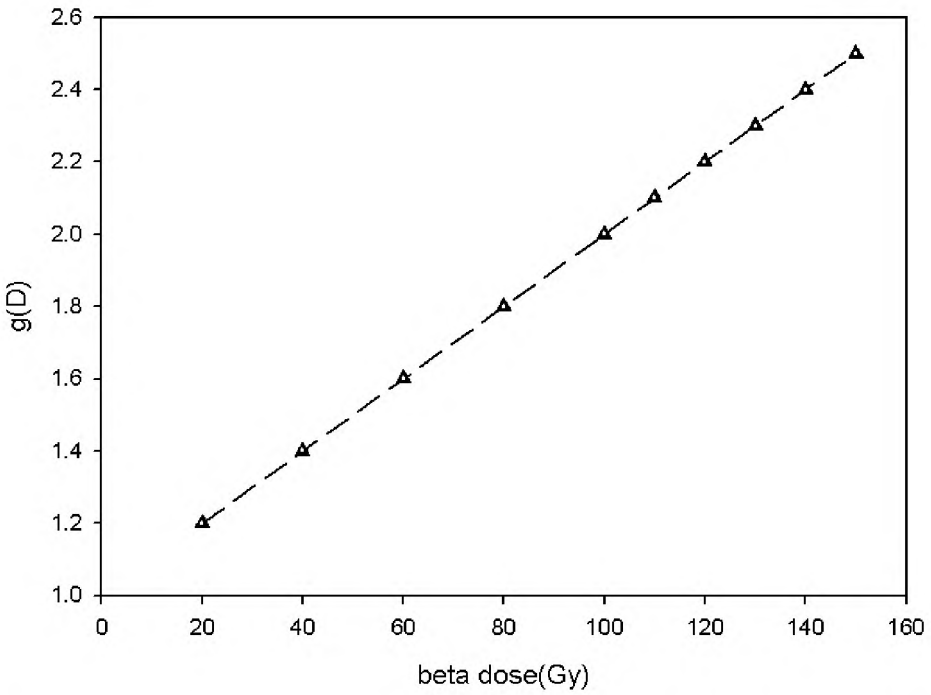

Figure 4.22: The superlinearity index g(D) against beta radiation dose.

Figure 4.23 shows the index $f(D)$ against dose. The values of $g(D) \geq 1$ from 20 to 40 Gy and 150 Gy. This behaviour means that dose response was superlinear. In the high dose from 80 to 140 Gy the value $f(D) < 1$ which illustrate that the dose response was supralinear. The increase of g(D) with dose, illustrate the change of the slope of beta dose in the sample.

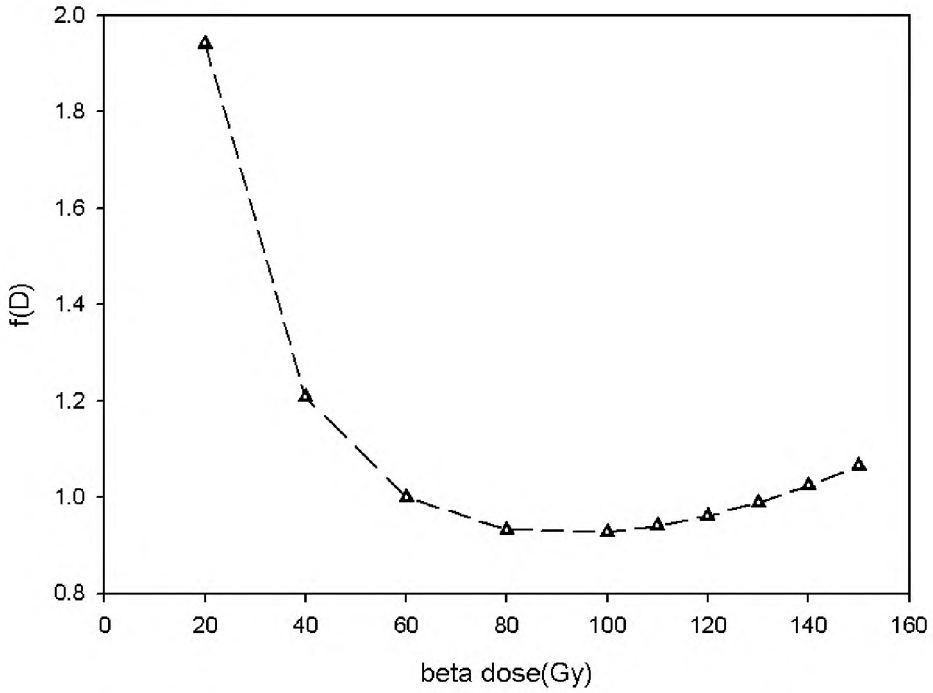

Figure 4.23: The supralinearity index f(D) against beta radiation dose.

Figure 4.24 shows that the peak temperature was independent of beta radiation dose from 20 to 150 Gy. This kind of behaviour is for first order kinetics.

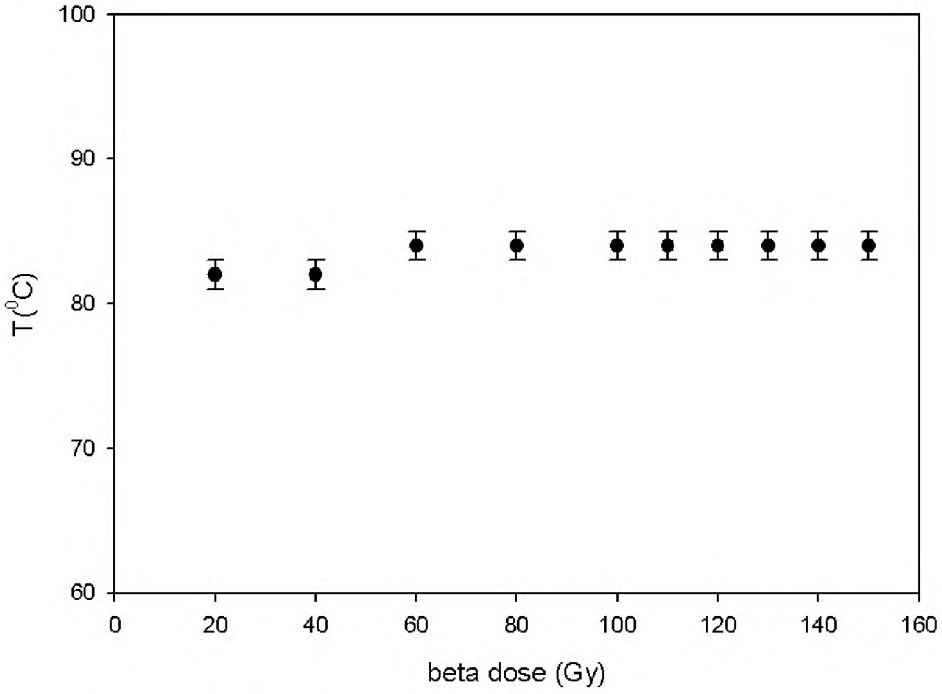

Figure 4.24: Peak temperature against beta radiation dose.

4.9 Kinetic analysis for peak III at 168 ^{0}C

The challenge in peak III was that not all methods were able to evaluate kinetic parameters. The cause of this is because of the procedures that each method uses. Only two methods were used, IRM and $VHRM$ to evaluate, E and s. When comparing the two peaks, I and III the was no huge difference for the data of each peak.

4.9.1 Kinetic analysis using initial rise method on TL glow peak III at 168 ^{0}C

Evaluation of kinetic parameters was also done using the initial rise method as shown in figure 4.25. The data points in the graph correspond with 10-15 % of the maximum intensity. These points were taken on rising side of main peak at 168 ^{0}C.

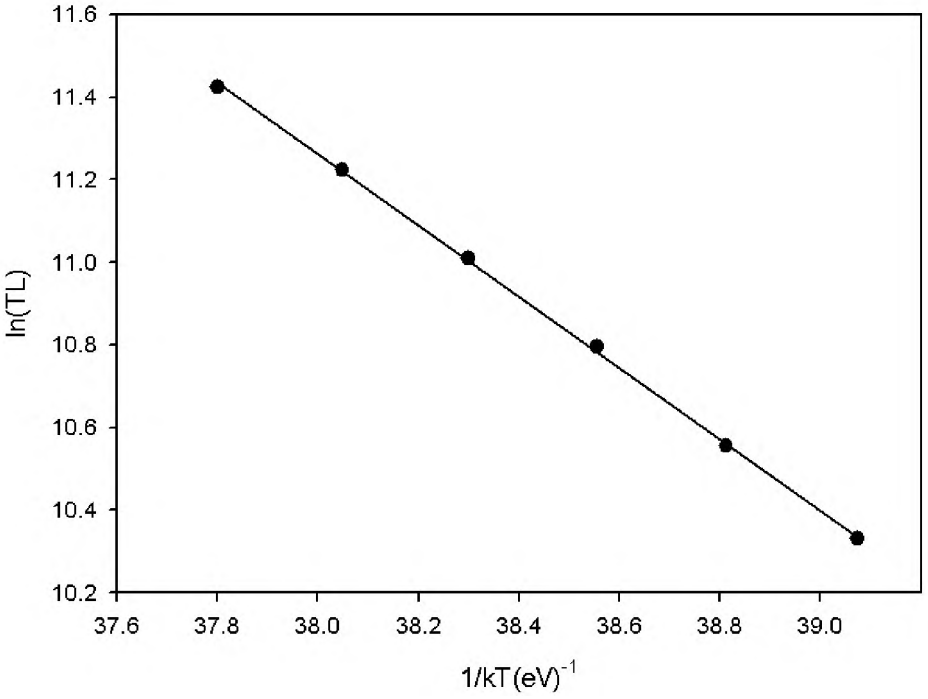

Figure 4.25: The graph of ln(TL) against 1/kT for peak III at 168 ^{0}C.

The slope of the graph gave the value of trap depth E as 0.85 $\pm$ 0.03 eV. The frequency factor was evaluated using equation (2.30) from the intercept was 2.3 $\times$ 10^8 s^{-1}.

4.9.2 Kinetic analysis of the peak at 168 ^0C using variable heating rate method

The variable heating rate (VHR) method uses different heating rates. Figure 4.26 shows the plot of $\ln(T_m^2/\beta)$ against $1/kT$. The slope of the graph yielded the value of E as 0.91 $\pm$ 0.01 eV. The intercept of the graph was used to find the frequency factor s and was found to be 3.1 $\times$ 10^9 s^{-1}.

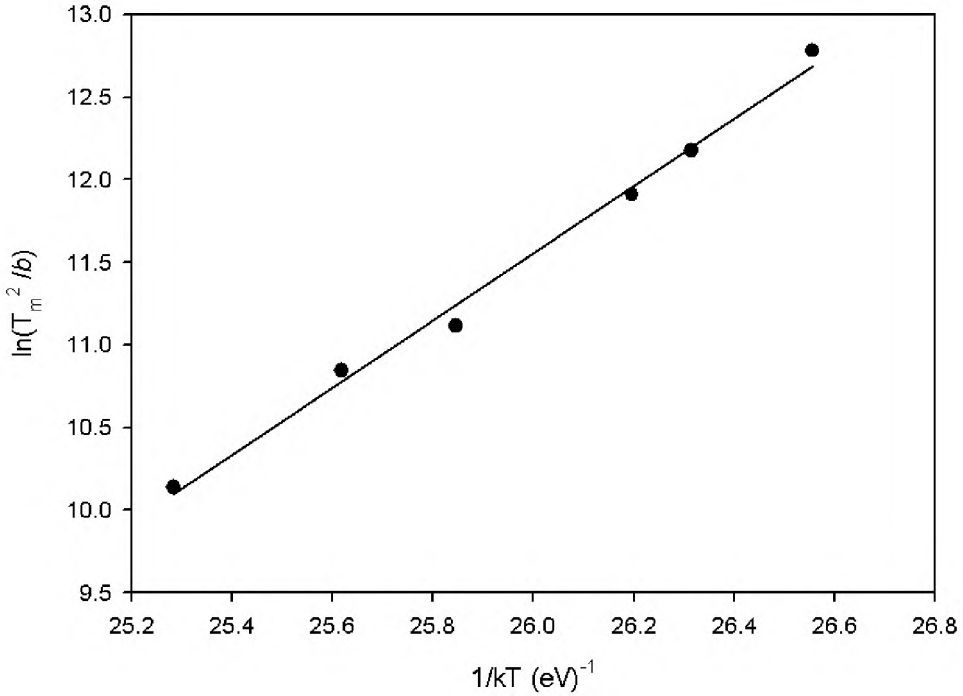

Figure 4.26: The graph of $\ln(T^2/\beta)$ against 1/kT of peak III at 168 ^{0}C.

Now the effect of heating rate on peak intensity was also observed. The sample was heated at various heating rates from 0.5 to 5 ^{0}C.s^{-1}. Figure 4.27 shows the relationship of TL peak intensity with heating rate. At low heating rate the TL peak intensity was high and at high heating rate the TL peak intensity was observed to be low. This behaviour may be caused by thermal quenching.

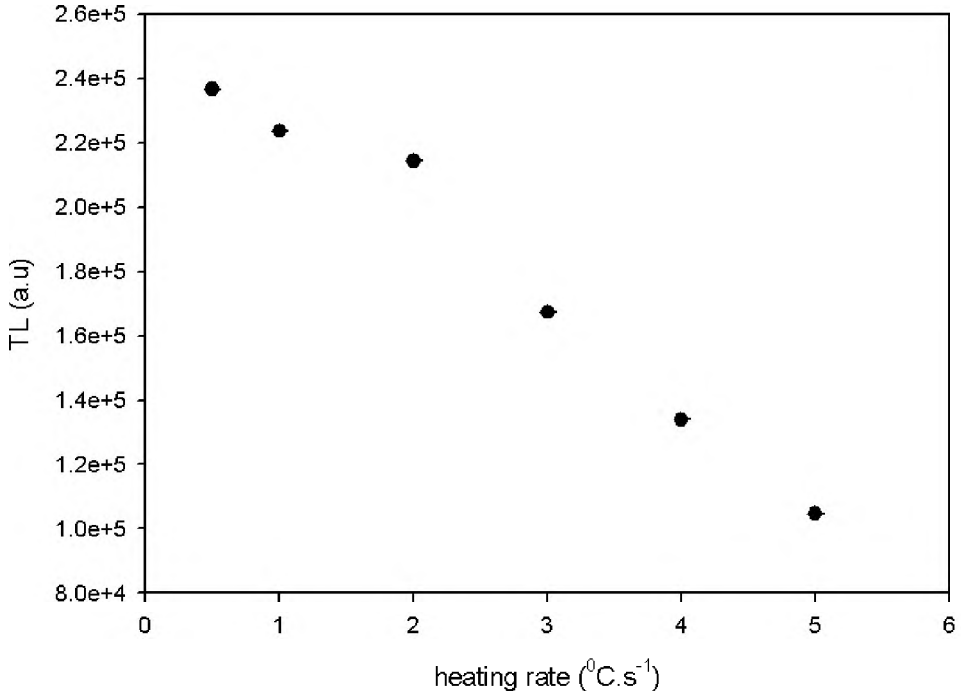

Figure 4.27: The TL intensity against heating rate from 0.5 to 5 ^{0}C.s^{-1} for peak III at 168 ^{0}C.

Figure 4.28 shows the peak position against heating rate. As the heating rate increases, the TL glow peak shifts to higher temperatures.

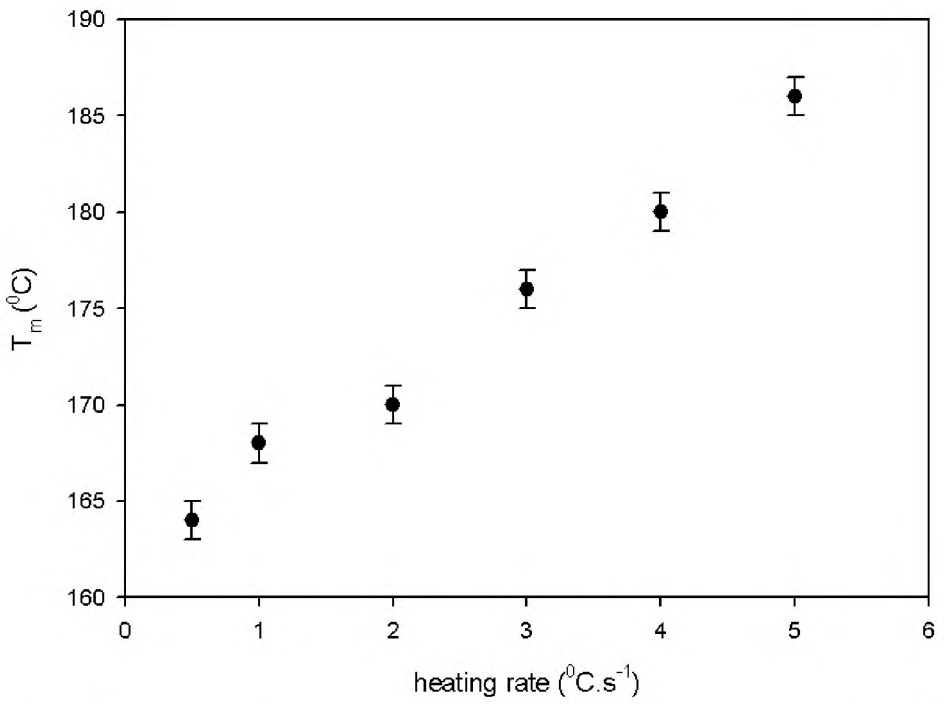

Figure 4.28: The peak temperature against heating rate for peak III at 168 ^{0}C.

The peak III at 168 ^{0}C was affected by the change of heating rate from 0.5 to 5 ^{0}C.s^{-1}.

4.10 Study of thermal fading

Now since TL materials are used in a variety of applications, it is important to be aware of the possibility of fading of the TL with time. Fading is noted when the TL peak intensity decreases with storage time at room temperature after irradiation of the sample has taken place. The measurements were on the same sample but treatment was different, since the sample was irradiated up to 100 Gy. This may be the cause shifting the peaks to new positions. By comparing the two figures 4.29 and 4.1 for 100 Gy and 10 Gy beta dose, as it is observed the shifting peaks.

4.10.1 Thermal fading for TL glow peaks at 70 ^{0}C and 174 ^{0}C

In this study the sample was first irradiated with a beta dose of 100 Gy, the resulting TL glow curve is shown in figure 4.29.

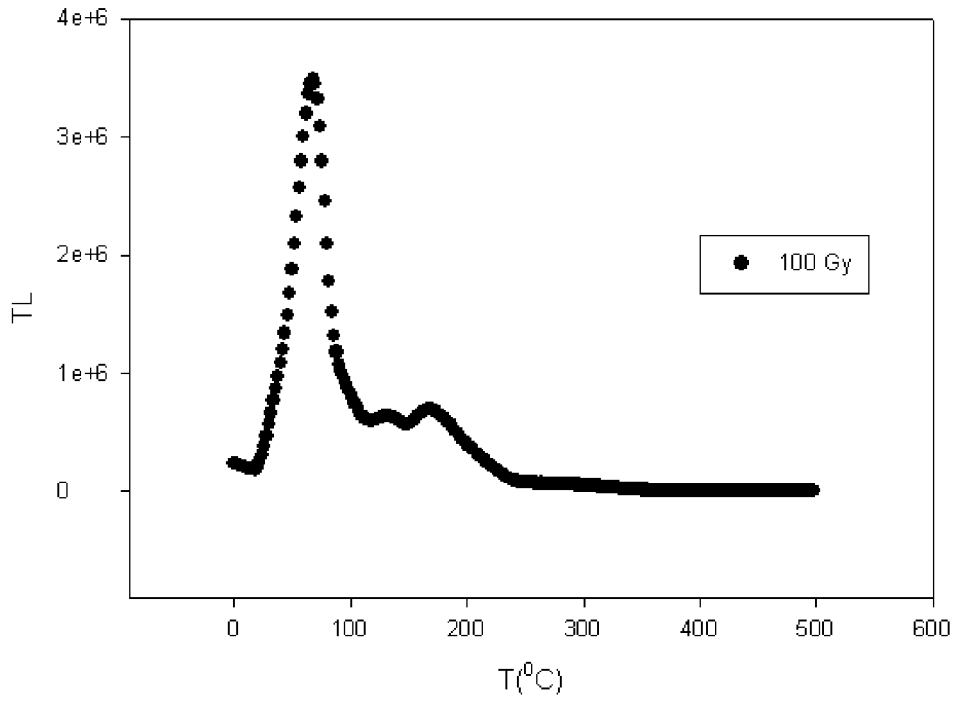

Figure 4.29: TL glow curve of a sample irradiated to 100 Gy .

Only peak I at 70 ^{0}C and peak III at 174 ^{0}C were analyzed for thermal fading. After irradiation the sample was stored for various times between 3 and 30 minutes.

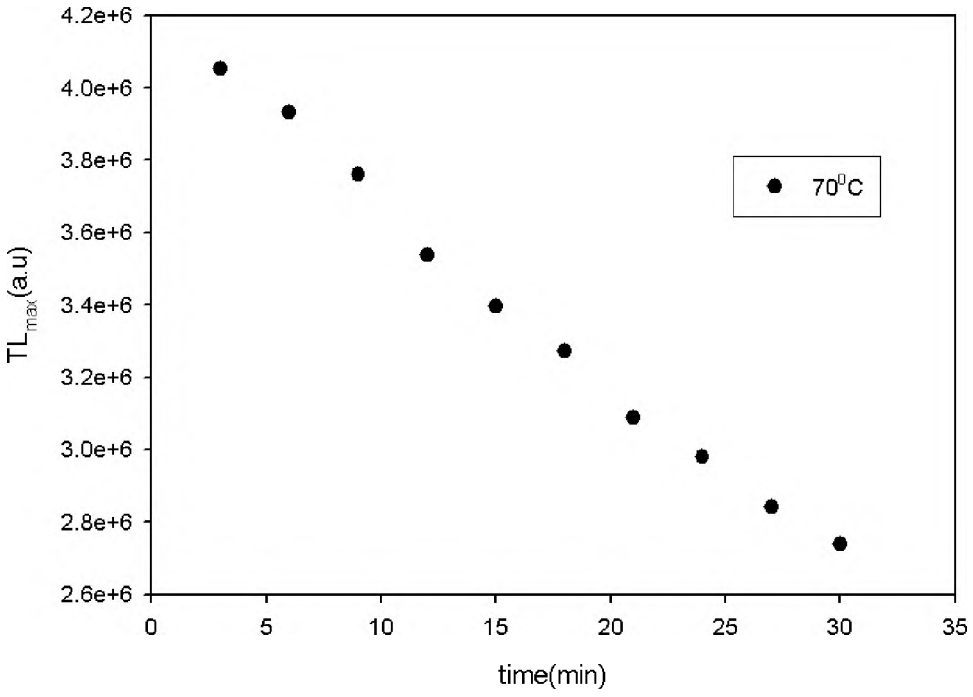

Figure 4.30: TL signal against storage time from 3 to 30 minutes for peak I at 70 ^{0}C. The sample was irradiated with beta radiation dose of 100 Gy.

Figure 4.30 shows the TL signal as a function of storage time. The TL intensity decreases with storage. Peak I at 70 ^{0}C was also affected by thermal fading. After the sample was irradiated with beta dose of 100 Gy and stored for 30 minutes at room temperature, thermal fading was observed.

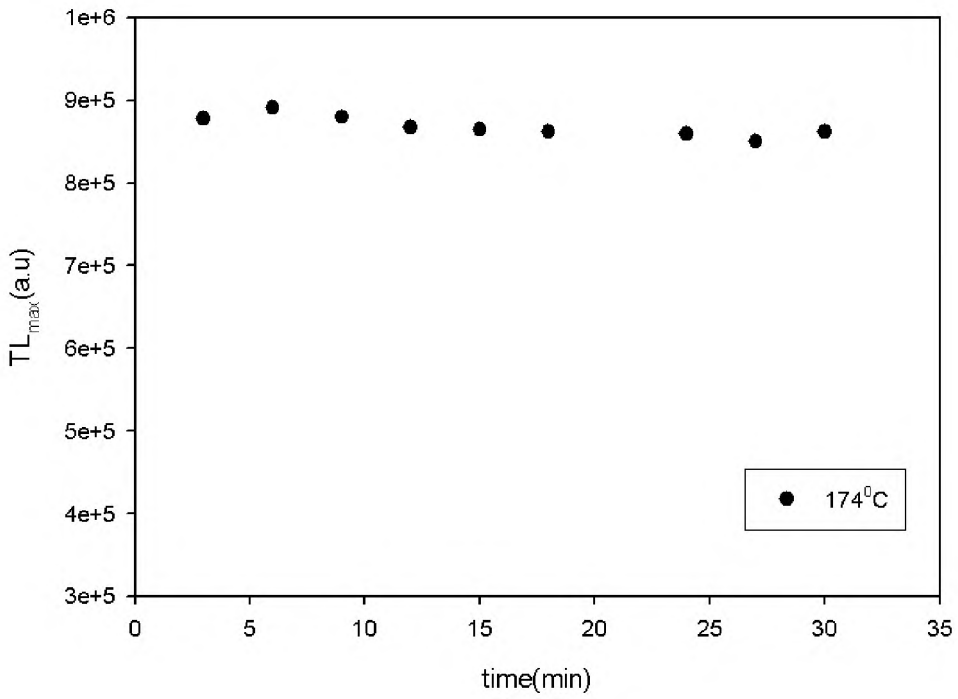

Figure 4.31: TL signal against storage time from 3 to 30 minutes for peak III at 174 ^{0}C, the sample was irradiated with beta radiation dose of 100 Gy

.

Figure 4.31 shows the intensity against storage time for peak III at 174 ^{0}C. The TL peak intensity is independent of storage time at room temperature. This behaviour shows that there was no thermal fading involved in peak III.

4.11 Effect of the TL dose response on the main peak (at 74 ^{0}C)

The sample was irradiated with beta radiation doses from 2 to 20 Gy. The values of maximum intensity corresponding to each dose was noted. The dose response is shown in figure 4.32. The experimental data were fitted by the following equation,

$$y(D) = aD^3 + bD^2 + cD + y_0 \tag{4.7}$$

where D is the given dose (Gy), a,b, c and y_0 are constants. Equations (4.5) and (4.6) were used to evaluate the functions $g(D)$ and $f(D)$ and also

to determine for which doses TL response is linear, superlinear, supralinear or sublinear.

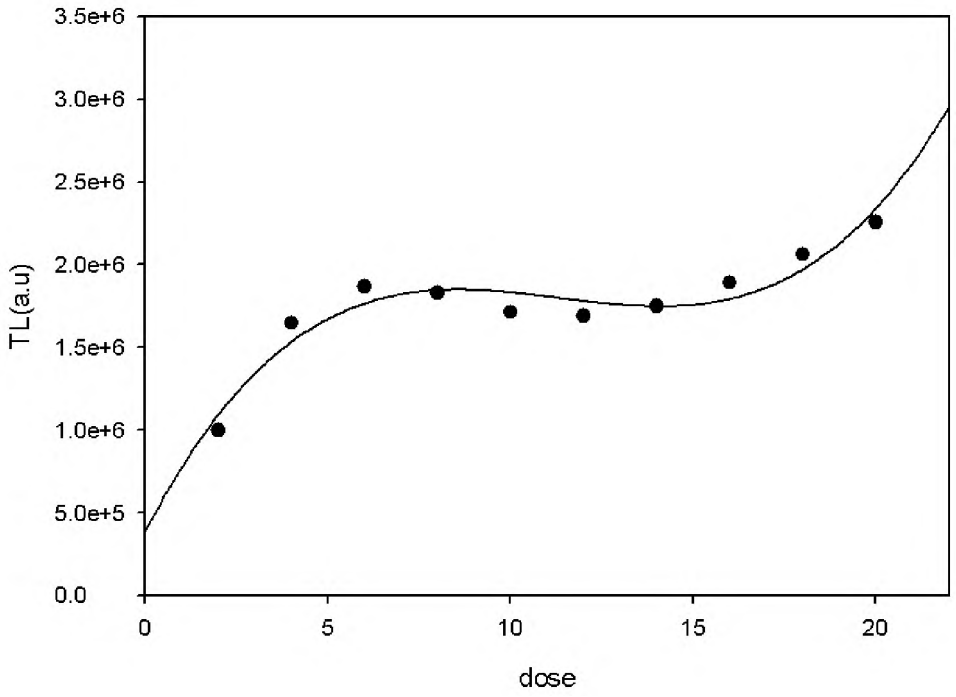

Figure 4.32: TL peak intensity against beta radiation doses from 2 to 20 Gy.

Figure 4.33 shows both indices $g(D)$ and $f(D)$ plotted against beta radiation dose.

At doses of 4 to 20 Gy the values of $g(D) > 1$ and $f(D) < 1$. This means that the TL dose response was superlinear then became sublinear.

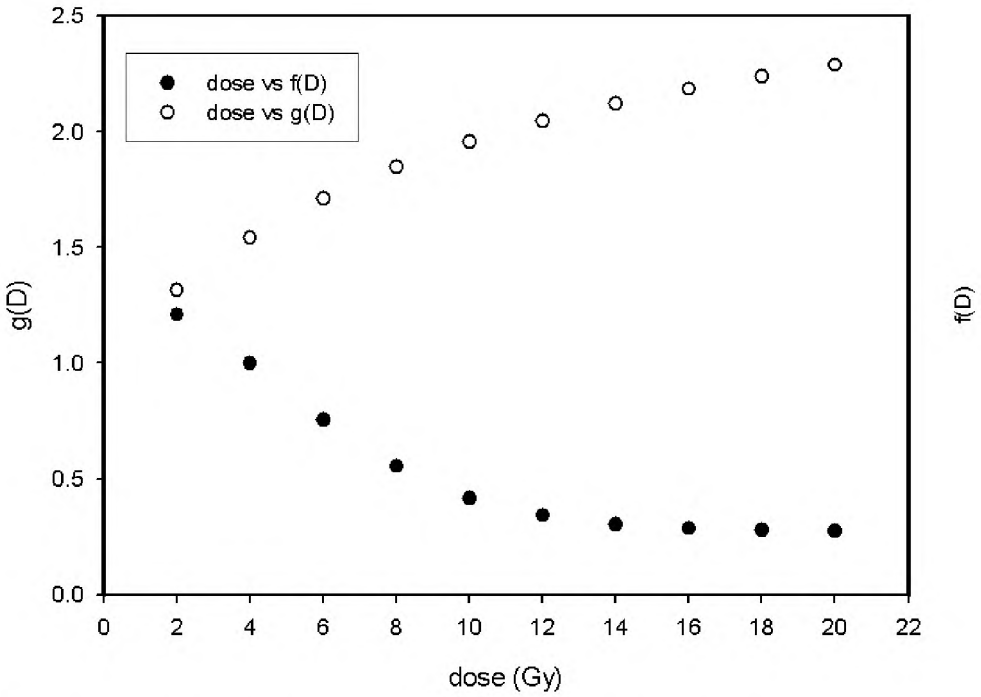

Figure 4.33: Indices, $g(D)$ and $f(D)$ plotted against beta radiation dose.

Supralinearity is caused by competition of traps during heating process of TL. During heating, electrons released from the traps may either recombine with holes or be retrapped in deeper traps. At low doses the probability of a free charge to recombine without falling into a competing trap is low by Townsend [17].

The sample was also irradiated with beta radiation dosse from 20 to 200 Gy. The resulting experimental data of TL peak intensity against beta dose is shown in figure 4.34. The experimental data was fitted by the following equation,

$$y(D) = y_0 + \frac{A}{1 + (\frac{D}{D_0})^B}. \tag{4.8}$$

where D is the given dose (Gy), D_0 normalisation dose (Gy) and y_0, A and B are constants. On equations (4.5) and (4.6) was used to evaluate the functions $g(D)$ and $f(D)$ and also to determine for which doses the TL response is linear, superlinear, supralinear or sublinear.

Figure 4.34 shows the TL intensity against doses from 20 to 200 Gy.The TL intensity is increases as the dose increase. The details on the graph are

more explained in figure 4.35.

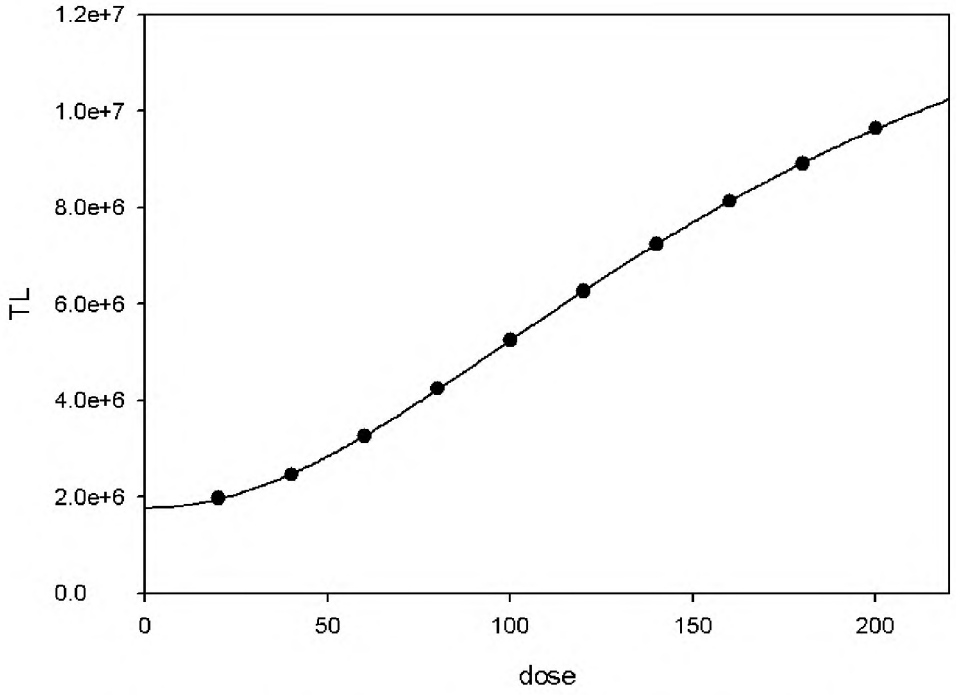

Figure 4.34: TL peak intensity against beta radiation dose from 20 to 200 Gy.

Figure 4.35 as shown at low dose 20 to 40 Gy shows the value of $g(D) = 1$ and the value of $f(D) > 1$, which means the TL response was linear then supralinearity response. High dose from 60 to 200 Gy the values of $g(D) > 1$ and $f(D) < 1$, which shows TL response was superlinear then became sublinear.

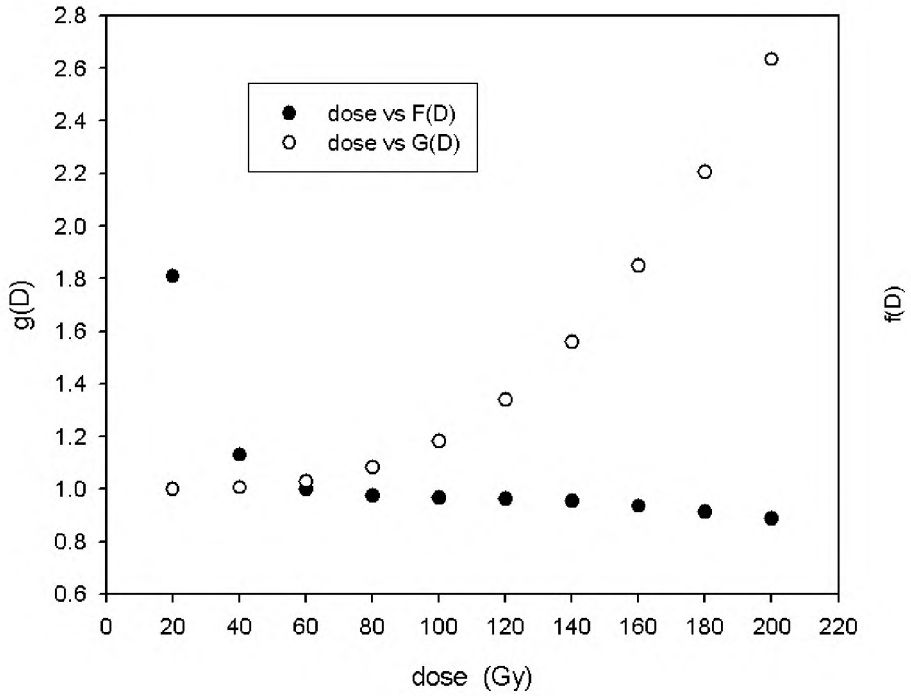

Figure 4.35: Indices, $g(D)$ and $f(D)$ against beta radiation dose from 20 to 200 Gy, at high doses.

Figure 4.36 shows peak temperatures as function of beta dose. The peak temperatures is independent of beta dose. This kind of behaviour is consistent with first order kinetics.

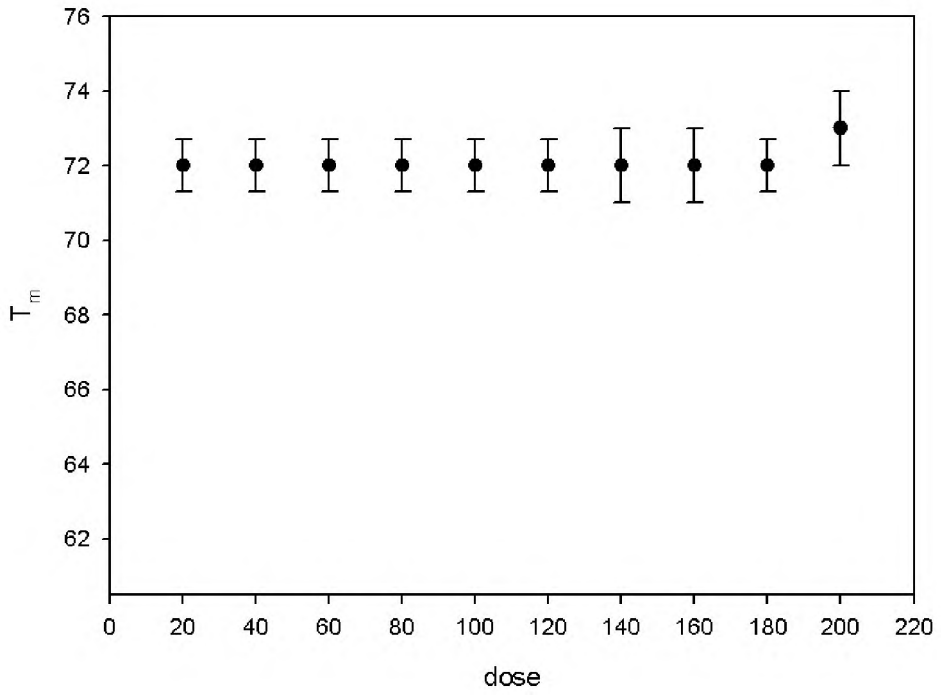

Figure 4.36: Peak temperatures as a function of beta radiation dose from 20 to 200 Gy.

Further analysis for high doses was done to observe which doses the sample saturates. The sample was irradiated to a beta dose of 100 Gy then heated at 1 ^{0}C$\cdot$ s^{-1}. There were three peaks observed as was shown in figure 4.29. Only two peaks at 70 ^{0}C and 174 ^{0}C where analyzed. The aim was to observe and reach the saturation region of the dose. The sample was irradiated with beta doses from 100 to 1600 Gy and after the sample was irradiated with beta doses from 100 to 2000 Gy.

Figure 4.37 shows the TL peak intensity as the function of beta dose for the peak at 70 ^{0}C. At low doses of 100 to 400 Gy, the peak intensity increases linearly. At high beta doses of 400 to 1200 Gy the behaviour was sublinear. The intensity saturated at high beta doses from 1200 to 1600 Gy.

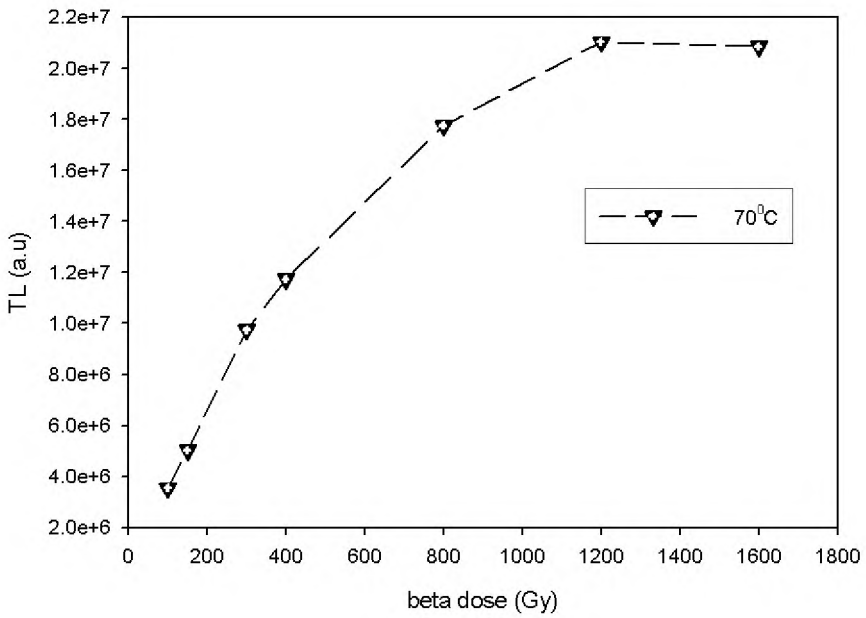

Figure 4.37: TL peak intensity as a function of beta radiation dose from 100 to 1600 Gy for the peak at 74 ^{0}C.

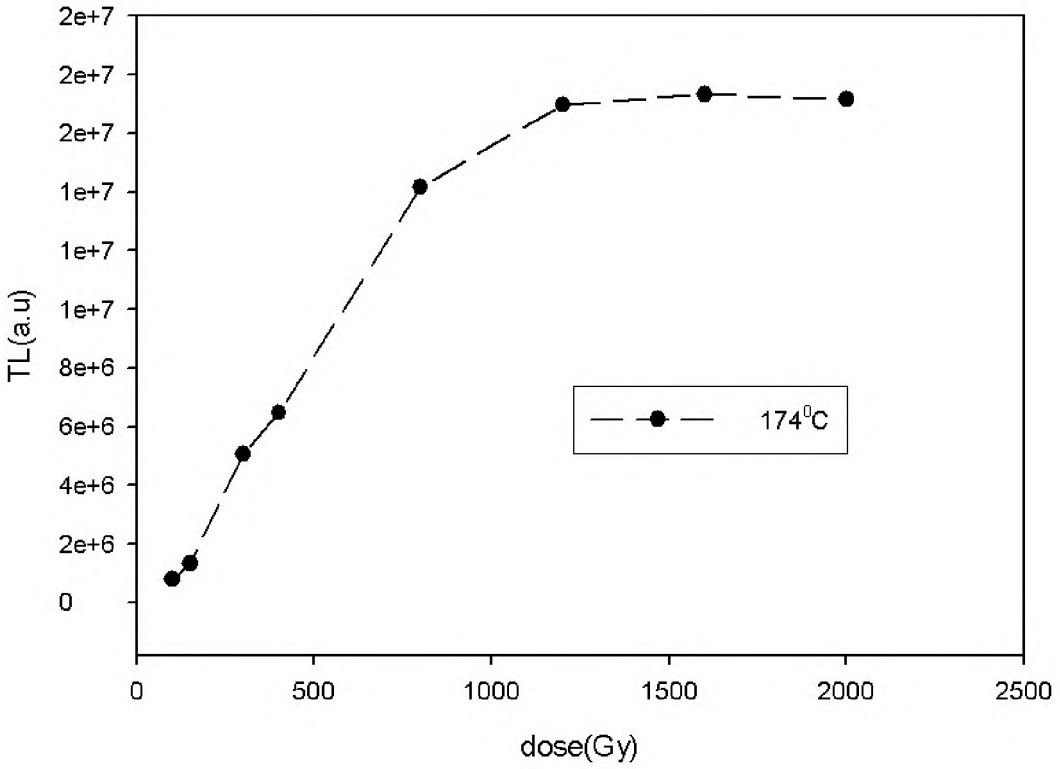

Figure 4.38: TL peak intensity as a function of beta radiation dose from 100 to 2000 Gy, for the peak at 174 ^{0}C.

Figure 4.38 shows the TL peak intensity as the function of beta dose for the peak at 174 ^{0}C. At low doses of 100 to 800 Gy, the peak intensity increases linearly. At high beta doses of 800 to 1400 Gy the behaviour was sublinear. The saturated level was observed at high beta doses from 1400 to 2000 Gy.

4.12 Summary of kinetic analysis of the TL glow peaks at 74 ^{0}C and 168 ^{0}C

The sample was irradiated up to 10 Gy then heated at linear heating rate of 1 ^{0}C·s^{-1} up to 500 ^{0}C. The TL glow curve with three TL glow peaks at 74 ^{0}C, 144 ^{0}C and 168 ^{0}C was observed. The analysis was only done on the peaks at 74 ^{0}C and 168 ^{0}C. Six methods were employed. The values of kinetic parameters E and s were found to be consistent with each other as shown in tables 4.4 and 4.5.

Table 4.4: Values of the trap depth and frequency factor found using various methods applied on the main peak at 74 ^{0}C.

Methods	E eV	frequency factor (s^{-1})
Initial rise	0.86± 0.03	10^{11}
Peak shape(E_τ)	0.86± 0.02	10^{11}
Peak shape(E_δ)	0.94± 0.02	10^{12}
Peak shape(E_ω)	0.87± 0.01	10^{11}
Peak shape(av)	0.89± 0.02	10^{13}
Variable heating rate	0.89± 0.01	10^{11}
Glow curve	0.80± 0.06	10^{9}
Glow curve deconvolution	0.90± 0.02	10^{12}
Isothermal	0.73± 0.03	10^{15}

Table 4.5: Values of the trap depth and frequency factor found using various methods applied on the peak at 168 ^{0}C.

Methods	E eV	frequency factor (s^{-1})
Initial rise	0.85± 0.03	10^{8}
Variable heating rate	0.91± 0.01	10^{9}

The peak temperature shifted with heating rate to high temperature. The TL intensity decreased as heating rate increased from 0.5 to 5 ^{0}C.s^{-1}. The decrease in TL against heating rate was caused by thermal quenching.

The T_m-T_{stop} method was applied over 54 to 64 ^{0}C . The T_m-T_{stop} method showed that the 74 ^{0}C peak is single and subjected to first order kinetics.

Thermal fading was observed after the sample was irradiated up to 100 Gy and the storage for 30 min.

At low dose from 2 to 20 Gy and TL dose response was superlinear, supralinear and sublinear. For high dose from 20 to 200 Gy and TL dose response was linear, supralinear, superlinear and sublinear. The peak temperature against beta dose from 20 to 200 Gy shows the firs order kinetics behaviour.

4.13 Phototransferred thermoluminescence

Phototransferred thermoluminescence (PTTL) was studied on a sample irradiated to 100 Gy Figure 4.39 shows the glow curve of an irradiated (100 Gy) sample heated to 500 ^{0}C at 1 ^{0}C.s^{-1}. The investigation was based on understanding how the electrons are transferred from deep to shallow traps. The glow curve shows three glow peaks which is similar to the TL glow curve shown in figure 4.1 when the sample was irradiated to 10 Gy. Figure 4.39

shows peak I at 70 ^{0}C has the intensity as compared with the other peak II at 136 ^{0}C and peak III at 174 ^{0}C.

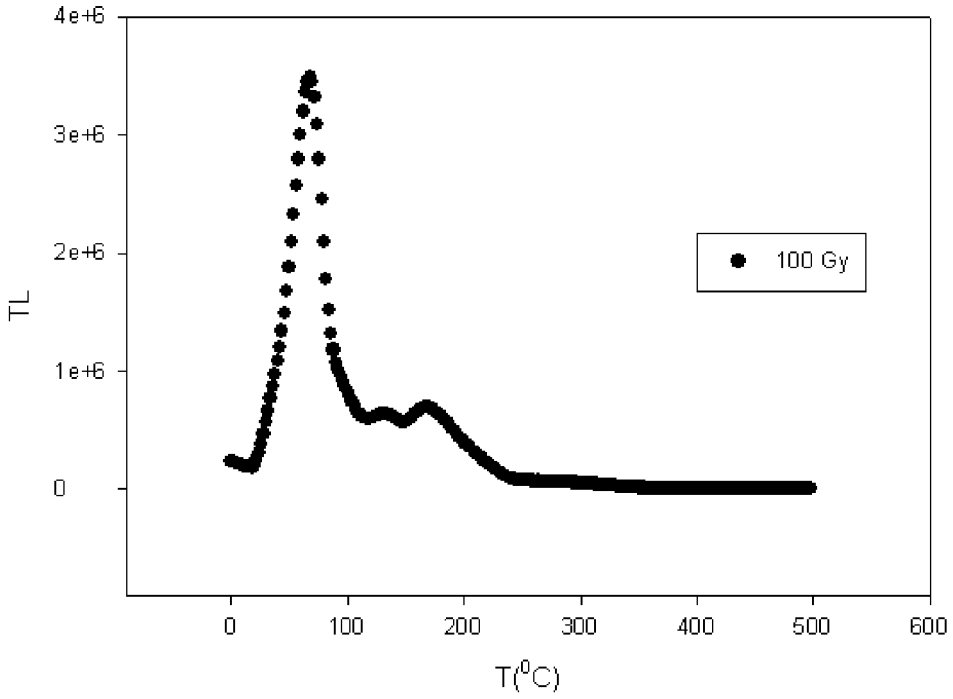

Figure 4.39: The sample was irradiated to 100 Gy was heated up to 500 ^{0}C .

4.13.1 Phototransferred TL following preheating to 430^{0}C

The sample was preheated up to 430 ^{0}C as shown in figure 4.40, to remove all the peaks I, II and III and then cooled to room temperature. The sample was then exposed 470 nm blue LEDs for periods from 3 to 29 s.

The sample was preheated at 430 ^{0}C, to erase the existing TL glow peaks . The PTTL for 430 ^{0}C curves was observed. Figure 4.40 shows that PTTL curve was characterized by three PTTL glow peaks, (I) at 72 ^{0}C, (II) 134 ^{0}C and (III) 176 ^{0}C. This kind of signal show that electrons were transfer from deep to acceptor traps.

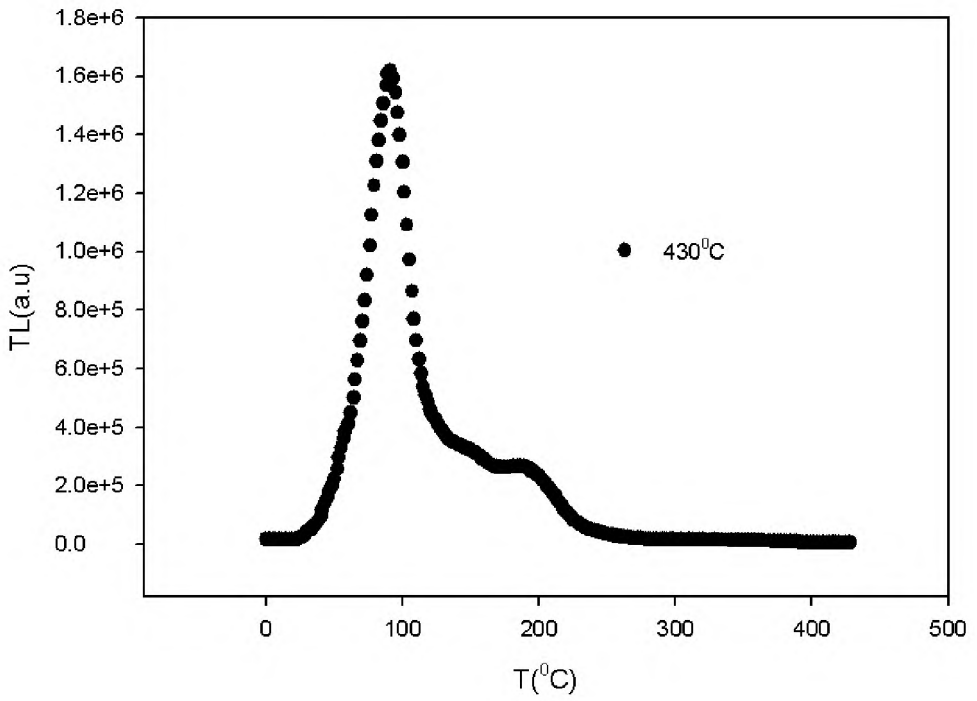

Figure 4.40: TL glow curve irradiated up to 100 Gy was preheated up to 430 ^{0}C.

Subsequently the sample was heated to measure TL from shallow traps. Figure 4.41 shows the results glow curve. There are three PTTL glow peaks labelled I, II and III. The three PTTL glow peaks, I, II and III were found at 72 ^{0}C, 134 ^{0}C and 176 ^{0}C. Only two PTTL glow peaks were analyzed, peak I and peak III. The low-intensity peak II was omitted from analysis.

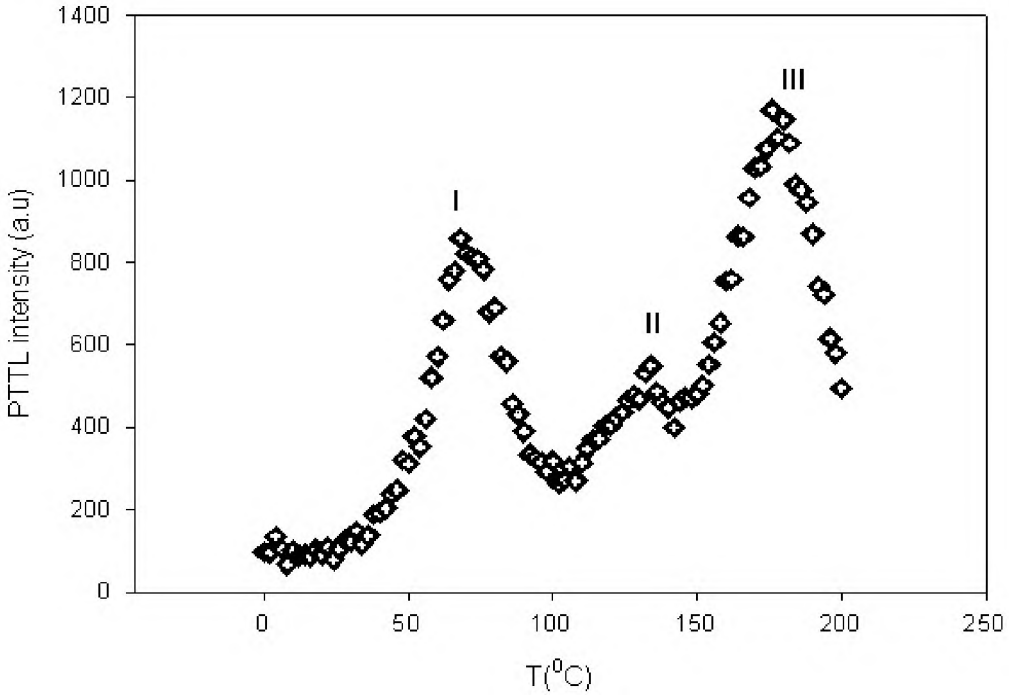

Figure 4.41: The PTTL glow peaks at 72 ^{0}C (peak I), 134 ^{0}C (peak II) and 176 ^{0}C (peak III) against temperature.

Effect of illumination time on PTTL peak I and III

Figures 4.42 shows the PTTL intensity (peak I) curves as a function of illumination time where each point represents peak intensity for a given time. The PTTL intensity increases and decreases with illumination time to 29 s. From 3 to 11 s PTTL peak intensity increases. At 13 s PTTL peak intensity reached maximum zone, then decreases from 13 to 21 s. From 25 to 29 s the PTTL intensity it seems to be stable or constant. The increase may be cause by filling the shallow traps by Wintle and Murray [18]. Even though electrons accumulate in shallow trap during illumination time, the number of holes decrease by Botter-Jensen [15].

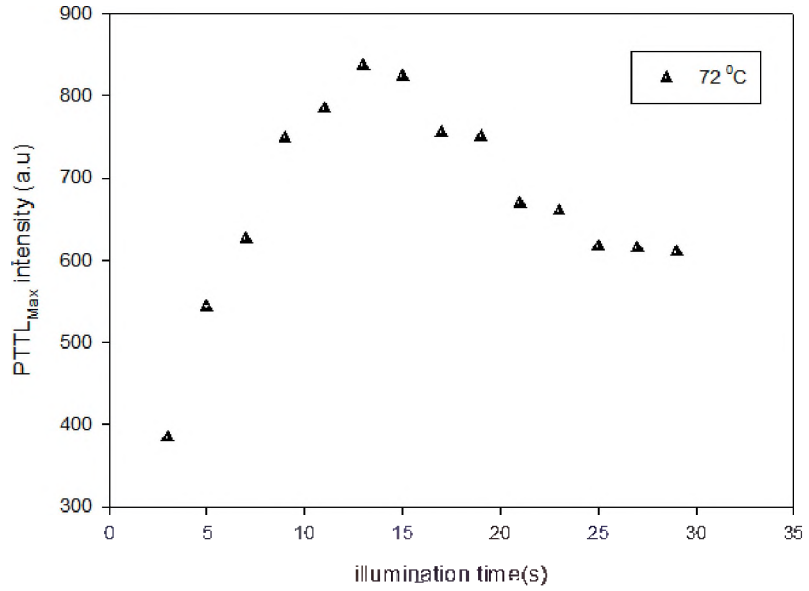

Figure 4.42: The PTTL intensity against illumination time for peak I.

Figure 4.43 shows the PTTL intensity (peak III) curves as a function of illumination time were each point represents peak intensity for a given time. The evidence shown in figure 4.43 is similar from the explanation of figure 4.42.

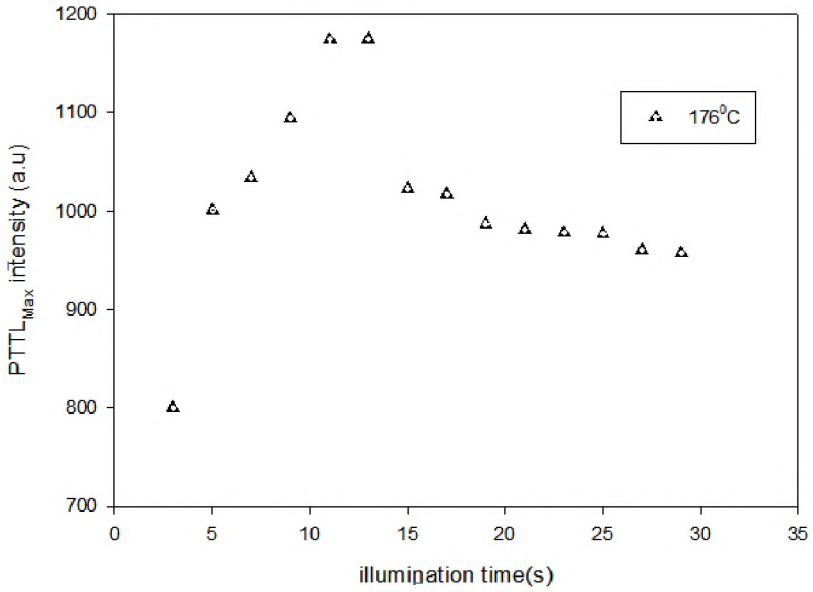

Figure 4.43: PTTL intensity against illumination time for peak III.

The maximum PTTL intensity of the peak I at 13 s is greater than maximum PTTL intensity of the peak III. The stabilization of the PTTL intensity of peak I was faster than stabilization of peak III, the cause of this kind behaviour may be the rate at which the electrons escape the electron trap.

4.13.2 Effect of heating rate on PTTL glow peaks I and III

The two PTTL glow peaks I and III were analyzed, by noting the effect of varying heating rate from 0.5 up to 5 ^{0}C.s^{-1}. Both figures 4.44 and 4.45 shows the PTTL intensity against heating rate for both peaks, I and III. The heating rate increases meanwhile the PTTL intensity decrease. This kind of relationship may be because the effect of thermal quenching.

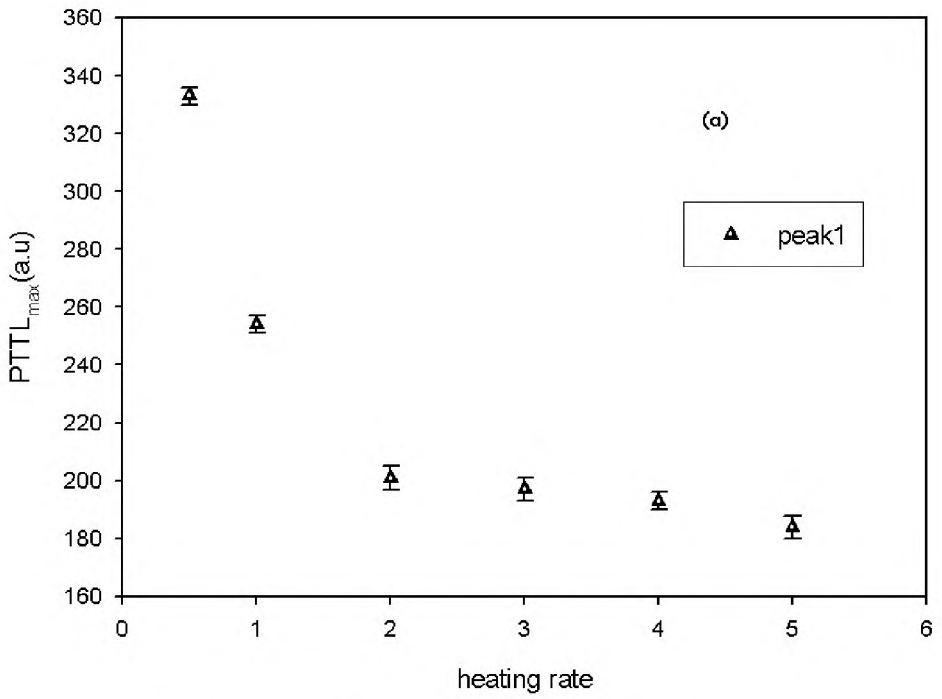

Figure 4.44: PTTL against heating rate for peak I.

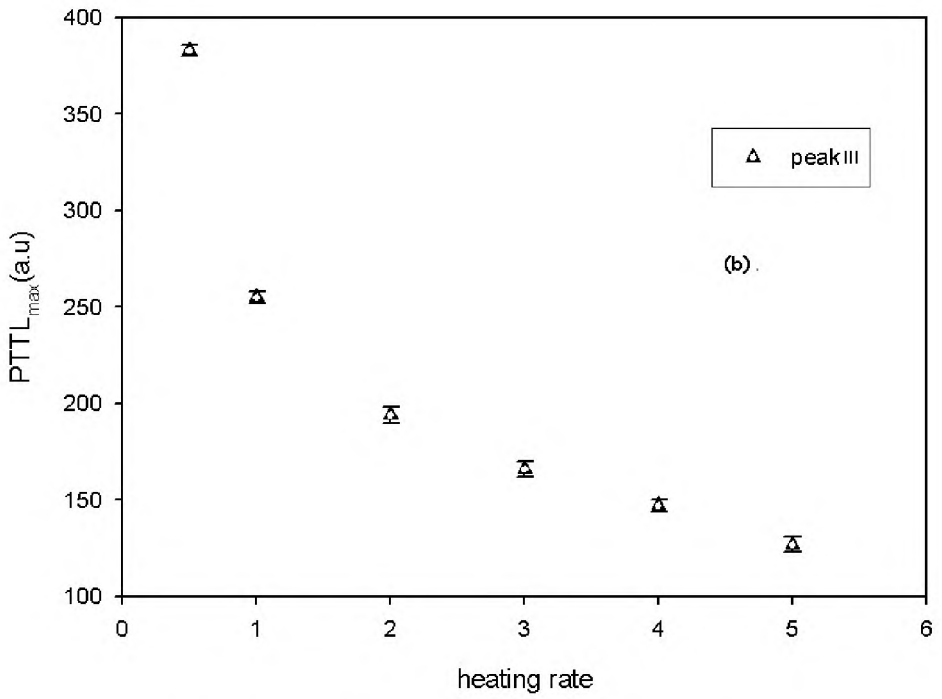

Figure 4.45: PTTL against heating rate for peak III.

4.13.3 Effect of peak temperature on PTTL glow peaks I and III

Figures 4.46 shows the PTTL intensity against peak temperature (peak I). The PTTL intensity decreases as the peak temperature increase.

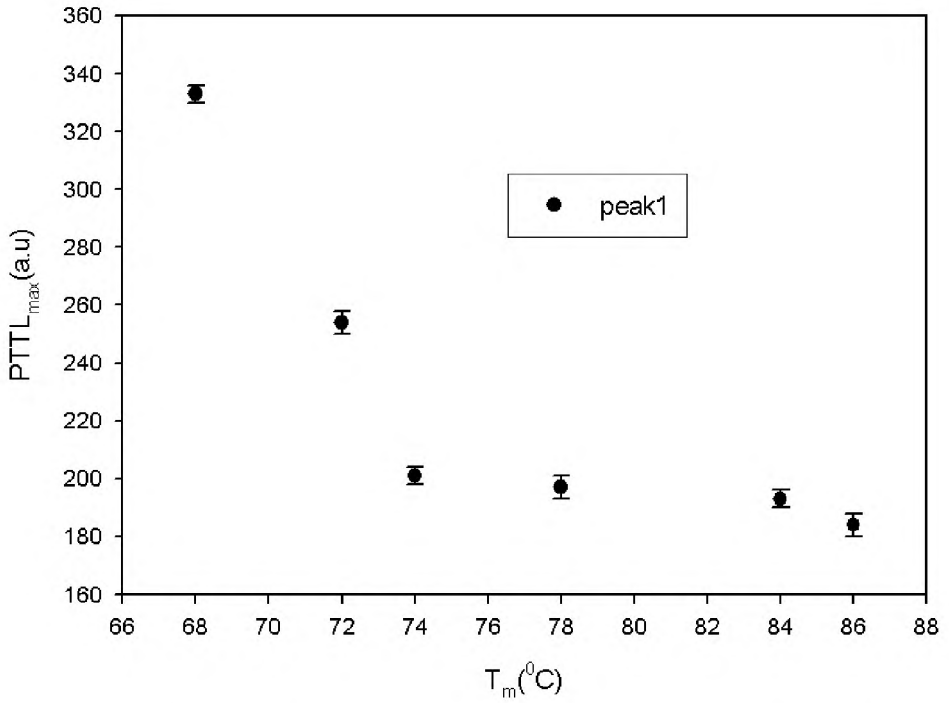

Figure 4.46: The PTTL against peak temperatures for peak I.

Figure 4.47 shows the PTTL intensity against peak temperature (peak III). The PTTL intensity decreases as the peak temperature increase. The peak temperature was noted meanwhile varying heating rate from 0.5 to 5 ^{0}C.s^{-1}.

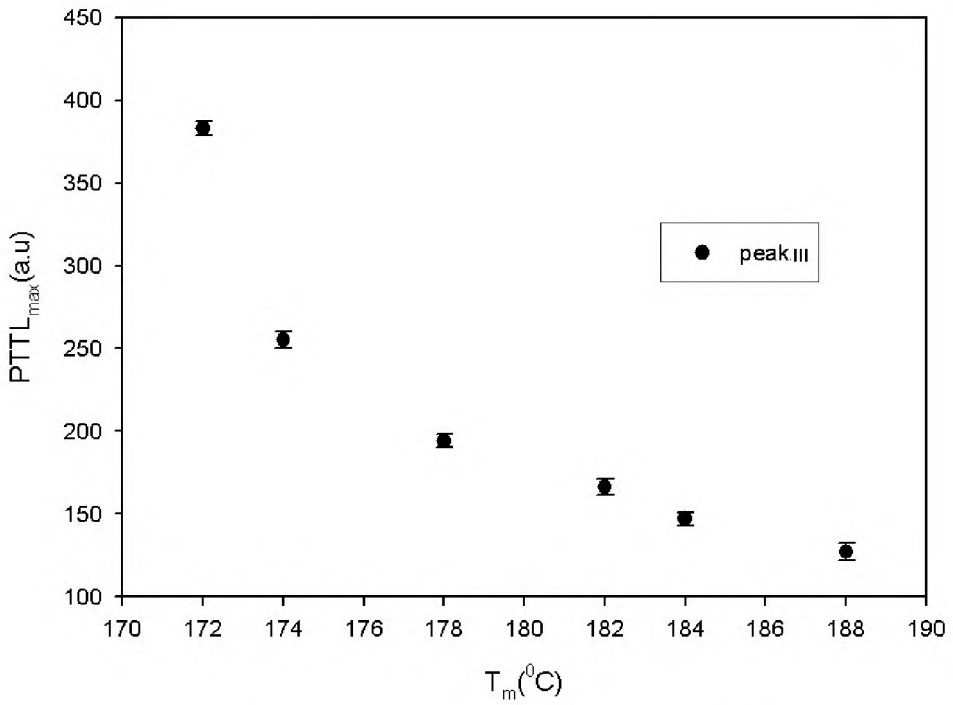

Figure 4.47: The PTTL against peak temperatures for peak III.

4.13.4 Effect of heating rate on the peak temperature of the PTTL glow peaks I and III

Figure 4.48 shows the peak temperature against heating rate (peak I). It is observed that when the heating rate increase also peak temperature increases 68 to 87 ^{0}C. This illustrate that peak temperature shifts to high temperature meanwhile heating rate increases as shown in figure 4.48 and 4.49. This behaviour shows that peak temperature is dependent in heating rate.

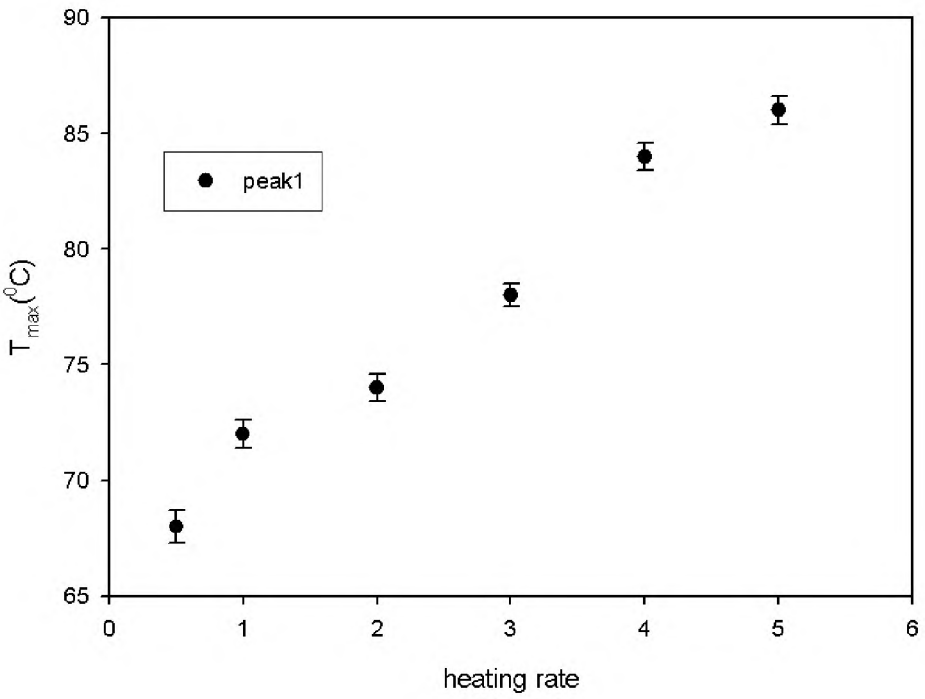

Figure 4.48: Effect of heating rates from 0.5 to 5 ^{0}C.s^{-1} on peak temperatures for peak I.

Figure 4.49 shows the peak temperature against heating rate (peak III).

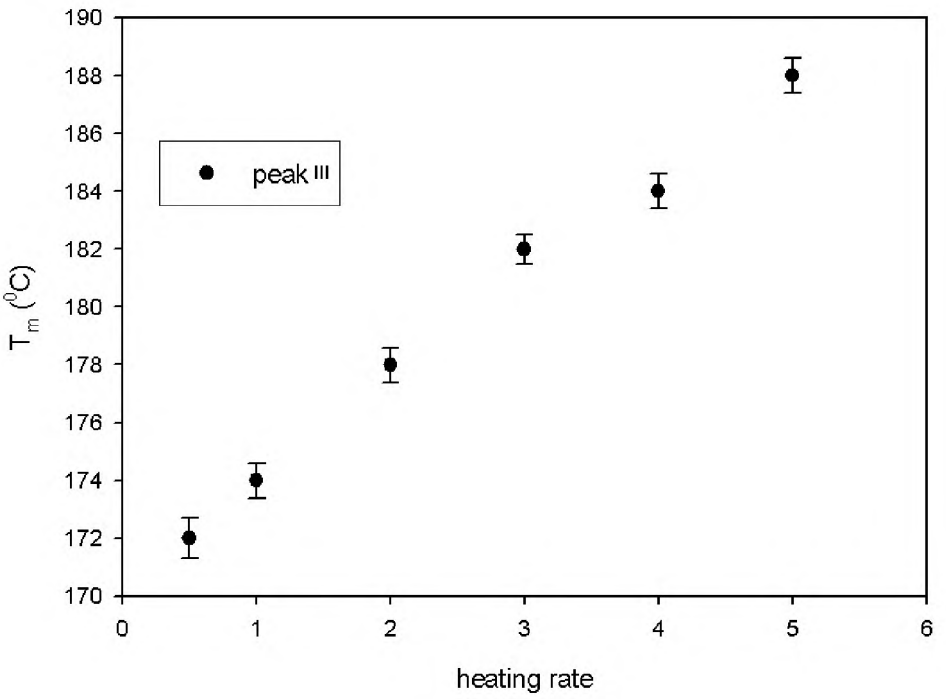

Figure 4.49: Effect of heating rates from 0.5 to 5 ^{0}C.s^{-1} on peak temperatures for peak III.

4.13.5 Pulse annealing

Since PTTL is governed by the stimulation of electrons from deep traps pulse annealing was employed to investigate the temperature range of the donor traps. The pulse annealing was performed using ten different temperatures from 50 to 500 ^{0}C at interval of 50 ^{0}C. During preheating from 50 to 100 ^{0}C, no PTTL signal was observed from both two PTTL glow peaks I and III.

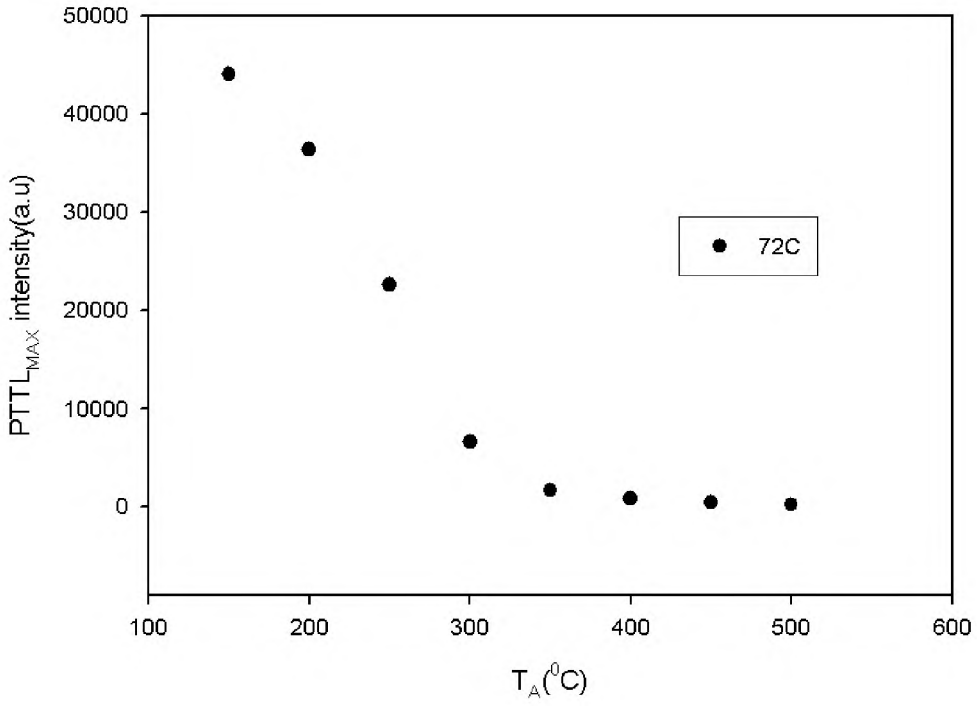

Figure 4.50: PTTL intensity of peak I plotted against annealing temperatures from 150 ^{0}C to 500 ^{0}C.

Figure 4.51 shows PTTL intensity of peak I against annealing temperature. For peak I the PTTL signal was observed from 150 ^{0}C up to 500 ^{0}C as shown in figure 4.50. The maximum PTTL intensity was found at 150 ^{0}C. As the preheating temperature increases, the PTTL intensity decreases from 150 ^{0}C up to 300 ^{0}C. Starting from 350 ^{0}C up to 500 ^{0}C the PTTL intensity was stable and approaching zero.

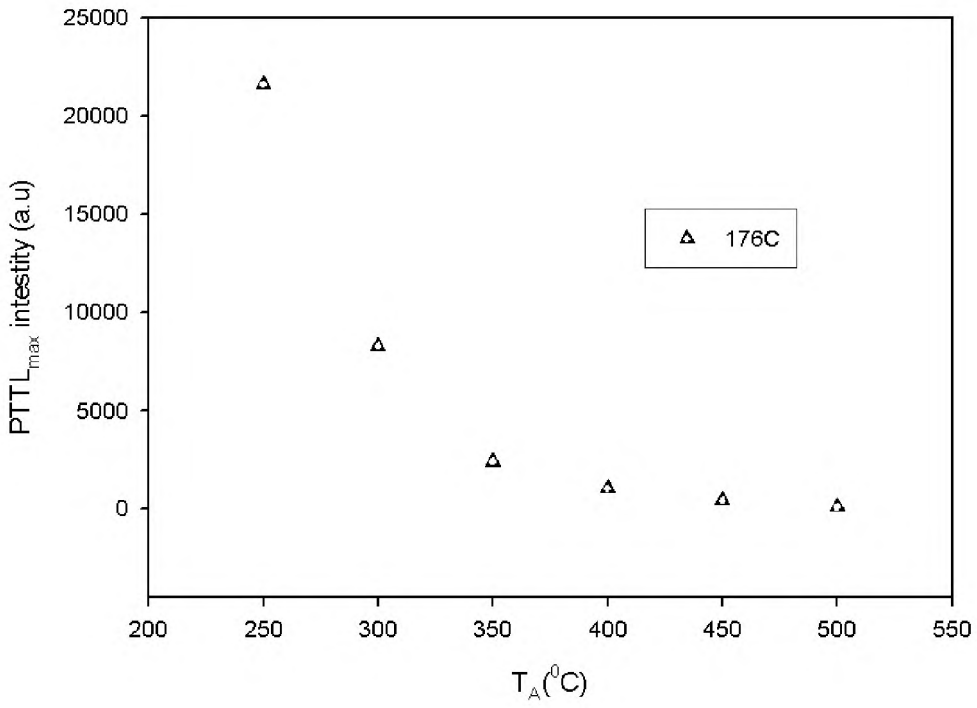

Figure 4.51: PTTL intensity of peak III plotted against annealing temperatures from 250 ^{0}C to 500 ^{0}C.

Figure 4.51 shows PTTL intensity of peak III against annealing temperature. For peak III the PTTL intensity signal was observed from 250 ^{0}C up to 500 ^{0}C to decrease as shown in figure 4.51. During pulse annealing, as the temperatures increases the PTTL intensity decreases. Beyond from 350 ^{0}C up to 500 ^{0}C the PTTL intensity was stable and approaching zero.

4.14 Kinetic analysis PTTL glow peaks (I and III) using initial rise method

Kinetic parameters of PTTL peaks was done using initial rise method. Figure 4.52 shows the plot of $ln(TL)$ against $1/kT$. The data points in the graph correspond with 10-15 % maximum intensity. The trap depth E found to be 0.60 $\pm$ 0.01 eV. The frequency factor was in order of 1.9 $\times$ 10^8 s^{-1}.

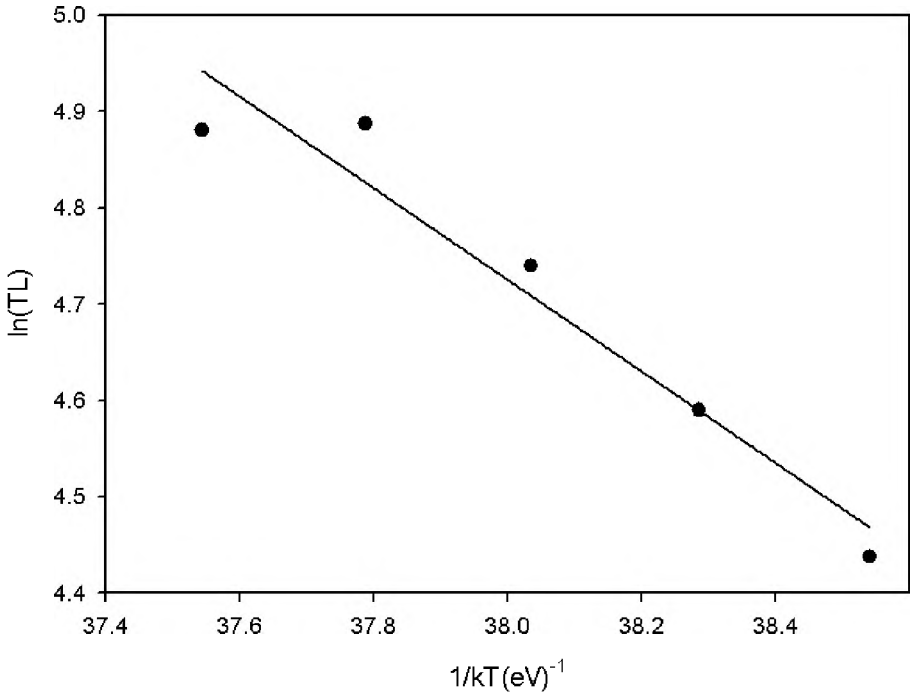

Figure 4.52: The relationship of ln(TL) against 1/kT for the peak (I) PTTL.

Figure 4.53 shows the plot of $ln(TL)$ against $1/kT$. The trap depth found to be 0.70 $\pm$ 0.03 eV. The frequency factor was found to be 2.9×10^8 s^{-1}.

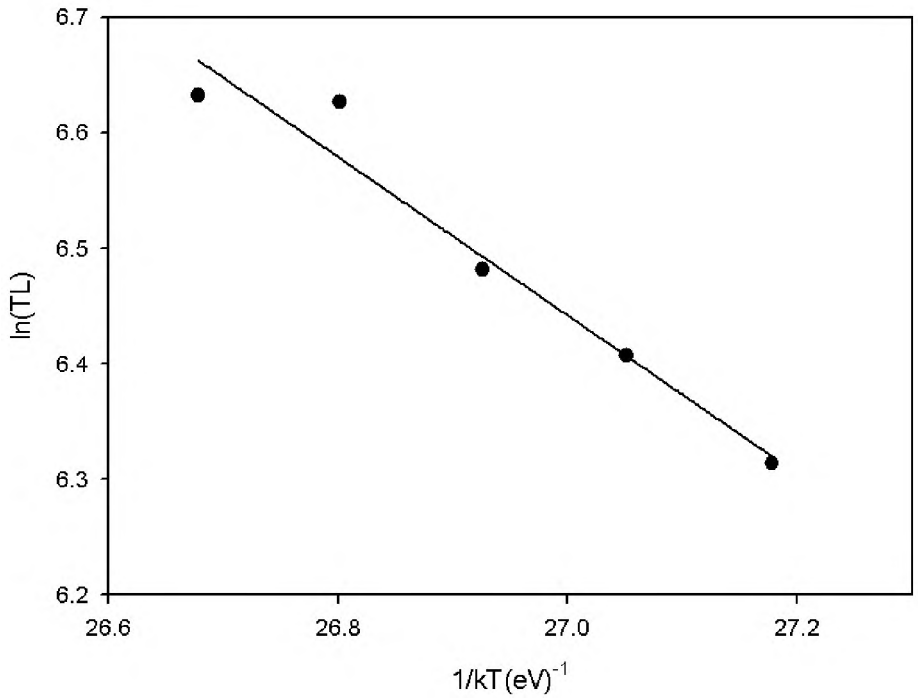

Figure 4.53: The relationship of ln(TL) against 1/kT for the peak(III) PTTL.

4.15 Kinetic analysis of PTTL glow peaks (I and III) using variable heating rate method

The variable heating rate (VHR) method was used to evaluate trap depth and frequency factor. Figure 4.54 shows a plot of $ln\left(\frac{T_m^2}{\beta}\right)$ against $1/kT$ for peak I. The trap depth E found to be 0.83 $\pm$ 0.02 eV and the frequency factor found to be 5.9×10^9 s^{-1}.

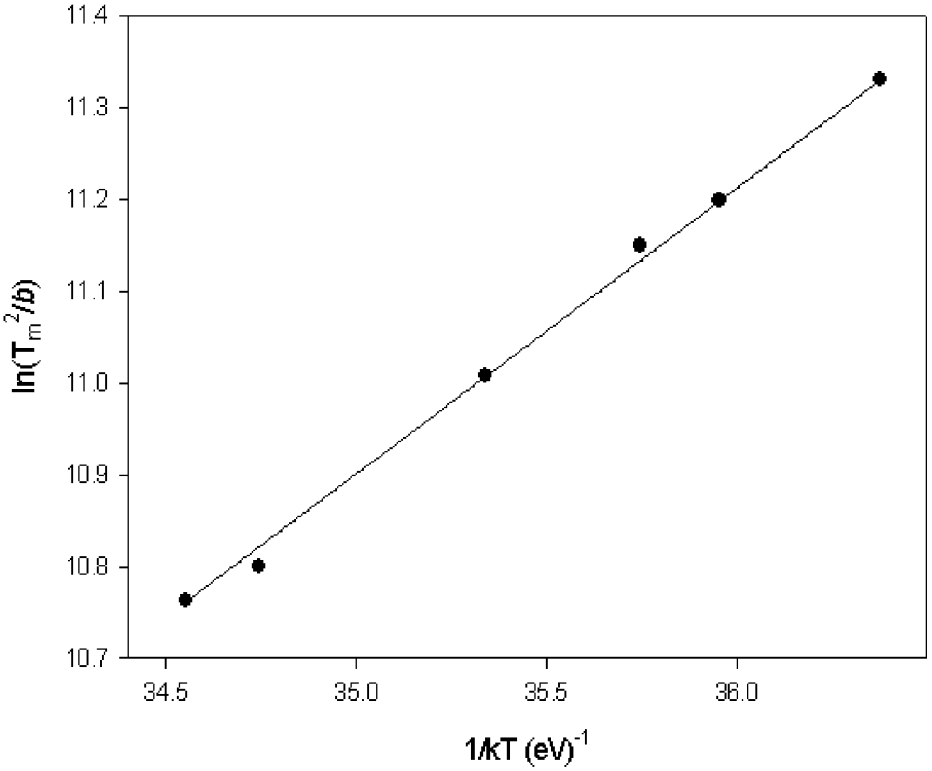

Figure 4.54: $\ln(T_m^2/\beta)$ against 1/kT for evaluation of trap depth on peak I.

Figure 4.55 shows a plot of $ln\left(\frac{T_m^2}{\beta}\right)$ against $1/kT$ for peak III. The value of E was 0.80 ± 0.03 eV and the frequency factor found to be 1.6 $\times 10^9$ s^{-1}.

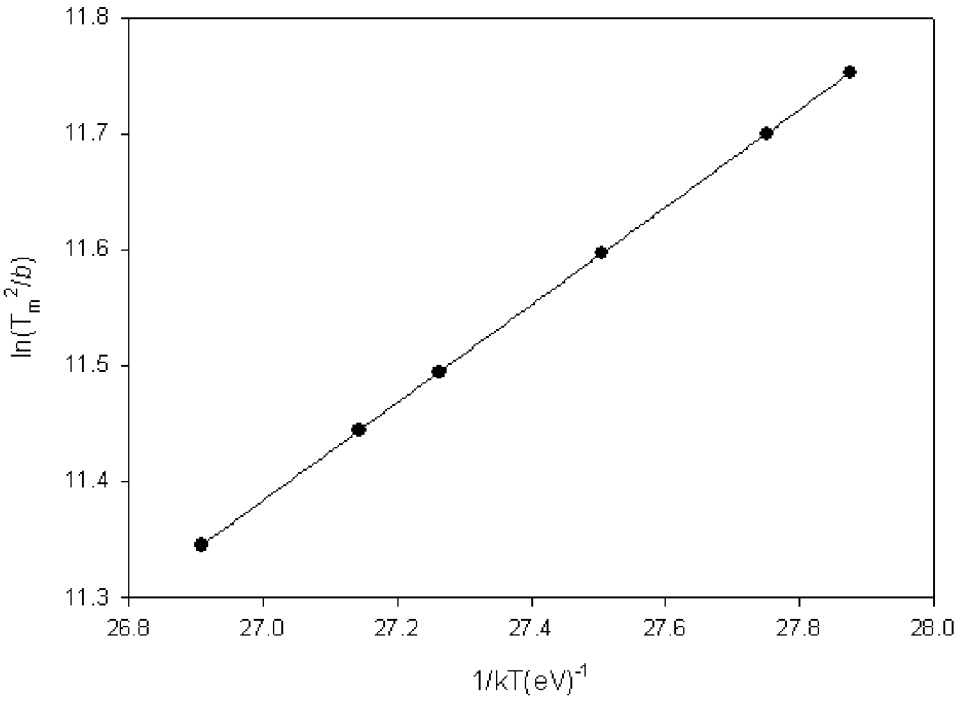

Figure 4.55: $\ln(T_m^2/\beta)$ against 1/kT for evaluation of trap depth for peak III.

4.15.1 Thermal fading of PTTL glow peaks

The investigation of the effect of thermal fading for PTTL peaks I and III was done. The sample was irradiated to a beta dose of 100 Gy, then preheated to 430 ^{0}C. From here the sample was cooled, then exposed to 470 nm blue LEDs and stored for 30 minutes at room temperature. The resultant PTTL glow peaks were analysed for thermal fading.

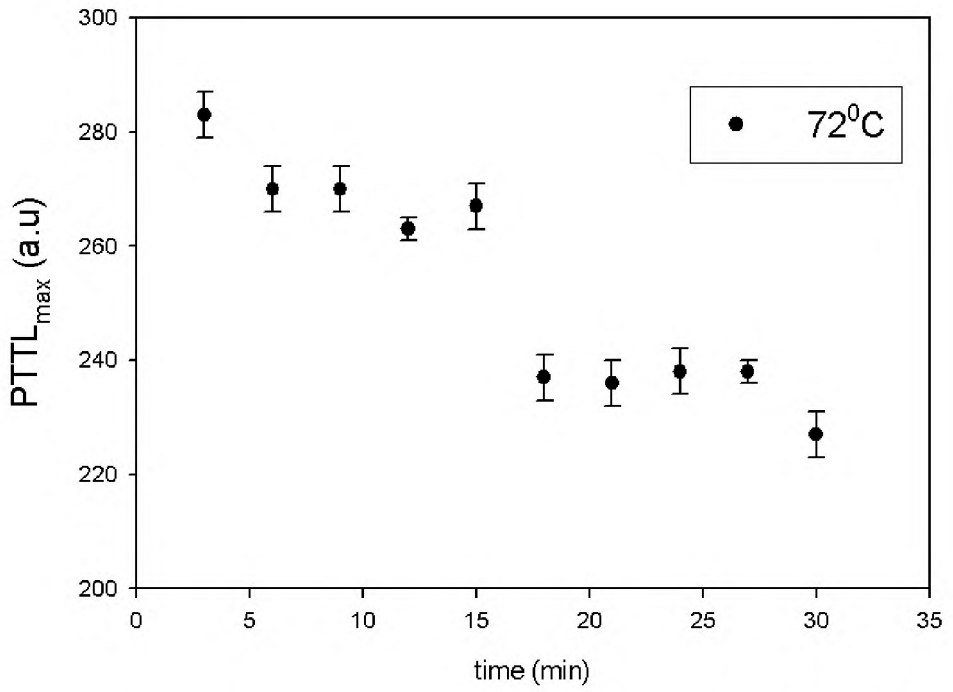

Figure 4.56: PTTL response as the function of storage time for peak I.

Figure 4.56 shows PTTL peak intensity against time for peak I. The PTTL signal decreases as the storage time increases.

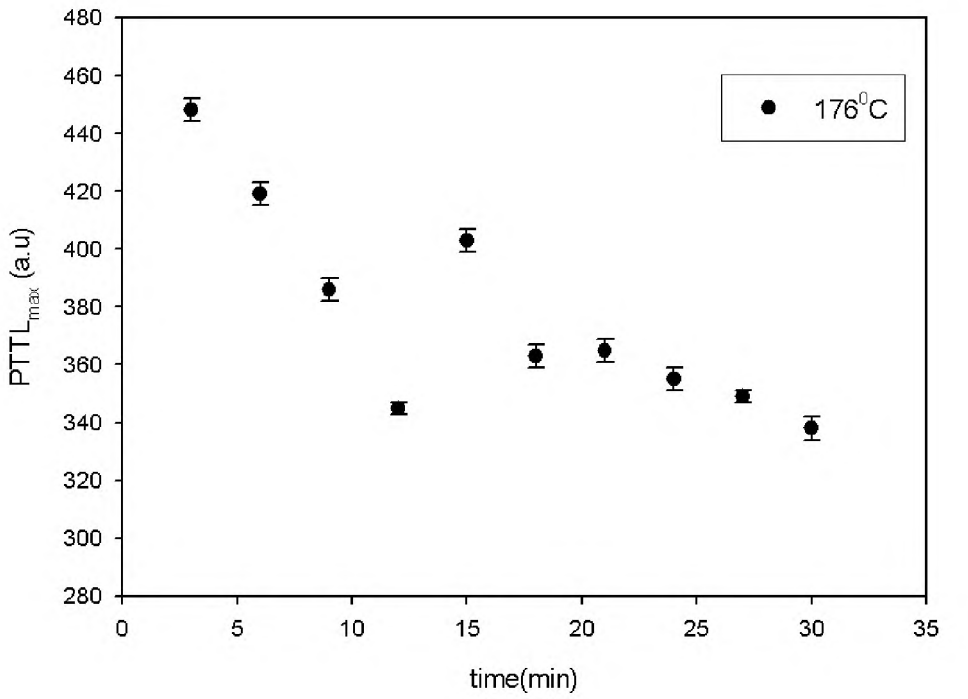

Figure 4.57: PTTL response as the function of storage time 3 to 30 minutes for peak III.

Similarly in figure 4.57 as shown PTTL against time for peak III, the PTTL signal decreases as storage time increases. From from 3 to 12 minutes PTTL peak intensity decrease uniformly. Then from 18 to 30 minutes the PTTL signal decreases.

4.15.2 Dose response of PTTL glow peaks

These two PTTL peaks, I and III, were not analysed in details. Figure 4.58 shows the TL peak intensity as a function of beta radiation doses from 20 to 200 Gy for peak I. The PTTL peak intensity increases as the dose increase.

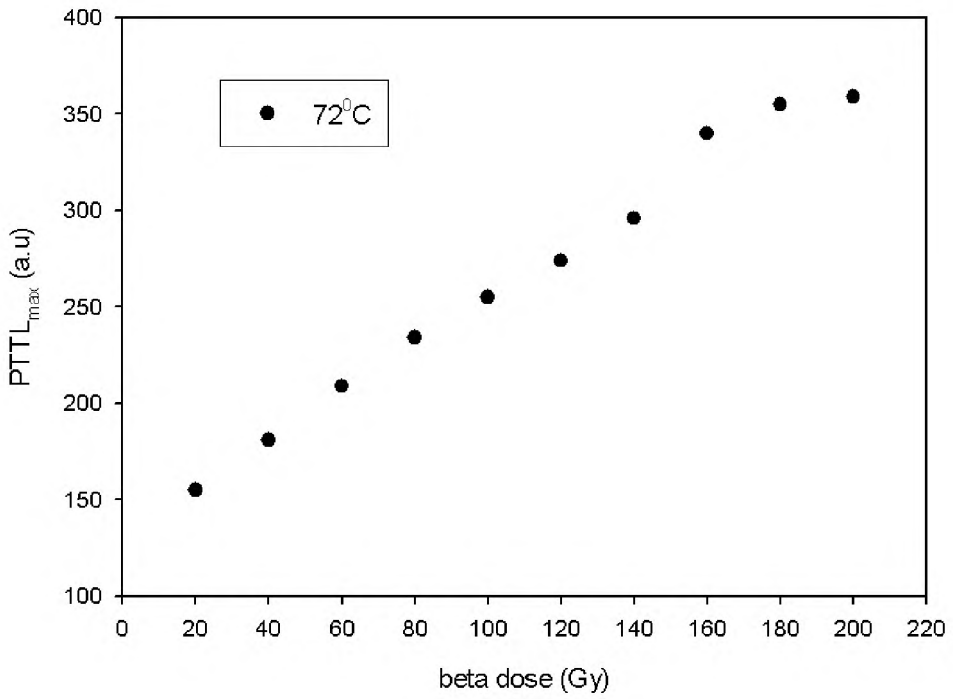

Figure 4.58: PTTL peak intensity against beta radiation doses from 20 to 200 Gy for peak I.

Figure 4.59 shows the PTTl intensity against beta radiation doses from 20 to 200 Gy for peak III. PTTL intensity increases as beta dose from 20 to 200 Gy.

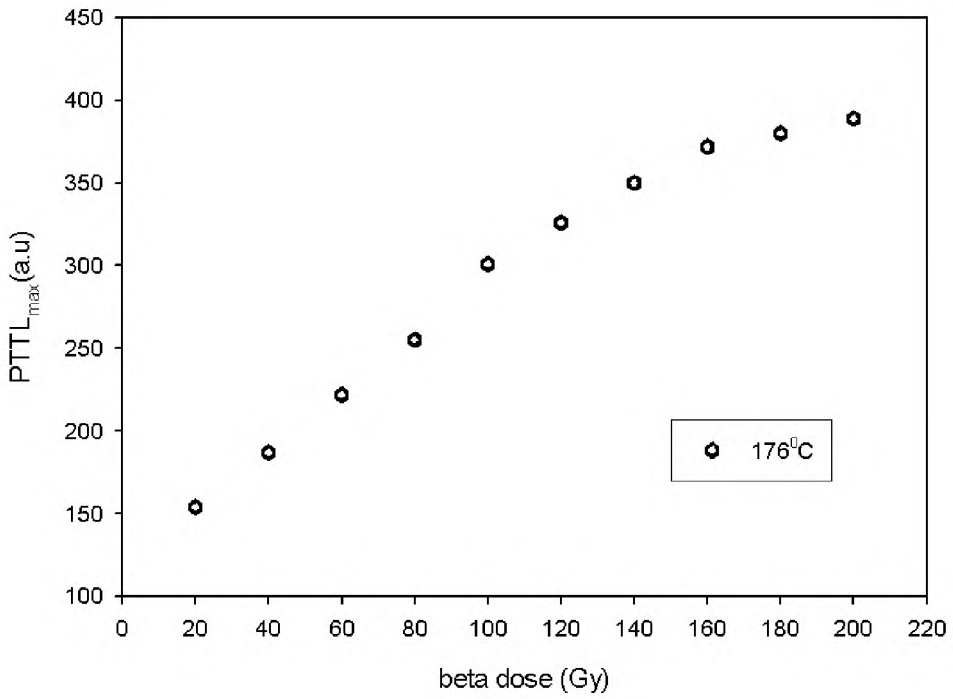

Figure 4.59: PTTL peak intensity against beta radiation dose from 20 to 200 Gy for peak III.

Peak temperature for PTTL glow peaks

Figure 4.60 shows peak temperatures as a function of beta radiation dose from 20 to 200 Gy. The peak temperatures are independent of beta radiation dose. This kind of behaviour is consistent with first order kinetics.

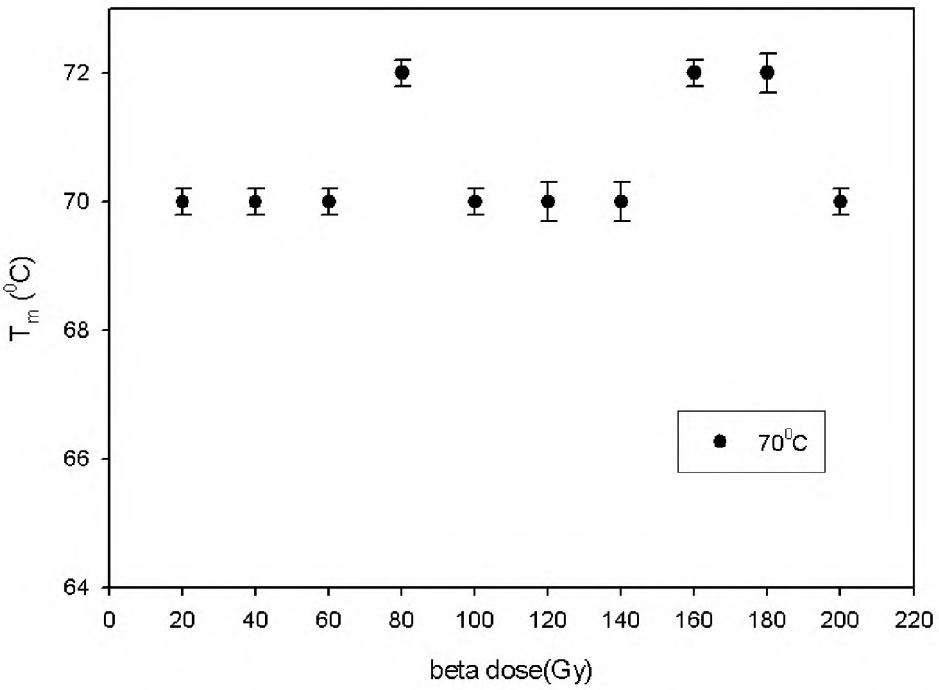

Figure 4.60: Peak temperatures as a function of beta radiation dose for peak I.

Figure 4.61 shows the peak temperatures as the function of beta radiation dose from 20 to 200 Gy for peak III. The peak temperatures is independent of beta doses.

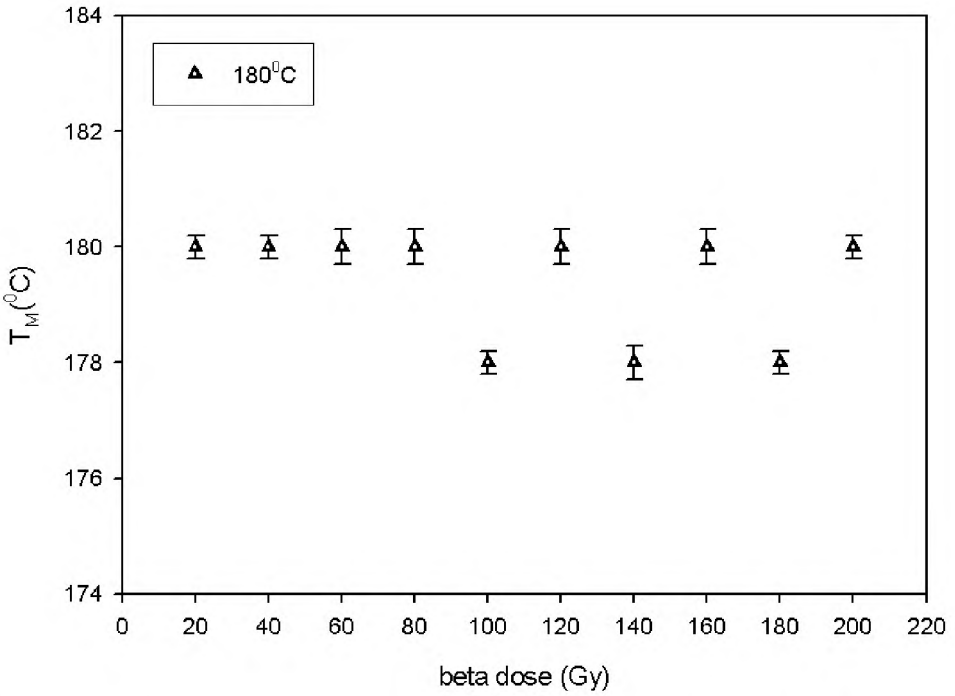

Figure 4.61: Peak temperatures as a function of beta radiation dose for peak III.

4.16 Summary for analysis of PTTL peak I and peak III

The sample was heated up to 430 ^{0}C then exposed to 470 nm blue LEDs for periods of time from 3 to 29 s at room temperature. Three PTTL glow peaks were observed as shown earlier in figure 4.41 but only peaks I and III were analyzed. Both peaks reached the maximum PTTL intensity at 13 s then decreases up to 29 s as was shown in figure 4.42 and figure 4.43. Kinetic analysis was done using two methods, the initial rise and the heating rate. The effect of heating rate on the TL peak intensity and peak temperature was observed. For peak I at 72 ^{0}C the donor of electrons to the shallow traps was find at 300 ^{0}C and peak III. On both PTTL glow peaks thermal fading was observed during storage time for 30 minutes. Peak temperature is independent of dose for both PTTL glow peaks I and III. During dose dependence for both peaks I and III, TL peak intensity was increasing with

beta dose. The two kinetics analysis methods shows the consistence of the values of trap depth and frequency factor. PTTL signal and its saturated region was observed. The effect of changing heat rate on the PTTL glow peaks was illustrated. During annealing the intensity both peaks were stablised between 350 ^{0}C and 500 ^{0}C.

Chapter 5

Conclusion

The resulting TL glow curve displayed three glow peaks located at 74 ^{0}C, 144 ^{0}C and 168 ^{0}C which represent electron traps in the sample below the temperatures of 500 ^{0}C. The main peak located at 74 ^{0}C could be useful for dosimetry application. The $T_m - T_{stop}$, shows that the was an overlapping peak in the rising part of the TL glow curve.

Kinetic analysis shows that all methods concur. All methods gave the values of the trap depth, that were consistence from 0.7 to 1.0 eV. Also for frequency factor the order was from 10^8 to 10^{15} s^{-1}. The characteristics of TL glow curve were observed to be first order kinetics. When using VHRM, the value of trap depth may not be accurate because of the choice of two parameters T_m and β is arbitrary and not all data points is used but sometimes it give a reasonable value when compared with other methods.

TL response was superlinear, supralinear and sublinear TL response. The peak temperature was independent of beta dose from 20 to 200 Gy showing first order kinetics.

After the sample was irradiated up to 100 Gy and stored for 30 minutes at room temperature. The sample shows thermal fading for only peak I, the fading behaviour may be cause of the electrons escaping the electron trap with time. No thermal fading was observed on peak III.

Only three peaks, I and III were responsible of photo transfer thermoluminescence (PTTL). The PTTL signal was observed between 3 to 29 seconds. The PTTL intensity increases and reached the maximum intensity at 13 s. Also the PTTL intensity decreases with increase in heating rate. The PTTL intensity shows the decrease as pulse annealing temperatures increases from 50 to 500 ^{0}C for peak I and III. During annealing the intensity of both peaks, I and III was stable between 350 ^{0}C and 500 ^{0}C. The donor trap was find at 350 ^{0}C. Also thermal fading was affecting both PTTL peaks, I and III.

Bibliography

[1] G.E.Yukihara and S. W. S. McKeever. *Optically stimulated luminescence fundamentals and applications.* Wiley, 2011.

[2] R. Chen and S. W. S. McKeever. *Theory of Thermoluminescence and Related Phenomena.* World Scientific, 1997.

[3] S. W. S. McKeever. *Thermoluminescence of solids.* Cambridge University Press, 1985.

[4] C. Furetta. *Handbook of Thermoluminescence.* World Scientific, 2003.

[5] J. T. Randall and M. H. F. Wilkins. Phosphorescence and electrons traps: I. the study of trap distributions. *Proc. R. Soc. London*, A 184 : 366 – 389, 1945.

[6] C. E. May and J. A. Partridge. Thermoluminescence kinetics of alpha irradiated alkali halides. *J. Chem. Phys.*, 40 : 1401 – 1415, 1964.

[7] R. Chen, G. Fogel, and N. Kristianpoller. Theoretical account of the sensitization and de-sensitization in quartz. *Radiat. Prot. Dosim.*, 23 : 277 – 279, 1994.

[8] G. F. J. Garlick and A. F. Gibson. The electron trap mechanism of luminescence in sulphide and silicate phosphors. *Proc. Phys. Soc.*, 60 : 574 – 589, 1948.

[9] R.Chen. *J. R. Electrochem. Soc.*, 116 : 1254, 1969.

[10] W. Hoogenstraaten. Method of measuring specific resistivity and hall effect of discs of arbirtary shape. *Philips. Res. Rep*, 13, 1958.

[11] G. Kitis, J. M. Gomez-Ros, and J. W. N. Tuyn. Thermoluminescence glow-curve deconvolution functions for first, second and general orders of kinetics. *J. Phys. D: Appl. Phys*, 31 : 2636 – 2641, 1998.

[12] S. W. S. McKeever and R. Chen. Luminescence models. *Radiat. Meas.*, 27 : 625 – 661, 1997.

[13] K. Inabe N. Takeichi and H. Nanto. On the general order kinetics of the thermoluminescence glow peak. *Wiley*, 10 : 159, 1975.

[14] A. J. J. Santos, J. F. de Lima, and M. E. G. Valerio. Phototransferred thermoluminescence of quartz. *Radiat. Meas.*, 33 : 427 – 430, 2001.

[15] L. Bøtter-Jensen, S. W. S. McKeever, and A. G. Wintle. *Optically Stimulated Luminescence Dosimetry.* Elsevier, 2003.

[16] V. Pagonis, G. Kitis, and C. Furetta. *Numerical and Practical Exercises in Thermoluminescence.* Springer, 2006.

[17] P. D. Townsend S. W. S. Mckeever, M. Moscovitch. *Thermoluminescence Dosimetry Materials:Properties and Uses.* Nuclear Technology, 1995.

[18] A. G Wintle and A. S. Murray. The relationship of quartz thermoluminescence, photo-transferred thermoluminescence, and optically stimulated luminescence. *Radiat. Meas.*, 27 : 611 – 624, 1997.